Ore Geology Reviews 89 (2017) 1030–1057

Contents lists available at ScienceDirect

Ore Geology Reviews

journal homepage: www.elsevier.com/locate/oregeo

Review

Cenozoic metallogeny of Greece and potential for precious, critical and rare metals exploration

Vasilios Melfos [a,*], Panagiotis Voudouris [b,*]

[a] Department of Mineralogy, Petrology and Economic Geology, Aristotle University of Thessaloniki, Thessaloniki 54124, Greece
[b] Department of Mineralogy-Petrology, National and Kapodistrian University of Athens, Athens 15784, Greece

ARTICLE INFO

Article history:
Received 13 July 2016
Received in revised form 23 May 2017
Accepted 29 May 2017
Available online 3 June 2017

Keywords:
Late orogenic extension
Detachment fault
Porphyry Cu–Mo-(Au)
Epithermal Cu-Au-Ag
Critical metals
Greece

ABSTRACT

The Cenozoic metallogeny in Greece includes numerous major and minor hydrothermal mineral deposits, associated with the closure of the Western Tethyan Ocean and the collision with the Eurasian continental plate in the Aegean Sea, which started in the Cretaceous and is still ongoing. Mineral deposits formed in four main periods: Oligocene (33–25 Ma), early Miocene (22–19 Ma), middle to late Miocene (14–7 Ma), and Pliocene-Pleistocene (3–1.5 Ma). These metallogenic periods occurred in response to slab-rollback and migration of post-collisional calc-alkaline to shoshonitic magmatism in a back-arc extensional regime from the Rhodopes through the Cyclades, and to arc-related magmatism along the active south Aegean volcanic arc. Invasion of asthenospheric melts into the lower crust occurred due to slab retreat, and were responsible for partial melting of metasomatized lithosphere and lower crustal cumulates. These geodynamic events took place during the collapse of the Hellenic orogen along large detachment faults, which exhumed extensive metamorphic core complexes in mainly two regions, the Rhodopes and the Cyclades. The detachment faults and supra-detachment basins controlled magma emplacement, fluid circulation, and mineralization.

The most significant mineralization styles comprise porphyry, epithermal, carbonate-replacement, reduced intrusion-related gold, intrusion-related Mo-W and polymetallic veins. Porphyry and epithermal deposits are commonly associated with extensive hydrothermal alteration halos, whereas in other cases alteration is of restricted development and mainly structurally controlled. Porphyry deposits include Cu-Au-, Cu-Mo-Au-Re, Mo-Re, and Mo-W variants. Epithermal deposits include mostly high- and intermediate-sulfidation (HS and IS) types hosted in volcanic rocks, although sedimentary and metamorphic rock hosted mineralized veins, breccias, and disseminations are also present. The main metal associations are Cu-Au-Ag-Te and Pb-Zn-Au-Ag-Te in HS and IS epithermal deposits, respectively. Major carbonate-replacement deposits in the Kassandra and Lavrion mining districts are rich in Au and Ag, and together with reduced intrusion-related gold systems played a critical role in ancient economies. Finally hundreds of polymetallic veins hosted by metamorphic rocks in the Rhodopes and Cyclades significantly add to the metal endowment of Greece.

Contents

* Corresponding authors.
E-mail addresses: melfosv@geo.auth.gr (V. Melfos), voudouris@geol.uoa.gr (P. Voudouris).

http://dx.doi.org/10.1016/j.oregeorev.2017.05.029
0169-1368/

1. Introduction

Greece is historically an important country as a metal producer especially during antiquity. Mining dates back to prehistoric times, focusing initially on gold, copper and iron. Later, in the Classical (5th to 4th centuries BC) and Hellenistic (4th to 2nd centuries BC) times, ore exploitation became more intense, especially for Au, Ag, Cu and Fe. Major mining centers operated around the Aegean, where a large number of underground galleries and metallurgical furnaces from that time are still preserved. Several metals, such as Ag, Au, Fe and Cu, were also produced during the Byzantine (4th to 15th centuries AD) and Ottoman periods (15th to 19th centuries AD). Since the beginning of the 20th century, especially after the Second World War (post-1945) several mines have operated for the exploitation of Cr, Ni, Al, Mn, Fe, Pb, Zn, Cu, Au and Ag from chromite, laterite, bauxite, iron-manganese, and Pb-Zn-(±Cu±Au±Ag) carbonate-replacement deposits (Tsirambides and Filippidis, 2012). However, the majority of these operations has been suspended in recent years for economic, political, social, and environmental reasons (Melfos and Voudouris, 2012). Nevertheless, Greece remains the most important country in the European Union (EU) for the production of Ni-Fe from laterites (2014 production: 2.4 Mt containing 18,500 t Ni) and Al from bauxites (2014 production: 1.8 Mt containing 170,000 t Al). The production of Mg from magnesite is also significant (2014 production: 270,000 t magnesite). More recent exploration has discovered deposits of gold, silver, copper, molybdenum, rhenium, antimony, tungsten, and tellurium, mainly in northern Greece (Melfos et al., 2002; Voudouris, 2006; Voudouris et al., 2009; Fornadel et al., 2011; Melfos and Voudouris, 2012; Voudouris et al., 2013a,b,c; Bristol et al., 2015; Stergiou et al., 2016).

The geological setting of the Hellenides (Fig. 1), part of the Alpine-Himalayan orogeny, comprises numerous geotectonic terranes formed in the complicated geodynamic environment of the Paleo- and Neotethys (Fig. 1; Pe-Piper and Piper, 2002; Schmid et al., 2008; Jolivet and Brun, 2010; Ring et al., 2010; Jolivet et al., 2013; Menant et al., 2016). During post-orogenic episodes, after the closure of the Vardar and Pindos (Neotethys) oceanic basins, large scale detachments formed that exhumed metamorphic core complexes. Meanwhile, Tertiary to Quaternary calc-alkaline to alkaline magmatism in the Aegean region occurred behind the active Hellenic subduction zone (Jolivet et al., 2013).

In this geotectonic regime several significant ore deposits and hundreds of smaller occurrences formed in association with magmatism and magmatic-hydrothermal systems. Deposits include porphyry, carbonate-hosted replacement Pb-Zn-Ag-Au, high-, intermediate- and low-sulfidation (IS and LS) epithermal polymetallic and precious metal vein, skarn, and intrusion-related gold deposits. They are mainly concentrated in two broad regions, the Rhodopes and the Cyclades (Figs. 1 and 2), which underwent similar tectono-metamorphic and magmatic evolution since the Cretaceous. These regions are the most promising targets for future exploration of precious, rare, and critical metals in Greece.

This paper focuses on the metallic mineral deposits of these two metallogenic provinces. The geology and ore types involved in each magmatic belt are reviewed, along with some specific features of these deposits including ore mineralogy, hydrothermal alteration, geochemistry, and age determinations and resource estimates where available. These data are used to evaluate the potential of these regions for future exploration and discovery of precious, rare, and critical metals.

2. Geological setting

2.1. Geodynamic overview of pre-Cenozoic to Cenozoic evolution in the Aegean region

The Hellenide orogen is a discrete terrane of the Alpine-Himalayan deformational belt and represents a geotectonic link between the southern Balkan Peninsula (e.g., the Dinarides/Albanides) and Turkey (e.g., Pontides, Anatolides). It consists, from north to south, of three continental blocks (Rhodopes, Pelagonia, and Adria-External Hellenides) and two intervening oceanic domains (Vardar and Pindos Suture Zones) (Kydonakis et al., 2015a,b). The Hellenides formed as a result of the ongoing Alpine collision between the African and Eurasian plates since the Late Jurassic to the present above the north-dipping Hellenic subduction zone. This convergence caused thrusting and SW-verging nappe-stacking of the Rhodopes, Pelagonia and Adria continental

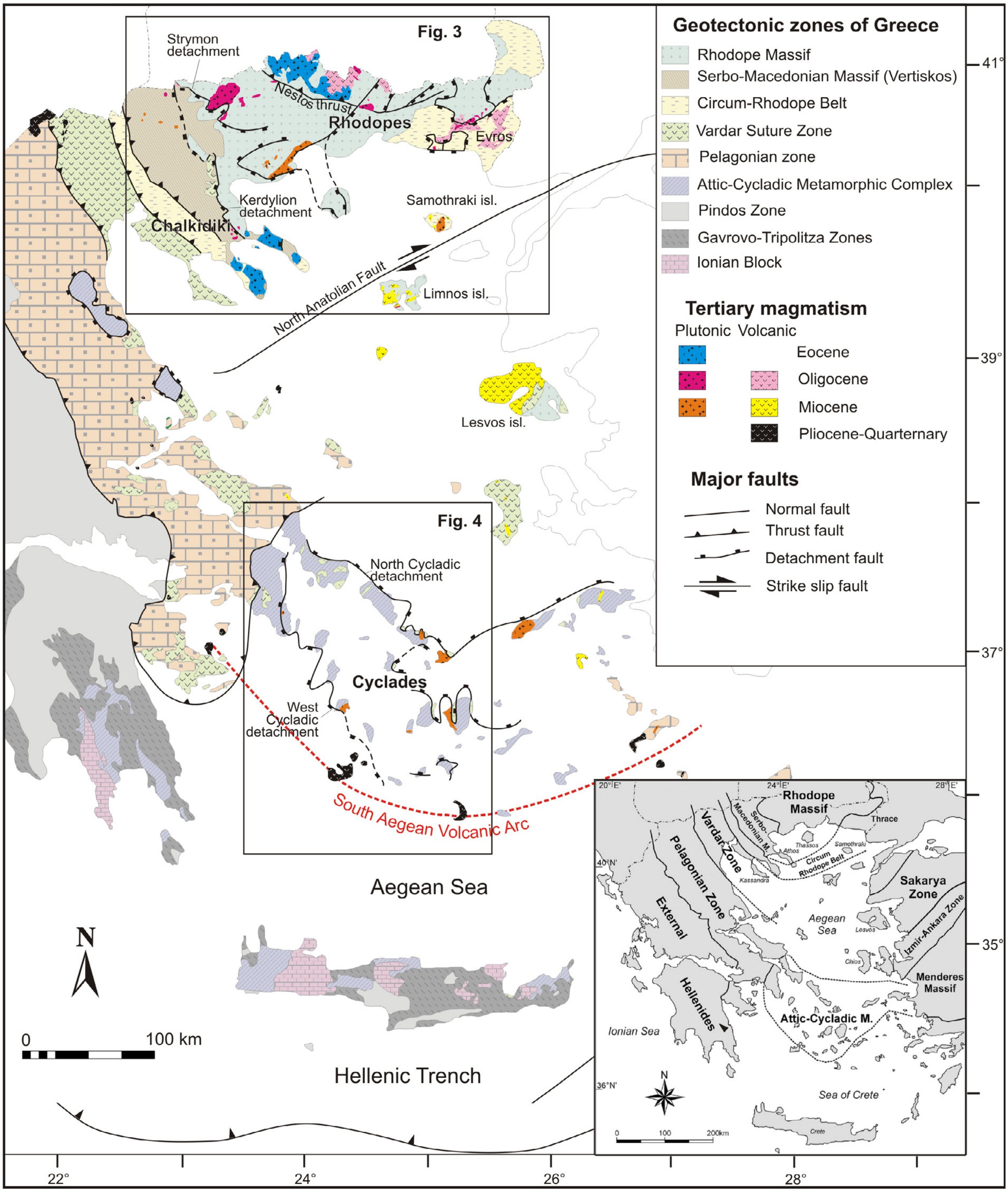

Fig. 1. Simplified geotectonic map of Greece showing the main tectonic zones and the major tectonic structures within the Hellenides and distribution of Cenozoic igneous rocks (modified after Pe-Piper and Piper, 2006; Schmid et al., 2008; Jolivet and Brun, 2010; Jolivet et al., 2013; Ersoy and Palmer, 2013). The geotectonic zones of the Hellenic orogen are shown in the inset.

blocks, and closure of the Vardar and Pindos oceanic domains of the Neotethys (Robertson, 2002; Schmid et al., 2008; Jolivet and Brun, 2010; Ring et al., 2010; Kydonakis et al., 2015a,b; Menant et al., 2016; Brun et al., 2016).

Late Precambrian to Late Jurassic evolution of the region was marked by the opening and closure of ocean basins and continental crust formation above the accompanying subduction zones (Anders et al., 2006; Himmerkus et al., 2006; Reischmann and Kostopoulos, 2007). A Permo-Carboniferous igneous event related to northward subduction of Paleotethys beneath the southern margin of Europe is recognized from the Pelagonia, Rhodope, and Attico-Cycladic areas, and records an active continental margin evolution in the Precambrian-Silurian basement of the Hellenides (Anders et al., 2006; Reischmann and Kostopoulos, 2007).

The Vardar Ocean opened during the Late Triassic–Early Jurassic, separating the Pelagonia and Rhodope continents (Robertson et al., 2013). Northeastward subduction created a Late Jurassic magmatic arc along the southern margin of the Rhodope

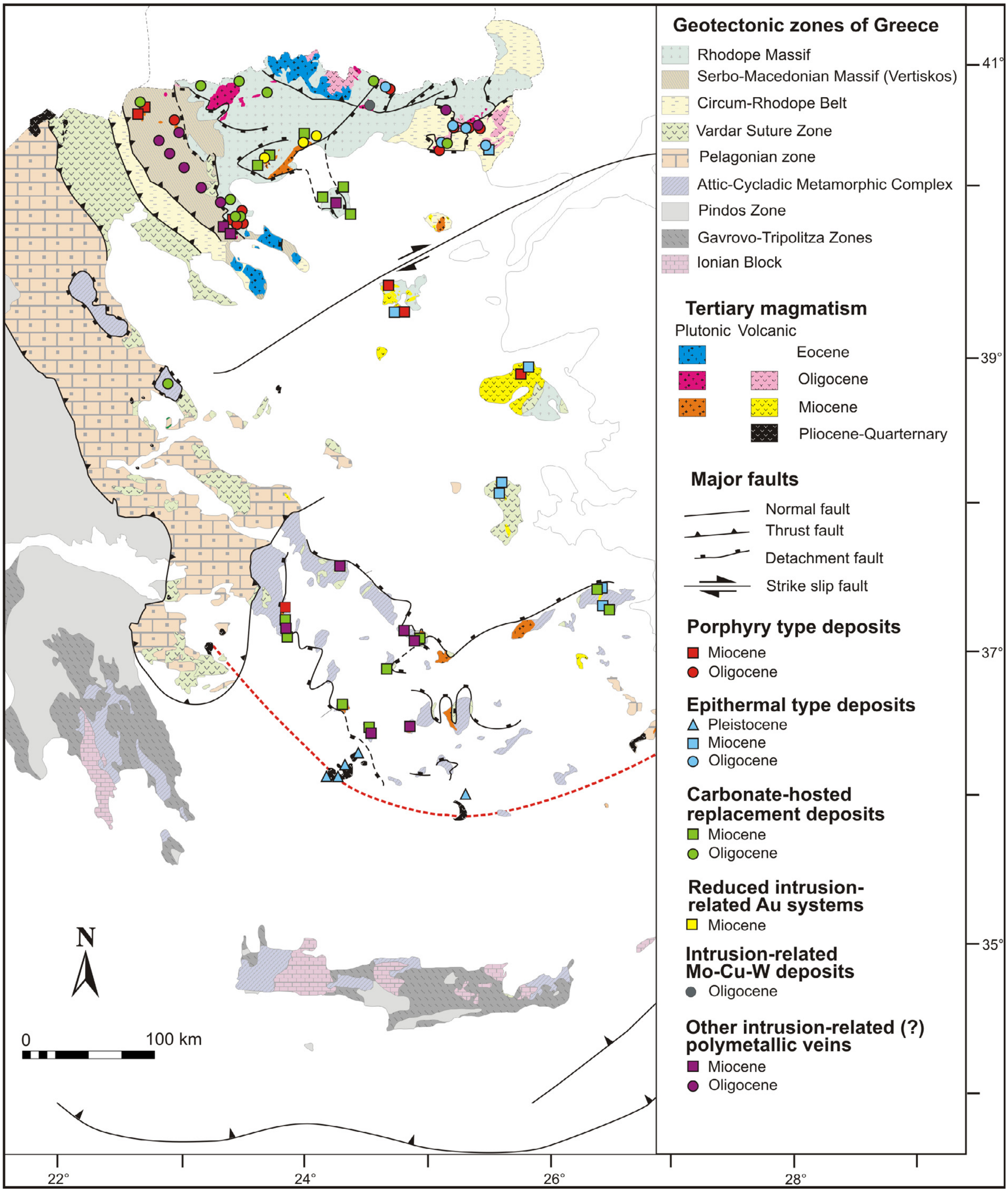

Fig. 2. Distribution of Cenozoic mineralization in Greece (references as in Fig. 1).

continent, while future ophiolites formed by supra-subduction zone spreading within the Vardar Ocean. Final collision between Europe and Pelagonia at the end of the Cretaceous closed the Northern Neotethys Ocean along the Vardar Suture Zone, as evidenced by obducted Jurassic ophiolites on the Pelagonia continental block (Robertson et al., 2013).

Accretion of the Pelagonia continental block to the Eurasian margin was followed by the onset of subduction of the Pindos oceanic basin in the Paleocene (~60–55 Ma) and then by its closure at ~35 Ma when the Adria and Pelagonia microcontinents collided (Brun and Faccenna, 2008; Ring et al., 2010; Jolivet et al., 2013; Menant et al., 2016). In the center of the Aegean, the Cyclades partly expose the buried parts of the Pindos Ocean and its continental margins (Menant et al., 2016). A single subduction zone was active from the Early Cretaceous, which consumed both oceanic and continental lithospheric mantle beneath the Aegean Sea (van Hinsbergen et al., 2005; Brun and Faccenna, 2008; Ring et al., 2010; Jolivet et al., 2013; Menant et al., 2016; Brun et al., 2016). The geodynamic evolution of the Aegean area includes slab roll-back since the Eocene, and slab tearing below western Anatolia during the Miocene. As a result of slab roll-back, collapse of the accretionary wedge and the opening of back-arc basins allowed for the post-orogenic exhumation of the lower parts of the stretched crust as metamorphic core complexes, such as in the Rhodopes and the Cyclades, with voluminous post-collisional magmatism (Fig. 1; Menant et al., 2016, and references therein).

2.2. The Rhodope Massif

The Rhodope Massif, together with other major units of the Balkan orogen in Serbia, Former Yugoslavian Republic of Macedonia (FYROM), Bulgaria and Greece (e.g., the Dacia-Serbo-Macedonian Mega-unit and, the Strandzha-Circum-Rhodope Belt), and the Sakarya block in western Turkey, are considered to have been part of the European continental margin (Schmid et al., 2008; Himmerkus et al., 2009a; Burg, 2012; Kydonakis et al., 2015a,b). The Rhodope Massif is bordered to the north by the Maritza shear zone separating the Rhodopes from the Srednogorie in Bulgaria, and to the south by the Vardar Suture Zone. The Rhodope Massif is a heterogeneous crustal body composed of three sub-domains (Fig. 3), namely the Northern Rhodope Domain, the Southern Rhodope Core Complex (both separated by the Nestos thrust fault), and the Chalkidiki Block, which coincides with the so-called Serbo-Macedonian Massif (excluding the Kerdylion Unit, which belongs to and has a common tectono-metamorphic history with the Southern Rhodope Core Complex; Kydonakis et al., 2015a,b). The Chalkidiki block and the Northern Rhodope Domain share a similar tectono-metamorphic history and participated in the same

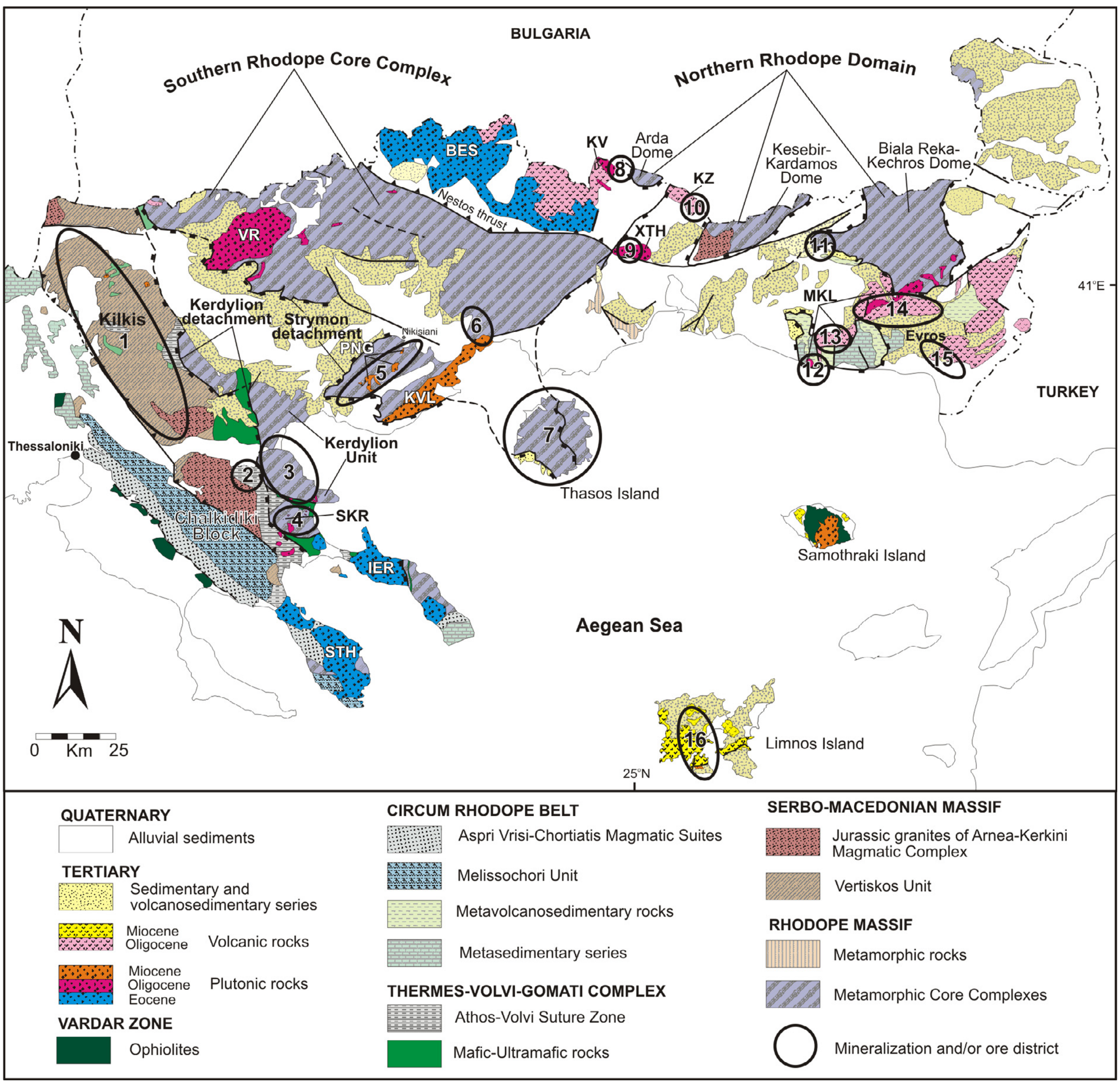

Fig. 3. Simplified geological map of the Greek Rhodope Massif and the Serbo-Macedonian Vertiskos Unit in northern Greece showing the major tectonic units referred to in the text, and the location of the main detachments, the Cenozoic magmatic rocks and the main mineralization and/or ore districts (adapted from Del Moro et al., 1988; Biggazzi et al., 1989; Christofides et al., 1998, 2004; Bonev et al., 2006a; Himmerkus et al., 2006; Brun and Sokoutis, 2007; Burg, 2012; Melfos and Voudouris 2012, 2016; Kilias et al., 2013a; Kydonakis et al., 2015a,b; Siron et al., 2016). Abbreviations of the magmatic rocks: BES: Barutin–Elatia-Skaloti, IER: Ierissos, KV: Kotyli-Vitinia, KZ: Kalotycho-Zlatograd, MKL: Maronia-Kirki-Leptokarya, SKR: Skouries, KVL: Kavala, PNG: Pangeon, STH: Sithonia, VR: Vrondou, XTH: Xanthi. Mineralization and/or ore districts: Western Rhodope Massif: 1. Kilkis (Vathi, Gerakario, Drakontio, Koronouda, Stefania, Laodikino); 2. Stanos, Nea Madytos; 3. Kassandra mining district (carbonate-replacement ore mineralization at Olympias, Madem Lakkos, Mavres Petres, Piavitsa); 4. Kassandra mining district (porphyry systems at Skouries, Fisoka, Alatina, Tsikara, Dilofon); 5. Pangeon; 6. Palea Kavala; 7. Thasos; Eastern Rhodope Massif: 8. Thermes; 9. Kimmeria of Xanthi; 10. Kalotycho-Melitena; 11. Kallintiri; 12. Maronia; 13. Petrota Graben (Perama Hill, Mavrokoryfi); 14. Kirki-Sapes-Kassiteres-Esimi (Pagoni Rachi, Konos Hill, Koryfes/Kasiteres, Myli, Viper, Scarp, St. Demetrios, St. Barbara, St. Philippos); 15. Evros (Pefka, Loutros); Northeastern Aegean region: 16. Limnos Island (Fakos, Sardes).

Mesozoic crustal-scale southwestward accretionary event before development of the Southern Rhodope Core Complex (Kydonakis et al., 2015a,b, 2016).

The Northern Rhodope Domain consists of the following main metamorphic units: (i) a lower unit of high-grade basement including orthogneisses derived from Permo-Carboniferous protoliths; this unit includes four metamorphic core complexes (the Arda, Biala Reka-Kechros, and Kesebir-Kardamos migmatitic domes); (ii) an intermediate unit of high-grade basement rocks that have both continental and oceanic affinities, and with protoliths ranging in age from Neoproterozoic through Ordovician, and Permo-Carboniferous to Early Cretaceous; and (iii) an overlying uppermost Mesozoic low-grade unit of the Circum-Rhodope Belt and the Evros ophiolite (Turpaud and Reischmann, 2010; Kirchenbaur et al., 2012; Meinhold and Kostopoulos, 2013; Bonev et al., 2015). The rocks of the intermediate unit experienced high to ultra-high pressure metamorphism with subsequent high-grade amphibolite-facies overprint (Mposkos and Kostopoulos, 2001).

The Chalkidiki Block (Fig. 3) represents a thrust system composed of four NW-trending units: the Vertiskos Unit including the Thermes-Volvi-Gomati (TVG) complex, the Circum–Rhodope Belt, the Chortiatis Magmatic Suite, and the eastern Vardar ophiolites. The latter two units comprise a Middle to Late Jurassic arc/back-arc spreading system (Bonev et al., 2015; Kydonakis et al., 2015a,b; Siron et al., 2016). The Vertiskos Unit is a Gondwana-derived basement fragment made of Silurian–Ordovician peraluminous orthogneiss with intercalated paragneiss, marble, amphibolite, eclogite, and serpentinite, and was incorporated into the Southern European Arcs by the end of the Palaeozoic (Himmerkus et al., 2009a). The Vertiskos Unit was affected by Palaeozoic deformation and a Late Jurassic–Cretaceous amphibolite-facies overprint (e.g., Kilias et al., 1999; Kydonakis et al., 2015a,b, 2016). A-type granitoids of the Arnea–Kerkini Magmatic Complex intruded during the Early Triassic (Himmerkus et al., 2009b). The Thermes-Volvi-Gomati (TVG) complex is a tectonic mélange separating the Vertiskos Unit from the southern Rhodope Kerdylion Unit (see below) and consists of the Athos-Volvi Suture Zone and mafic and ultramafic rocks (Siron et al., 2016). The Circum–Rhodope Belt comprises low-grade metasedimentary rocks of Triassic–Jurassic protolith age and minor rhyolites, fringing the crystalline basement of the Vertiskos Unit (Meinhold and Kostopoulos, 2013).

The Southern Rhodope Core Complex (SRCC), which is tectonically juxtaposed against the Vertiskos Unit, is composed of Permo-Carboniferous orthogneiss and massive Triassic marble intercalated with amphibolitic and metapelitic rocks (Dinter et al., 1995; Brun and Sokoutis, 2007; Turpaud and Reischmann, 2010). The SRCC displays intense, penetrative, top-to-the-southwest shearing under amphibolite and greenschist facies conditions (Burg et al., 1996). Parts of the SRCC have experienced partial melting and formation of migmatites at Thasos Island and the Kerdylion Unit. These Permo-Carboniferous orthogneisses in the SRCC may be equivalent to those in the Arda, Biala Reka-Kechros, and Kesebir-Kardamos migmatitic domes in the Northern Rhodope Domain (Fig. 3; Brun and Sokoutis, 2007; Kydonakis et al., 2015b).

2.3. The Cyclades

In the center of the Aegean Sea the Cyclades consist of three main units (Bonneau, 1984): the lowermost Pre-Alpidic Cycladic Basement Unit, the intermediate Cycladic Blueschist Unit, and the uppermost Pelagonian Unit (Fig. 4). The Blueschist Unit represents a polymetamorphic terrane which tectonically overlies the basement gneiss and consists of a metamorphosed volcano-sedimentary sequence of clastic metasedimentary rocks, marbles, calc-schists, and mafic and felsic meta-igneous rocks (Parra et al., 2002; Bröcker and Pidgeon, 2007; Katzir et al., 2007; Ring et al., 2010; Jolivet et al., 2013; Scheffer et al., 2016).

The Cyclades have been exhumed since the Eocene as metamorphic core complexes formed in low, medium, and/or high temperature environments (Menant et al., 2016, and references therein). The Cycladic Blueschist Unit experienced two stages of metamorphism during the Tertiary: the first occurred during the Eocene (∼52–53 Ma), which was marked by high-pressure eclogite- to blueschist-facies metamorphism at 15–20 kbar, and ∼500 °C. Exhumation of the Cycladic Blueschists first occurred between 45 and 35 Ma in a syn-orogenic context, following a cold retrograde path (Menant et al., 2016; Laurent et al., 2017). The Cycladic Blueschist Unit underwent an early Oligocene medium temperature-medium pressure metamorphic overprint (∼9 kbar, 550–570 °C) followed by greenschist-facies retrograde metamorphism. Finally, in the early Miocene, high-temperature medium-pressure metamorphism (5–8.5 kbar, 500–700 °C) and associated migmatites developed in the central Cyclades (Jolivet and Brun, 2010; Grasemann et al., 2012; Menant et al., 2016, and references therein; Scheffer et al., 2016). The amphibolite to greenschist metamorphic event occurred during extension-related exhumation and was coeval with back-arc extension at the Rhodopes in northern Greece (Altherr et al., 1982; Lister et al., 1984; Gautier and Brun, 1994; Jolivet et al., 2010; Ring et al., 2010).

The upper Pelagonian Unit did not experience Eocene high-pressure metamorphism, and consists of various klippen of unmetamorphosed Late Permian to Jurassic volcaniclastic rocks, ophiolites, and carbonates, greenschist facies rocks of Cretaceous to Tertiary age, and Late Cretaceous medium-pressure and/or high temperature rocks and granitoids (Reinecke et al., 1982; Bröcker and Pidgeon, 2007). It was thrust onto the Blueschist Unit at ∼25–20 Ma (Boronkay and Doutsos, 1994).

Exhumation of the Cycladic rocks as metamorphic core complexes was accommodated during the Oligocene–Miocene by several ductile to brittle detachment systems (see below). The extensional event also allowed for various granitoids (granite, granodiorite, leucogranite) to be intruded throughout the Cyclades between 15 and 7 Ma (Altherr et al., 1982; Pe-Piper and Piper, 2002; Skarpelis et al., 2008).

2.4. Back-arc extension and metamorphic core complexes in the Aegean

In the Rhodope region, Paleogene-Neogene exhumation of the metamorphic pile and core complexes followed the Cretaceous syn-metamorphic SW-directed thrusting (Burg et al., 1996; Kilias et al., 1999; Bonev et al., 2006a,b; Brun and Sokoutis, 2007; Burg, 2012; Kydonakis et al., 2015a,b; Brun et al., 2016). In the Northern Rhodope Domain, early (syn-orogenic) exhumation was initiated in the early Eocene (∼55 Ma) and lasted up to ∼42 Ma (middle Eocene), and was coeval with the accretion of Pelagonia following the closure of the Vardar Ocean (Wüthrich, 2009; Menant et al., 2016). Two later stages of extension and metamorphic core complex formation occurred in the Rhodope Massif from ∼42–35 Ma and ∼24–12 Ma (Wüthrich, 2009; Jolivet and Brun, 2010; Márton et al., 2010; Moritz et al., 2010; Burg, 2012; Jolivet et al., 2013; Kounov et al., 2015). The first phase of core complex formation in the Rhodopes (40–35 Ma) was coeval with the subduction of the Pindos Ocean following accretion of the Pelagonian continental block to the Eurasian margin (Brun and Faccenna, 2008; Wüthrich, 2009). The second phase of core complex-related extension took place after suturing of the Pindos oceanic domain (∼35 Ma; Ring et al., 2010), and was coeval with the accretion and subduction of continental blocks of the external Hellenides, and back-arc

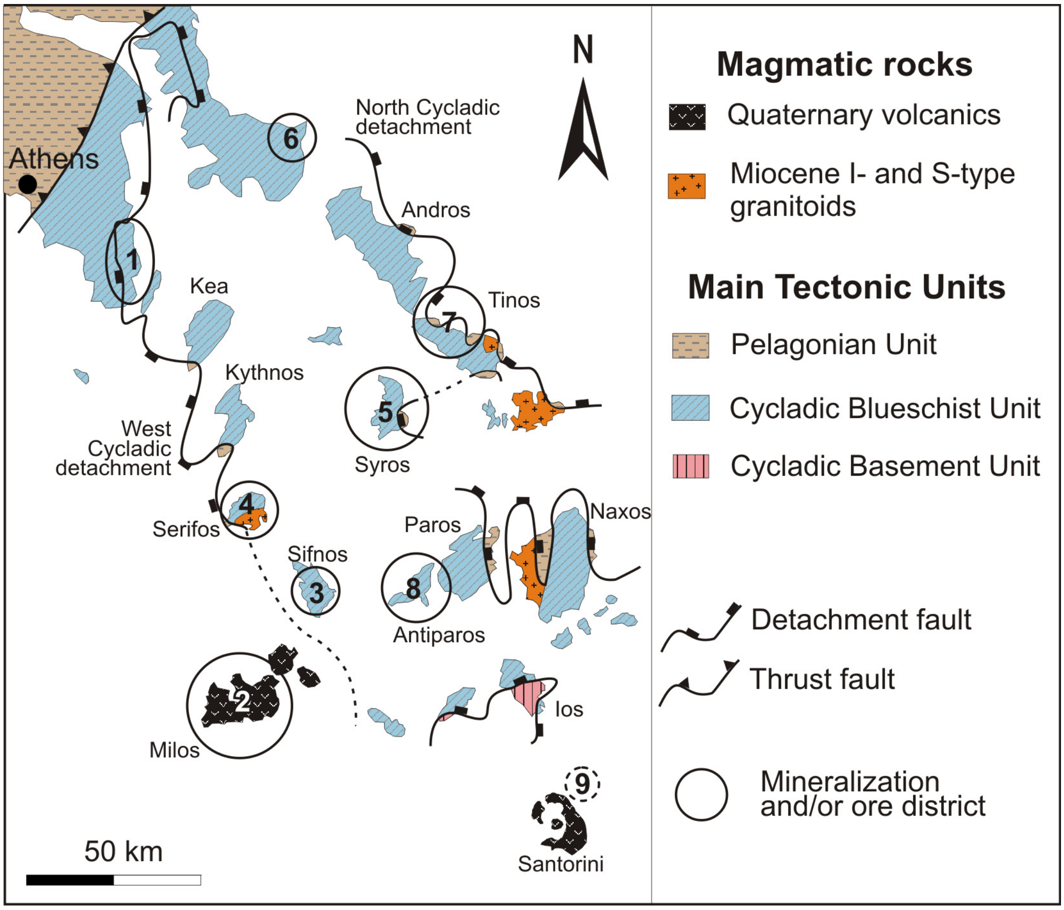

Fig. 4. Simplified geological map of the Cyclades showing the locations of the major detachments, magmatic rocks and mineralization and/or ore deposits and prospects (adapted from Grasemann et al., 2012; Jolivet et al., 2013, 2015; Scheffer et al., 2016). Mineralization and/or ore districts: 1. Lavrion (Plaka, Kamariza-Sounio); 2. Milos (Profitis Ilias, Chondro Vouno, Triades-Galana, Kondaros-Katsimouti-Vani); 3. Sifnos; 4. Serifos; 5.Syros; 6. Kallianou; 7. Tinos; 8. Antiparos; 9. Kolumbo.

extension initiated by the onset of the subduction of the Mediterranean Ocean.

In the central and eastern Rhodope area of Bulgaria and Greece (e.g., the Northern Rhodope Domain core complexes), the Arda, Biala Reka-Kechros, and Kesebir-Kardamos migmatitic domes (Fig. 3) were progressively exhumed along several ductile to brittle shear zones, all active from ~42–35 Ma (Bonev et al., 2006a,b, 2010; 2013; Wüthrich, 2009; Márton et al., 2010; Moritz et al., 2010; Kaiser-Rohrmeier et al., 2013). In the South Rhodope Core Complex, cooling/exhumation of the metamorphic rocks occurred along two major detachment faults (Brun and Sokoutis, 2007; Wüthrich, 2009; Kounov et al., 2015): the ductile Kerdylion detachment, active from ~42 to 24 Ma; and the ductile-to-brittle Strymon detachment (~24–12 Ma). The Kerdylion detachment, which separates the Serbo-Macedonian Vertiskos Unit from the Rhodope Kerdylion Unit, controlled the exhumation of the SRCC (Brun and Sokoutis, 2007; Kydonakis et al., 2015b; Brun et al., 2016).

In the Aegean back-arc domain at ~35–30 Ma ago, an increase of the rate of slab retreat led to the initiation of post-orogenic extension, largely accommodated by large-scale structures such as the North Cycladic Detachment System (NCDS), active from ~35–10 Ma (Jolivet et al., 2013) (Fig. 4). The North Cycladic detachment system records a NE-directed normal shear sense, which separates the Cycladic Blueschist Unit in the footwall from the Upper Unit in the hanging wall (Jolivet et al., 2010). Grasemann et al. (2012) proposed the existence of another large-scale low-angle normal fault system, the West Cycladic detachment system, which is exposed on Kea, Kythnos, and Serifos, with a strike length of at least 100 km, and possibly extending to the southeast. The West Cycladic detachment system dips toward SW with top-to-the-SSW kinematics. Two more detachment systems, the South Cycladic Detachment System and the Central Cycladic Detachment (Naxos and Paros), have been recognized in the Cyclades (Iglseder et al., 2011, and references therein). New $^{40}Ar/^{39}Ar$ and U-Th/He thermochronological data suggest that the West Cycladic Detachment System accommodated extension throughout the Miocene (Grasemann et al., 2012). The evolution of the western Cyclades can be resolved into a coherent and uniform tectonic progression involving SSW-directed ductile to brittle extension, localized plutonism, and rapid cooling of the footwall between 9 and 6 Ma. Because both the North and the West Cycladic Detachment Systems were active until the late Miocene but exhibit opposing shear sense, Grasemann et al. (2012) proposed that a large part of the stretching of the Aegean crust was accommodated by these two bivergent crustal-scale detachment systems.

In the Rhodope Massif the exhumation of metamorphic core complexes along detachment faults resulted in the formation of Palaeocene to early Eocene, late Eocene–Oligocene, and Miocene supra-detachment sedimentary basins (Bonev et al., 2006a,b; Márton et al., 2010; Kilias et al., 2013a). Sediments transgressively or tectonically overlie the metamorphic units of the domes in fault-bounded half-grabens located along the hanging wall of the low-angle detachment faults. Continental extension in Biga and the northeastern Aegean islands of Limnos and Lesvos, as well as in the Cyclades, also resulted in a system of back-arc E–W- to

NNW–SSE-oriented extensional sedimentary basins (Bonev and Beccaletto, 2007; Burchfiel et al., 2008; Brun and Sokoutis, 2007). Since ~16 Ma, extension in the Aegean region has been controlled by the westward extrusion of Anatolia along the North Anatolian Fault (Jolivet et al., 2013).

2.5. Cenozoic magmatic evolution

Several possible causes for the post-collisional volcanic and plutonic activity in the Aegean–west Anatolian region have been proposed, including slab roll-back, post-orogenic collapse and lithospheric thinning, delamination of crustal/lithospheric slices, and slab break-off (e.g., Fytikas et al., 1984; de Boorder et al., 1998; Pe-Piper et al., 1998; Ersoy and Palmer, 2013, and references therein). However, mantle tomographic images indicate that a single slab was subducted since at least the latest Cretaceous, and was responsible for the geodynamic events in the Aegean domain (Jolivet and Brun, 2010). The relationships between subduction dynamics and magmatic evolution in the Aegean region has been studied by Pe-Piper and Piper (2006), Ersoy and Palmer (2013), Jolivet et al. (2013, 2015), and Menant et al. (2016), and their work is summarized below.

Initial "Andean-style" subduction of the Vardar-Izmir-Ankara Ocean and associated Late Cretaceous (~92–67 Ma) arc magmatism resulted in the Apuseni–Banat–Timok–Srednogorie–Pontides magmatic belt (Gallhofer et al., 2015). This was followed by post-collisional Paleocene-Eocene (56–40 Ma) adakite-like magmatism derived from slab melts, in the Rhodope and the west Srednogorie regions, and is part of a 250 km-long NW-trending belt which continues through northern Turkey (Marchev et al., 2013). This magmatic belt includes, among others, the Pirin, Rila, Barutin–Elatia–Skaloti, Sithonia, and Ierissos plutons in Bulgaria and Greece (Fig. 3). Adakite-like magmatism was related to a deep slab break-off (Vardar Ocean) and was followed by asthenospheric upwelling, fast exhumation, and the first period of core complex formation in the Rhodopes from 42 to 35 Ma (Marchev et al., 2013). A slab break-off model has also been proposed for the generation of the adakite-like Eocene magmatic rocks in NW Anatolia (Ersoy and Palmer, 2013).

Asthenospheric upwelling and the first stage of core complex-formation in the Rhodopes was followed by orogenic collapse, steep faulting, and extensional late Eocene to Miocene magmatism that started at ~35 Ma (Marchev et al., 2013). The late Eocene–Miocene post-collisional magmatism in the Rhodopes (Greece and Bulgaria), and northwestern Turkey (Biga Peninsula and Eastern Thrace), is part of the major NW- to EW-trending arcuate magmatic-metallogenic zone running from the Dinarides (Serbia, Kosovo, FYROM) and the Rhodopes, to Anatolia in Turkey and beyond (Heinrich and Neubauer, 2002; Neubauer, 2002; Cvetković et al., 2004; Yigit, 2009, 2012). Slab roll-back is consistent with the progressive southward migration of magmatic activity from the Tertiary in the Rhodope Massif (from 35–30 Ma) to the present in the South Aegean volcanic arc, and with the development of the Aegean subduction zone (Fytikas et al., 1984; Pe-Piper and Piper, 2002, 2006; Jolivet and Brun, 2010; Jolivet et al., 2013, 2015). Pliocene shoshonitic volcanic and subvolcanic rocks also occur in the Voras-Allchar area (Greece-FYROM border).

Late Eocene–Oligocene igneous rocks have calc-alkaline, shoshonitic, to ultrapotassic affinity and mafic-intermediate and felsic composition; they cover large areas in the Rhodope and Serbo-Macedonian block (Fig. 3) and in northwestern Turkey (Innocenti et al., 1984; Jones et al., 1992; Pe-Piper and Piper, 2002; Christofides et al., 2004; Perugini et al., 2004; Marchev et al., 2005, 2013; Ersoy and Palmer, 2013). Within the Rhodope area, major Oligocene intrusive and volcanic areas occur in Borovitsa, Lozen, Madzharovo, Iran Tepe, Zvezdel, Kotyli-Vitinia, Kalotycho-Zlatograd, and Xanthi (Innocenti et al., 1984; Marchev et al., 2005). Other volcanic areas belong to the so-called Evros volcanic rocks, which include the Tertiary basins in Rhodopi and Evros counties (Arikas and Voudouris, 1998; Christofides et al., 2004). Several plutons (e.g., Vrondou, Xanthi, Maronia-Kirki-Leptokarya) intruded contemporaneously with detachment faulting (e.g., in the footwall of detachments) and are partly mylonitized. In the Kassandra mining district, Oligocene intrusives were emplaced at ~27–25 Ma, contemporaneous with movement of the Kerdylion detachment (Brun and Sokoutis, 2007; Hahn et al., 2012; Siron et al., 2016). The late Eocene–Oligocene magmatism in Bulgaria and Greece, Serbia, Kosovo, and FYROM shows a decreasing influence of crustal contamination with time and an increasing input from the mantle, until the eruption of purely asthenospheric magmas. The magmatism evolved from K-rich trachybasalts (34 Ma) via shoshonites, calc-alkaline and high-K calc-alkaline basalts (33–31 Ma), to alkaline basalts (28–26 Ma), and is considered to have resulted from the melting of depleted mantle, metasomatized by earlier subduction processes (Cvetković et al., 2004; Marchev et al., 2005, 2013; Prelević et al., 2005; Schefer et al., 2011; Bonev et al., 2013; Lehmann et al., 2013). It is further suggested that the late Eocene-Oligocene (~35–25 Ma) magmatism in the Rhodope Massif was caused by convective removal of the lithospheric mantle (lithospheric delamination) and subsequent upwelling of the asthenosphere (Christofides et al., 2004; Marchev et al., 2005; Pe-Piper and Piper, 2006).

Early Miocene magmatism in the northeastern Aegean islands of Limnos and Lesvos (Figs. 1 and 3) and in western Turkey occurred mostly to the south of the Oligocene igneous activity of the Rhodope block and was coeval with the second phase of core complex-related extension in the Rhodope Massif and with the entrance of the Mediterranean Ocean into the Hellenic subduction zone (Dinter and Royden, 1993; Pe-Piper and Piper, 2002; Pe-Piper et al., 2009). The early Miocene igneous rocks form a belt of shoshonitic and calc-alkaline plutonic, subvolcanic and volcanic rocks on the Greek islands of Lesvos, Limnos, and Samothraki (Fig. 1), and in western Turkey (Pe-Piper and Piper, 2002; Pe-Piper et al., 2009; Ersoy and Palmer, 2013).

Early Miocene (22–17 Ma) calc-alkaline to shoshonitic magmatism was also present in the Rhodope Massif (e.g., Skouries monzonite porphyry; Kroll et al., 2002; and Kavala and Pangeon granitoids; Dinter et al., 1995), with the latter being emplaced contemporaneously to movement along the Strymon detachment (Dinter and Royden, 1993; Brun and Sokoutis, 2007).

During the Miocene (from ~17 to ~7 Ma) several intrusions, partly associated with coeval volcanic rocks, were emplaced during the exhumation of metamorphic core complexes in the footwall of major detachments in the Menderes Massif and Cyclades (Altherr and Siebel, 2002; Pe-Piper and Piper, 2006; Iglseder et al., 2009; Denèle et al., 2011; Menant et al., 2016). Magmatic rocks are of high-K calc-alkaline to shoshonitic affinity, and granitoids are of both I- and S-type (Altherr and Siebel, 2002; Ersoy and Palmer, 2013). For these magmas, a subduction-modified metasomatized mantle source with the contribution of crustal sources has been proposed (Altherr and Siebel, 2002; Stouraiti et al., 2010; Ersoy and Palmer, 2013). Typical arc-related volcanism with medium-K calc-alkaline composition has been erupted since the Pliocene along the active South Aegean Volcanic Arc (Fytikas et al., 1984).

3. Types and styles of magmatic-hydrothermal ore deposits

The Oligocene-Miocene and Pliocene-Pleistocene magmatic belts in the Rhodopes and the Cyclades are considered among the most endowed areas within the Alpine-Balkan-Pontide-Anatolide segment of the Western Tethyan belt, which extends from Serbia to Turkey, Armenia, and Iran (Janković, 1997; Arikas and Voudouris, 1998; Heinrich and Neubauer, 2002; Marchev et al., 2005; Voudouris and Alfieris, 2005; Voudouris, 2006; Arvanitidis, 2010; Melfos and Voudouris, 2012, 2016; Yigit, 2012; Siron et al., 2016; Voudouris et al., 2016a,b). These belts are rich in precious, rare, and critical metal deposits including Cu-Au, Cu-Mo-Au-Re, and Mo porphyries, Cu-Au-Te high- sulfidation (HS), Pb-Zn-Ag-Au intermediate- sulfidation IS), and Au-Ag low-sulfidation (LS) epithermal deposits, as well as Fe-Cu-W-Au skarns, Pb-Zn-Ag-Au carbonate-replacement deposits, and reduced intrusion-related gold systems with proximal to distal mineralization (e.g., intrusion-hosted Au-Ag±Bi±Te±W sheeted-veins, structurally controlled Au-As rich lodes, and distal-disseminated Carlin-style Au mineralization). The location of Cenozoic deposits in Greece, as well as their characteristics, is presented in Figs. 2–4 and in Tables 1–4. All these deposits are related to post-collisional magmatic rocks, which are in part controlled by detachment faults and exhumation of metamorphic core complexes in a back-arc setting. Arc-magmatism along the active South Aegean Volcanic Arc is related to shallow-submarine epithermal deposits at Milos (Alfieris et al., 2013) and to active VMS-epithermal ore deposition at Kolumbo volcano, near Santorini Island (Kilias et al., 2013b).

3.1. Porphyry deposits

In northern Greece, porphyry deposits are mainly concentrated at both in the eastern (e.g., Maronia, Pagoni Rachi, Konos, Kassiteres, Myli, Melitena; Fig. 3) and western parts of the Rhodope Massif (e.g. Skouries, Fisoka, Tsikara, Vathi and Gerakario; Fig. 3). The porphyry systems in the eastern part of the Rhodopes (e.g., the Northern Rhodope Domain) are associated with felsic to intermediate subvolcanic rocks of calc-alkaline to high-K calc-alkaline affinity with subalkaline to alkaline character, and of Oligocene age (Ortelli et al., 2009, 2010; Moritz et al., 2010; M. Ortelli, pers. commun., 2010). Most of these porphyry systems show epithermal overprinting evidenced by Au-Ag-rich polymetallic veins. The porphyry systems in the Northern Rhodope Domain are not well explored and generally contain low Cu with variable Au, Mo and Re concentrations (Voudouris et al., 2013c).

3.1.1. Porphyry deposits in the eastern Rhodope Massif

The Maronia porphyry Cu-Mo-Re-Au mineralization, exposed at Ktismata Hill, is related to a microgranite porphyry emplaced within the Maronia pluton, which consists mainly of monzonite with an age of 29.8 ± 1.3 to 28.4 ± 0.9 Ma (Rb-Sr on whole rock and biotite, and fission-track dating of apatite; Kyriakopoulos 1987; Del Moro et al., 1988; Biggazzi et al., 1989). Sodic-potassic, propylitic, sericitic, and argillic alteration styles predominate, and mineralization is mainly associated with three highly silicified zones within the sericitic zone (Melfos et al., 2002). Molybdenite contains very high Re concentrations of up to 2.88 wt.%. Surface samples show concentrations of up to 7600 ppm Mo, 5460 ppm Cu, and 1 ppm Au. Drilling yielded a 10 m intercept grading 12 ppm Au, 17 ppm Ag, and 2 wt.% Cu, which is probably related to a high-sulfidation epithermal overprint suggested by the presence of famatinite, tennantite and pyrophyllite, as well by the locally unexpected high Au concentration (Melfos et al., 2002).

The Pagoni Rachi Cu-Mo-Re-Au deposit in the Kirki ore district is associated with a granodiorite-tonalite porphyry and is characterized as a telescoped porphyry-epithermal system (Voudouris et al., 2013b). Mineralization occurs in four paragenetic stages: (a) sodic/potassic-calcic alteration with gold-rich magnetite-bornite-chalcopyrite quartz veins (A- and M-type) and distal propylitic alteration; (b) sodic/potassic alteration with pyrite-chalcopyrite-molybdenite-quartz veins (B-type); (c) sericitic alteration with "transitional" porphyry to epithermal pyrite-chalcopyrite-molybdenite veins (D-type) that include native gold and Ag-, Bi-, Te-, and Se-bearing minerals; and (d) argillic alteration with quartz-calcite base and precious metal epithermal veins (E-type) rich in Au, Ag and Te, with a possible genetic relationship with D-type veins (Voudouris et al., 2013b). Bulk chemical analyses of the ore, based on surface samples, revealed up to 5.1 ppm Au, up to 0.5 wt.% Cu, up to 40 ppm Te, up to 2000 ppm Mo, and up to 20 ppm Re reflecting the extremely high Re content in molybdenite (up to 4.69 wt.%) and the presence of rheniite (Voudouris et al., 2009).

The Konos Hill porphyry Cu-Mo-Re deposit at Sapes is hosted in an Oligocene granodiorite porphyry stock. The main alteration style is sericitic, and mineralization consists mainly of pyrite, molybdenite, rheniite, chalcopyrite, enargite and bornite both in quartz stockworks and disseminated in the rock matrix. Epithermal-style quartz veins with pyrite-tetrahedrite-tennantite-enargite crosscut earlier porphyry veins (Voudouris et al., 2006; Ortelli et al., 2009).

The Kassiteres porphyry Cu deposit occurs within a microdiorite porphyry exposed around Koryfes Hill (Voudouris et al., 2006). The system is characterized by sodic/potassic alteration, which progressively changes into a pervasive propylitic alteration halo. The sodic/potassic alteration is partly overprinted by sericitic alteration, which is structurally controlled. Hydrothermal biotite was dated at 32.0 ± 0.5 Ma by $^{40}Ar/^{39}Ar$ (Ortelli et al., 2010).

The Myli Cu-Mo-Au deposit in the Esymi area is a telescoped porphyry-epithermal system related to a granodiorite porphyry, characterized by sericite alteration. The mineralization occurs mainly as chalcopyrite, molybdenite, and native gold in disseminations and within A- and B-quartz veins (Fig. 5a), and pyrite D-veins (Voudouris et al., 2013c). A late epithermal overprint is evidenced by quartz-carbonate-barite-bearing polymetallic veins rimmed by sericite and carbonate alteration of the host granodiorite. The veins contain pyrite, sphalerite, galena and tennantite.

The Melitena porphyry Mo deposit is hosted by a silicified and sericitized granodiorite porphyry which intrudes metamorphic rocks of the Rhodope Massif (Voudouris and Melfos, 2012; Voudouris et al., 2013c). Pyrite and molybdenite, with minor galena, chalcopyrite, and pyrrhotite occur in quartz veins and disseminations in the wall rocks. Rhenium contents in molybdenite reach up to 1.74 wt.%. Bulk ore chemical analyses of porphyry-mineralized samples revealed 400 ppm Cu, 6000 ppm Mo and up to 0.3 ppm Au. High-sulfidation epithermal style alteration is superimposed upon the porphyry quartz stockwors and is characterized by the development of advanced argillic- and silicic alteration and pyrite mineralization.

3.1.2. Porphyry deposits in the western Rhodope Massif

In the western part of the Rhodope Massif, major porphyry deposits are clustered within the Kerdylion Unit of the South Rhodope Core Complex (Siron et al., 2016), as well as within the Serbo-Macedonian Vertiskos Unit (Kockel et al., 1975) (Figs. 2 and 3).

Skouries is a Cu-Au porphyry deposit in the Kassandra mining district, NE Chalkidiki, with proven and probable reserves of 152.7 Mt grading 0.8 g/t Au, and 0.5% Cu, for 3.8 Moz Au and 776 Mt Cu (Eldorado Gold Corp., 2017). Economou-Eliopoulos and Eliopoulos (2000) and Eliopoulos et al. (2014) also reported up to 41 ppb Ru, up to 150 ppb Pt, and up to 610 ppb Pd in drill-hole samples. The mineralization is associated with a Miocene monzonite porphyry (Kroll et al., 2002; Siron et al., 2016) and occurs in the form of stockwork veins and disseminations (Frei, 1995). The main ore minerals are pyrite, chalcopyrite, bornite, magnetite, minor galena and tetrahedrite, and traces of molybdenite (Fig. 5b). Gold grains occur commonly as inclusions within chalcopyrite. Rare Pd-Pt-Au-Ag tellurides also occur (McFall et al.,

Table 1
Characteristics and reserves or resources data of most significant Tertiary porphyry type mineralizations in Greece. HR: Host Rock; ALT: Alteration; MIN: Mineralization.

Deposit name	Ore district	Geotectonic belt or unit	Commodities	Deposit style	Morphology of ore bodies	Main host rocks	Age: HR, ALT, MIN	Tonnage and grades	References
Eastern Rhodope Massif									
Maronia		Circum-Rhodope belt	Cu Fe Mo Au Pb Zn Sb As	High-K calc-alk Cu-Mo	Stockwork, disseminated, veins	Microgranite porphyry	Oligocene		Melfos et al., 2002
Pagoni Rachi	Kirki-Sapes-Kassiteres-Esimi	Circum-Rhodope belt	Cu Mo Fe Re	High-K calc-alk Cu-Mo	Stockwork, disseminated, veins	Granodiorite-tonalite porphyry	Oligocene		Voudouris et al., 2013b
Konos	Kirki-Sapes-Kassiteres-Esimi	Circum-Rhodope belt	Cu Mo Fe Re	High-K calc-alk Cu-Mo	Stockwork, disseminated	Granodiorite porphyry	Oligocene (ALT: 33.1–31.2 Ma)		Voudouris et al., 2006; Ortelli et al., 2010
Kassiteres (Koryfes)	Kirki-Sapes-Kassiteres-Esimi	Circum-Rhodope belt	Cu Au Mo Pb Zn Ag Bi Te	High-K calc-alk Cu	Disseminated, vein, stockwork	microdiorite porphyry	Oligocene (ALT: 32.0 ± 0.5 Ma)		Voudouris et al., 2006; Ortelli et al., 2010
Myli	Kirki-Sapes-Kassiteres-Esimi	Circum-Rhodope belt	Cu Mo Au Re Pb Zn Ag As	High-K calc-alk Cu-Mo	Stockwork, disseminated, vein	Granodiorite porphyry	Oligocene		Voudouris et al., 2013c
Melitena	Kalotycho-Melitena	Rhodope massif	Mo Cu Fe Re Pb	High-K calc-alk Mo	Vein, stockwork, disseminated	granodiorite porphyry	Oligocene		Voudouris and Melfos, 2012; Voudouris et al., 2013c
Western Rhodope Massif									
Skouries	Kassandra mining district	Kerdylion Unit	Cu Au Pd Ru Te Mo	Sub-alk Cu-Au	Breccia, disseminated, veins, stockwork	Monzonite porphyry	Miocene (HR: 20.56 ± 0.48 to 19.59 ± 0.17 Ma; ALT: 19.9 ± 0.9 Ma)	Reserves: 152,736 Mt at 0.8 g/t Au, and 0.5 % Cu, for 3.8 Moz Au and 776 Mt Cu	Frei, 1995; Hahn et al., 2012; Siron et al., 2016; Eldorado Gold Corp., 2017
Fisoka	Kassandra mining district	Kerdylion Unit	Cu Au Pb Zn	High-K calc-alk Cu-Au	Breccia, disseminated, veins, stockwork	Diorite and granodiorite porphyries	Oligocene (HR: 24.47 ± 0.14 Ma; ALT: 24.5 ± 1.2 to 23.0 ± 1.2 Ma)		Gilg and Frei, 1994; Tompouloglou 1981; Siron et al., 2016
Alatina	Kassandra mining district	Kerdylion Unit	Cu Au	High-K calc-alk Cu	Breccia, disseminated, veins, stockwork	Diorite and granodiorite porphyries	Oligocene		Gilg and Frei, 1994
Tsikara	Kassandra mining district	Kerdylion Unit	Cu Au Pb Zn	High-K calc-alk Cu-Au	Breccia, disseminated, veins, stockwork	Granodiorite and monzodiorite porphyries	Oligocene (HR: 27.00 ± 0.19 to 26.65 ± 0.31 Ma; ALT: 21.2 ± 1.03 Ma)		Tompouloglou, 1981; Gilg and Frei, 1994; Siron et al. 2016
Dilofon	Kassandra mining district	Kerdylion Unit	Cu Au Pb Zn	High-K calc-alk Cu	Breccia, disseminated, veins, stockwork	Diorite and granodiorite porphyries	Oligocene-Miocene?		Gilg, 1993
Vathi	Kilkis	Vertiskos Unit	Cu Au Ag Fe Mo U	Sub-alk Cu-Au	Stockwork, veinlets, veins, disseminated	Qtz-monzonite porphyry, trachydacite	Miocene (HR: 18 ± 0.5 to 17 ± 1 Ma)	Resources: 15 Mt at 0.8 g/t Au, and 0.3 % Cu	Veranis and Tsamantouridis, 1991; Stergiou et al., 2016
Gerakario	Kilkis	Vertiskos Unit	Cu Au	Sub-alk Cu-Au	Vein, disseminated	Syenite and granodiorite porphyries	Miocene (HR: 34 ± 0.5 and 22 ± 0.8 Ma)	Probable reserves: 28 Mt at 0.9 g/t Au and 0.4% Cu	Frei, 1992; Tsirambides and Filippidis, 2012
Northeastern Aegean region									
Fakos Limnos		Rhodope massif	Cu Mo Au Ag Bi Te	Sub-alk Cu-Mo porphyry	Stockwork, breccia, disseminated, vein	Quartz monzonite porphyry	Miocene (HR: 21.3 ± 0.7 to 20.2 ± 0.2 Ma)		Voudouris and Alfieris, 2005; Fornadel et al., 2012
Sardes Limnos		Rhodope massif	Cu Mo Au As Zn Pb	Sub-alk Cu-Mo	Veinlets, stockworks, disseminated	Quartz monzonite porphyry, sandstones, marls	Miocene (HR: 21.3 ± 0.7 to 20.2 ± 0.2 Ma)		Voudouris and Alfieris, 2005
Stipsi Lesvos		Rhodope massif	Cu Mo Re Bi Pb Se Ag Au	Sub-alk Mo	Veinlets, stockwork, disseminated	Dacite porphyry	Miocene (HR: 18.4 ± 0.5 Ma)		Voudouris and Alfieris, 2005
Cyclades									
Plaka Lavrion		Attic-Cycladic crystalline Belt	Cu Mo W	Sub-alk Cu-Mo porphyry	Sheeted quartz veins, stockwork	Granodiorite porphyry	Miocene (HR: 9.4 to 7.1 ± 0.6 Ma)		Altherr and Siebel, 2002; Voudouris et al., 2008a

Table 2
Characteristics and reserves or resources data of most significant Tertiary epithermal type mineralizations in Greece. HR: Host Rock; ALT: Alteration; MIN: Mineralization.

Deposit name	Ore district	Geotectonic belt or unit	Commodities	Deposit style	Morphology of ore bodies	Main host rocks	Age: HR, ALT, MIN	Tonnage and grades	References
Eastern Rhodope Massif									
Perama Hill	Petrota Graben	Circum-Rhodope Belt	Au Ag Cu Bi Pb Te Se	High and intermediate sulfidation	upper parts: oxidized; deeper parts: disseminated, vein, massive sulfide lodes	Andesite, conglomerate, sandstone	Oligocene	Reserves: 9.697 Mt at 3.13 g/t Au and 4 g/t Ag, with a total of 0.975 Moz Au and 1.151 Moz Ag	Voudouris et al., 2011a; Eldorado Gold Corp., 2017
Mavrokoryfi	Petrota Graben	Circum-Rhodope Belt	Ag Au Cu Te	High sulfidation	Vein, massive sulfide lodes, breccia	Andesite, hyaloclastite	Oligocene		Voudouris, 2011
Viper	Kirki-Sapes-Kassiteres	Circum-Rhodope Belt	Cu Au As Sb Ag Pb Zn Bi Te Se	High and intermediate sulfidation	Breccia, disseminated, veinlets, vugs fillings	Granodiorite-tonalite porphyry, tuff, rhyodacite	Oligocene	Resources: 0.28 Mt at 19.5 g/t Au, 9 g/t Ag, and 0.4% Cu	Voudouris et al., 2006; Glory Resources, 2012
Scarp	Kirki-Sapes-Kassiteres	Circum-Rhodope Belt	Cu Au	High sulfidation	Breccia, disseminated	Granodiorite-tonalite porphyry, tuff, rhyodacite	Oligocene	Resources: 0.87 Mt at 2.2 g/t Au, and 1.5 g/t Ag	Ortelli et al., 2010; Glory Resources, 2012
St. Demetrios	Kirki-Sapes-Kassiteres	Circum-Rhodope Belt	Cu Au As Sb Ag Pb Zn Bi Te Se	High and intermediate sulfidation	Breccia, disseminated, veinlets, vugs fillings	Granodiorite-tonalite porphyry, tuff, rhyodacite	Oligocene (ALT: 31.9 ± 0.6 Ma)	Reserves: 0.21 Mt at 3.5 g/t Au, and 5.2 g/t Ag	Voudouris et al., 2006; Ortelli et al., 2010; Glory Resources, 2012; Voudouris, 2014
St. Barbara	Kirki-Sapes-Kassiteres	Circum-Rhodope Belt	Cu Au As Sb Ag Pb Zn Bi Te Se	High and intermediate sulfidation	Veins, breccia	Andesite, tuff, monzodiorite	Oligocene (ALT: 31.2 ± 0.4 Ma)		Voudouris et al., 2006
St. Philippos	Kirki-Sapes-Kassiteres	Circum-Rhodope Belt	Pb Zn Ag As Cu Bi Sn Cd In Ga Ge Au	Intermediate and high sulfidation	Vein, breccia, disseminated	Sandstone, conglomerate, marl, tuff, microgranite porphyry	Oligocene	Past mining produced 0.2 Mt at 7.5 % Pb + Zn	Voudouris et al., 2013b
Pefka	Evros	Circum-Rhodope Belt	Cu Au Ag Pb Zn Bi Sn Ge Ga In Mo V As Hg Te Se	High and intermediate sulfidation	Veins	Tuffs, andesite, rhyodacite, latite	Oligocene (HR: 30.7 Ma)		Voudouris, 2006; Repstock et al., 2015
Loutros	Evros	Circum-Rhodope Belt	Fe Pb As Ag	Intermediate sulfidation	Veins	Rhyolite	Miocene (HR: 19.53 ± 0.75 Ma)		Melfos and Voudouris, 2016
Kalotycho	Kalotycho-Melitena	Rhodope massif	Fe	High sulfidation	Veins	Tuffs, andesite, trachyte, dacite, rhyolite	Oligocene (HR: 33 ± 1.2 to 24.6 ± 0.6 Ma)		Innocenti et al., 1984; Voudouris and Melfos, 2012
Northeastern Aegean region									
Fakos (Limnos)		Rhodope massif-Pontide Unit	Cu Mo Au Ag Bi Te As Sb Zn Pb	High and intermediate sulfidation	Stockwork, breccia, disseminated, vein	Quartz monzonite porphyry	Miocene (HR: 21.3 ± 0.7 to 20.2 ± 0.2 Ma)		Voudouris and Alfieris, 2005; Fornadel et al., 2012
Megala Therma (Lesvos)		Rhodope-Pontide Unit	Au Ag Pb Zn Fe Cu Mo	Intermediate sulfidation	Veinlets, veins, breccia	Andesite, latite	Miocene (HR: 21.5 ± 1.5 Ma)		Pe-Piper and Piper, 1993; Voudouris and Alfieris, 2005
Cyclades									
Profitis Ilias (Milos)	Attic-Cycladic ore belt	Attic-Cycladic crystalline Belt	Pb Zn Ag Au Cu Sb Te	Intermediate sulfidation	Massive to semi-massive ore, veins	Rhyolite, pyroclastic rocks	Pliocene to Pleistocene (HR: 2.7 Ma)	Reserves: 5 Mt at 4.4 g/t Au	Kilias et al., 2001; Naden et al., 2005; Alfieris et al., 2013
Chondro Vouno (Milos)	Attic-Cycladic ore belt	Attic-Cycladic crystalline Belt	Pb Zn Ag Au Cu Sb Te	Intermediate sulfidation	Veins	Pyroclastic rocks	Pliocene to Pleistocene (HR: 2.7 Ma)	Reserves: 3.3 Mt at 4.2 g/t Au	Kilias et al., 2001; Naden et al., 2005; Alfieris et al., 2013
Triades-Galana (Milos)	Attic-Cycladic ore belt	Attic-Cycladic crystalline Belt	Ag Au As Bi W Mo	Intermediate sulfidation	Veins	Dacites, andesites, pyroclastic and volcanosedimentary rocks	Pliocene to Pleistocene (HR: 2.5 to 1.4 Ma)	Resources: 1.2 Mt at 1 g/t Au and 124 g/t Ag	Stewart and McPhie, 2006; Alfieris et al., 2013
Kondaros-Katsimouti-Vani (Milos)	Attic-Cycladic ore belt	Attic-Cycladic crystalline Belt	Ag Au As Bi W Mo	Intermediate sulfidation	Massive to semi-massive ore, veins, stratabound and stratiform layers	Dacite, andesite, pyroclastic and volcanosedimentary rocks	Pliocene to Pleistocene (HR: 2.5 to 1.4 Ma)		Alfieris et al., 2013; Papavassiliou et al. 2017

Table 3

Characteristics and reserves or resources data of most significant Tertiary carbonate replacement and skarn type mineralizations in Greece. HR: Host Rock; ALT: Alteration; MIN: Mineralization; apy: arsenopyrite.

Deposit name	Ore district	Geotectonic belt or unit	Commodities	Deposit style	Morphology of ore bodies	Main host rocks	Age: HR, ALT, MIN	Tonnage and grades	References
Rhodope Massif									
Olympias	Kassandra mining district	Rhodope massif	Au Ag Pb Zn Cu Sb	Carbonate replacement, vein	Mantos, veins, disseminated	Marble	Oligocene (MIN, apy: 26.1 ± 5.3 Ma)	Reserves: 16.1 Mt at 7.9 g/t Au, 128 g/t Ag, 4.3% Pb and 5.7% Zn	Kalogeropoulos et al., 1989; Gilg, 1993; Forward et al., 2011; Hahn et al., 2012; Eldorado Gold, 2017
Madem Lakkos	Kassandra mining district	Rhodope massif	Au Ag Pb Zn Cu	Carbonate replacement, vein	Mantos, veins, disseminated	Marble, pegmatite, amphibolite, gneiss	Oligocene	Past mining produced 13.5 Mt of Ag-Pb-Zn ore	Gilg, 1993; Eldorado Gold, 2017
Mavres Petres	Kassandra mining district	Rhodope massif	Au Ag Pb Zn Cu	Carbonate replacement, vein	Mantos, veins, disseminated	Marble, amphibolite, gneiss	Oligocene	Reserves: 1.87 Mt at 160 g/t Ag, 6% Pb and 8.8% Zn	Gilg, 1993; Forward et al, 2010; Eldorado Gold Corp., 2017
Piavitsa	Kassandra mining district	Rhodope massif	Pb Zn Mn As Au	Carbonate replacement, vein	Mantos, breccia, disseminated, banded epithermal veins	Marble, amphibolite, gneiss	Miocene	Resources: 10.54 Mt at 5.7 g/t Au	Siron et al., 2016; Eldorado Gold Corp., 2017
Thermes		Rhodope massif	Pb Zn Fe Cu Mn As Sb Cd Te Ag Au	Carbonate replacement, vein	Veins, manto	Marble, amphibolite, orthogneiss	Oligocene		Kalogeropoulos et al., 1996
Kimmeria		Rhodope massif	Fe Cu Zn W Bi Au	Skarn	Massive, disseminated	Marble, gneiss,, amphibolite	Oligocene (HR: 28.8 ± 0.7 to 26.3 ± 0.1 Ma)	Resources: 2 Mt at 20 g/t Ag and 1.98 % Cu	Liati, 1986; Kyriakopoulos, 1987
Thasos, E- and S-part	Thasos	Rhodope massif	Pb Zn Fe Cu As Cd Ag	Carbonate replacement, vein	Mantos, veins	Marble, schist, amphibolite, gneiss	Miocene?		Vavelidis and Amstutz, 1983
Thasos, W- and N-part	Thasos	Rhodope massif	Cu Fe Mn As Ni Bi Te Ag Au	Carbonate replacement, vein	Mantos, veins, breccia	Marble, schist, amphibolite, gneiss	Miocene?	Past mining produced: 2 Mt with 12% Zn + Pb, and 3 Mt with 44% Fe	Vavelidis and Amstutz, 1983
Attic-Cycladic Belt									
Lavrion (Kamariza-Sounio-Plaka)	Lavrion	Attic-Cycladic crystalline belt	Pb Zn Ag Fe Cu As Sb Bi Te Ni Cd Ge In Sn Au	Carbonate replacement, vein	Massive, disseminated, layers, veins	Marble, schist	Miocene (HR: 9.4 ± 0.3 to 7.3)	Past mining produced: Antiquity 6th-1st c. BC: 13 Mt at 400 g/t Ag and 20% Pb - 1864–1978: 1.5 Mt ancient slags at 50 g/t Ag and 10% Pb and 30 Mt ore at 140 g/t Ag and 3% Pb; Resources: 4 Mt with 7% Pb + Zn	Marinos and Petrachek 1956; Conophagos, 1980; Voudouris et al., 2008b; Bonsall et al., 2011
Serifos	Attic-Cycladic ore belt	Attic-Cycladic crystalline belt	Fe Cu As Pb Zn	Skarn	Massive ore, veins	Marble, schist, gneiss	Miocene (HR: 11.6 ± 0.1 to 9.5 ± 0.1)	Past mining produced: 6.6 Mt for Fe	Salemink, 1985; Ducoux et al. 2017
Sifnos	Attic-Cycladic ore belt	Attic-Cycladic crystalline belt	Fe Cu Au Pb Zn Mn Ag	Shear zone and detachment fault related	Veins, massive, lenses	Gneiss, schist, marble	Miocene		Vavelidis, 1997; Neubauer, 2005
Syros	Attic-Cycladic ore belt	Attic-Cycladic crystalline belt	Pb Zn Fe Cu Mn As Sb Bi Te Cd Ag Au	Carbonate replacement, vein	Dissemination, massive bodies, veins	Marble, schist, gneiss	Miocene	Past mining produced 21–26 Kt of Fe-Pb-Zn ore; Resources: 0.1 Mt of Fe-Pb-Zn	Melidonis and Constantinides, 1983; Voudouris et al., 2014

Table 4
Characteristics of most significant Tertiary intrusion related Au & Mo-Cu-W mineralizations in Greece. HR: Host Rock; ALT: Alteration; MIN: Mineralization; py: pyrite.

Deposit name	Ore district	Geotectonic belt or unit	Commodities	Deposit style	Morphology of ore bodies	Main host rocks	Age: HR, ALT, MIN	Tonnage and grades	References
Reduced intrusion-related gold systems in the Rhodope Massif									
Palea Kavala	Palea Kavala	Rhodope Massif	Fe Cu Pb Zn Mn Cd As Sb Bi Te Ag Au	Intrusion hosted veins, carbonate replacement, vein	Veins, disseminated, massive fissures (pods), mantos, breccia	Granodiorite, marble, schist	Miocene (HR-granodiorite: 21.1 ± 0.8 to 19.7 ± 0.3 Ma)	Resources: 1,5 Mt containing up to 34.5 g/t Au, up to 180 g/t Ag, up to 13% Pb + Zn, up to 40% Fe and up to 42% Mn	Fornadel et al., 2011
Pangeon	Pangeon	Rhodope Massif	Fe Pb Zn Cu Mn As Sb Cd Bi W Te Ag Au	Intrusion hosted veins, carbonate replacement, vein	Mantos, veins	Granodiorite, marble, schist	Miocene (HR-granodiorite: 21.7 ± 0.5 to 18.8 ± 0.6 Ma)		Eliopoulos and Kilias, 2011; Vaxevanopoulos, 2017
Intrusion-related Mo-Cu-W deposits									
Kimmeria		Rhodope Massif	Cu Mo W Bi	Vein	Veins	Granodiorite	Oligocene (HR-granodiorite: 28.8 ± 0.7 to 26.3 ± 0.1 Ma)		Walenta and Pantzartzis, 1969; Voudouris et al., 2010; Theodoridou et al., 2016
Other intrusion-related (?) polymetallic veins									
Rhodope Massif									
Kallintiri		Circum-Rhodope Belt	Sb Pb Zn Ag Au Te Hg Tl	Detachment fault related	Veins	Marble, schist, sediments	Oligocene?		Kanellopoulos et al., 2014
Thasos	Thasos	Rhodope Massif	Cu Ag Fe As Bi Te Ni Au	Carbonate replacement, vein	Veins	Schist	Miocene?		Vavelidis et al., 1995; Vavelidis and Melfos, 2004
Stanos		Thermes-Volvi-Gomati complex	Cu Au Ag Bi Te	Shear-zone hosted	Massive, veins, disseminated	Orthogneiss, amphibolite, metagabbro, schist	Miocene (MIN-py: 19.2 ± 2.1 Ma)		Voudouris et al., 2013a; Bristol et al., 2015
Nea Madytos		Thermes-Volvi-Gomati complex	Cu Au Ag Pb Te Bi	Shear-zone hosted	Massive, veins, disseminated	Gneiss, amphibolite	Oligocene-Miocene?		Vavelidis and Tarkian, 1995
Drakontio	Kilkis	Vertiskos Unit	Cu Pb Zn Ag Au	Shear-zone hosted	Massive, veins, disseminated	Gneiss, schist, amphibolite	Oligocene-Miocene?		Vavelidis et al., 1999
Koronouda	Kilkis	Vertiskos Unit	Cu Au Ag Zn Pb Fe As Ni Co Sb Te Bi	Shear-zone hosted	Massive, veins, disseminated	Gneiss, pegmatoids	Oligocene-Miocene?		Vavelidis et al., 1996
Stefania	Klikis	Vertiskos Unit	Cu Ag Au Bi Te Co Ni As	Shear-zone hosted	Massive, veins, disseminated	Gneiss, schist	Oligocene-Miocene?		Melfos et al., 2001
Laodikino	Kilkis	Vertiskos Unit	Cu Au Fe As Zn Pb Te Co Ni Sb Bi	Shear-zone hosted	Massive, veins, disseminated	Gneiss, schist	Oligocene-Miocene?		Thymiatis, 1995
Attic-Cycladic Belt									
Kallianou	Attic-Cycladic ore belt	Attic-Cycladic crystalline belt	Fe As Pb Cu Zn Sb Te Cd Ag Au	Detachment fault related	Veins, dissemination	Schist, marble	Miocene		Voudouris et al., 2011b
Tinos	Attic-Cycladic ore belt	Attic-Cycladic crystalline belt	Fe Zn As Cu Au Ag Pb Sb Ni Co Cd Sn Te W	Epithermal veins	Veins	Marble, schist	Miocene (HR: ~18–15 Ma)		Tombros et al., 2007
Sifnos	Attic-Cycladic ore belt	Attic-Cycladic crystalline belt	Fe Cu Au Pb Zn Mn Ag	Shear zone and detachment fault related	Veins, massive, lenses	Gneiss, schist, marble	Miocene		Vavelidis 1997; Neubauer 2005
Antiparos	Attic-Cycladic ore belt	Attic-Cycladic crystalline belt	Ag	Vein	Veins	Marble, schist	Miocene		Kevrekidis et al., 2015

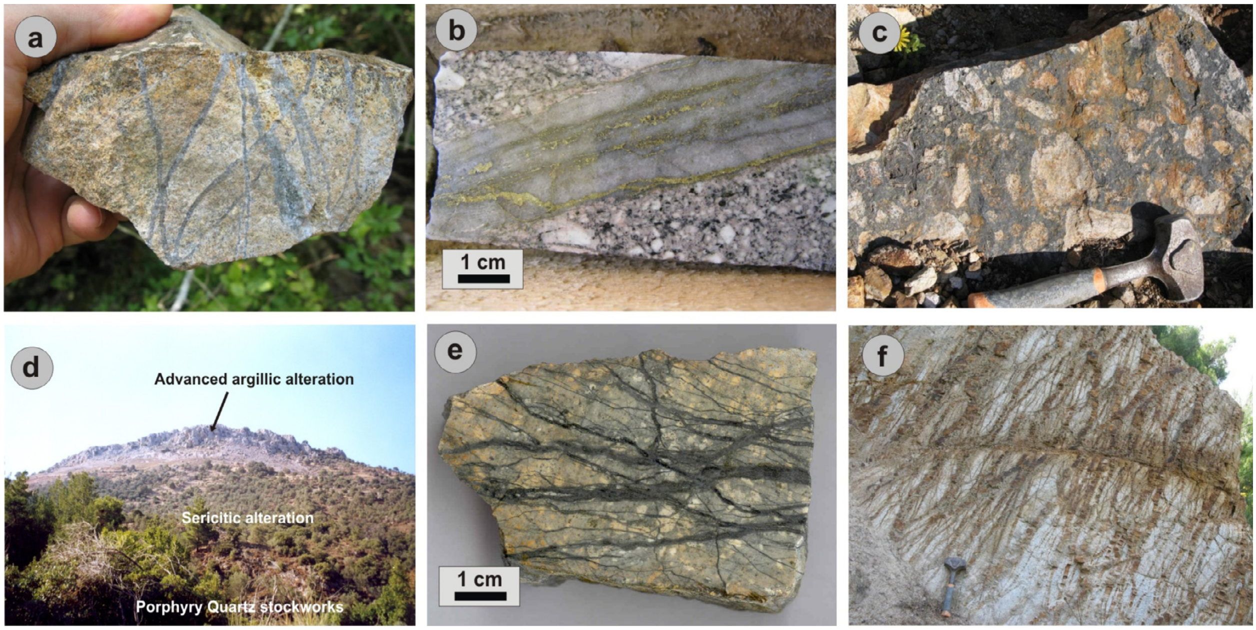

Fig. 5. Field photographs and hand specimens demonstrating various features of porphyry-style mineralization in Greece: (a) hand specimen of sericite-carbonate altered granodiorite porphyry from Myli that contains sinuous to planar porphyry-style quartz veinlets; (b) hand specimen of Skouries drill core showing planar quartz vein (B-type?) with chalcopyrite cutting potassic-altered monzonite porphyry; (c) hydrothermal breccia composed of sericitized fragments of monzonite porphyry cemented by tourmaline (Fakos deposit, Limnos Island); (d) view of alteration zoning at Stipsi porphyry deposit: porphyry-style stockworks hosted in granodiorite porphyry at lower levels grade upwards into sericite-altered and then advanced argillic-altered volcanic rocks; (e) hand specimen of sericite-carbonate-altered granodiorite porphyry from Stipsi that contains sinuous porphyry-style quartz veinlets; (f) sugary quartz stockworks and sheeted veins with oxidized Mo-W mineralization cutting potassic-altered granodiorite at Lavrion.

2016). A 40 m-thick oxidation zone with malachite, azurite and limonite is underlain by a 2–3 m-thick enrichment zone, where covellite, chalcocite, chalcopyrite, pyrite and magnetite coexist with malachite and azurite. At least three phases of monzonite porphyry are recognized, which are related to intense potassic and propylitic alteration.

Other porphyry deposits in the Kassandra mining district occur at Fisoka, Alatina, Tsikara, Aspra Chomata, and Dilofo where extensive alteration zones are associated with porphyritic intrusions of granodioritic, syenitic, monzodioritic, and dioritic compositions. Whole-rock K-Ar ages have been obtained at the Tsikara and Fisoka porphyry systems by Tompouloglou (1981). In Tsikara, the monzodiorite porphyry was dated at 21.2 ± 1.03 Ma and in Fisoka the diorite porphyry has an age of 24.55 ± 1.22 Ma; a K-Ar date for sericite gave an age of 23.01 ± 1.15 Ma. However, recent zircon U-Pb geochronology indicates late Oligocene ages (27–25 Ma) for both the Tsikara and Fisoka intrusive rocks (Siron et al., 2016). Hydrothermal alteration is dominated by sericitic alteration, which is locally superimposed on propylitic and a potassic alteration.

In the Kilkis district, the most important porphyry deposit is located at Vathi, which is estimated to contain 15 Mt ore with grades of 0.30% Cu and 0.8 g/t Au (Veranis and Tsamantouridis, 1991; Stergiou et al., 2016). The mineralization is associated with quartz monzonite porphyry dikes with ages of 18 ± 0.5 to 17 ± 1 Ma (U-Pb zircon; Frei, 1992), which intrude basement gneiss and a trachydacite porphyry. The trachydacite porphyry is characterized by weak potassic and strong propylitic alteration, overprinted by sericitic alteration and silicification. The quartz monzonite is affected by a strong potassic alteration and subsequent sericite alteration (Frei, 1992; Stergiou et al., 2016). The mineralization forms stockworks, sheeted veins, and quartz-pyrite D-veins, and a mineralized phreato-magmatic breccia intrudes the trachydacite porphyry with an ENE-WSW trend. Surface oxidized samples of the mineralized trachydacite porphyry contain in average 2607 ppm Cu, 335 ppm Mo, 0.73 ppm Au, up to 330 ppm U, up to 500 ppm La, and up to 715 ppm Ce (Stergiou et al., 2016).

The Gerakario porphyry-epithermal system is located very close to Vathi, with probable reserves of 28 Mt grading 0.4% Cu and 0.9 g/t Au (Tsirambides and Filippidis, 2012). Copper mineralization is associated with potassically altered syenite porphyry and a sericitically and propylitically altered granodiorite porphyry. U-Pb ages obtained on zircons from the syenite porphyry and granodiorite porphyry yielded ages of 22 ± 0.8 Ma and 34 ± 0.5 Ma, respectively (Frei, 1992). The mineralization occurs as pyrite-chalcopyrite disseminations and magnetite-pyrite-chalcopyrite veins. Stibnite bearing quartz veins in the adjacent gneiss are attributed to a subsequent epithermal stage.

3.1.3. Porphyry deposits in the northeastern Aegean region

In the northeastern Aegean region, the Limnos and Lesvos Islands host at least three Miocene porphyry-style deposits at Fakos, Sardes and Stipsi respectively (Figs. 2 and 3; Voudouris and Alfieris, 2005; Fornadel et al., 2012). The Fakos deposit is hosted by a ~20 Ma quartz monzonite porphyry stock (Fornadel et al., 2012). Early stage A- and B-type quartz veinlets are associated with potassic and propylitic alteration and contain pyrite, chalcopyrite, galena, bornite, sphalerite, molybdenite, magnetite, and hematite. A subsequent mineralization stage is related to quartz-tourmaline-sericite veins and breccias and is composed mostly of disseminated pyrite, arsenopyrite, and molybdenite (Fig. 5c). Porphyry-style mineralization was overprinted by high- to intermediate-sulfidation epithermal quartz veins, which are spatially associated with sericitic and argillic alteration. Bulk chemical analyses of surface samples from quartz stockworks yielded up to 780 ppm Cu and up to 83 ppm Mo.

The Sardes porphyry system in the northwestern part of Limnos Island comprises a stockwork quartz veinlets containing pyrite and molybdenite, hosted within a Miocene monzonite porphyry and quartz-sericite-tourmaline-altered sedimentary rocks (Voudouris and Alfieris, 2005).

The Stipsi porphyry Cu-Mo prospect in the north-central part of Lesvos Island is hosted by a high-K calc-alkaline granodiorite porphyry and the surrounding volcanic rocks. It is characterized by intense propylitic, sericite-carbonate, argillic, and at the upper levels, advanced argillic and silicic alteration (Fig. 5d; Voudouris and Alfieris, 2005). Maximum concentrations based on bulk chemical analyses from surface samples of the Stipsi prospect were 0.48 ppm Au, 1330 ppm Cu, 170 ppm Mo, and 1.7 ppm Ag. The porphyry-style mineralization consists of dense quartz stockworks containing molybdenite, bismuthinite, and galena (Fig. 5e), overprinted by intermediate-sulfidation epithermal quartz-carbonate veins (Voudouris and Alfieris, 2005).

3.1.4. Porphyry deposits in the Cyclades

In the Cyclades, porphyry Mo-W mineralization occurs as sheeted quartz veins and stockworks cutting a late Miocene granodiorite stock in the Plaka area of the Lavrion mining district (Figs. 2, 4 and 5f; Altherr and Siebel, 2002; Voudouris et al., 2008a). The sheeted veins strike generally NW-SE and their thickness reaches 40 cm. The mineralization consists of pyrite, molybdenite, chalcopyrite, pyrrhotite and minor scheelite. Quartz, hydrothermal biotite, K-feldspar and sericite are gangue minerals. The granodiorite was intensely altered to potassic, sodic, propylitic, and sericitic asemblages, locally with silicification. Chemical analyses of surface ore samples revealed up to 1200 ppm Mo, 760 ppm W, and 3 wt.% Fe. The granodiorite intruded the footwall of a detachment fault. Hydrothermally altered and locally mineralized variably deformed felsic dikes and sills crosscut both the granodiorite and the metamorphic footwall and hanging wall rocks, and occur along the detachment fault, indicating that the intrusion of the magma took place during the detachment movement. Geochronological dating of the granodiorite and porphyritic dikes and sills based on K-Ar ages on biotite, feldspar and whole rock, fission track age from apatite, and U-Pb and (U-Th)/He ages on zircon, provided an age of 9.4–7.1 Ma for the igneous activity in Lavrion (Altherr et al., 1982; Skarpelis et al., 2008). Zircon (U-Th)/He thermochronometry from footwall granitoids at Plaka area between 7.9 ± 0.6 and 7.1 ± 0.6 Ma indicate that mineralization and rapid cooling of the footwall through ~180 °C occurred at ca. 7.6 Ma (Berger et al., 2013).

3.2. Epithermal deposits

3.2.1. Epithermal deposits in the eastern Rhodope Massif

Several polymetallic epithermal deposits and prospects containing Au, Ag, Cu, Te, Se, Bi, In, and Ga occur in the Greek part of the eastern Rhodope Massif (Figs. 2 and 3). These deposits are mostly high-sulfidation Cu-Au-Ag systems (Perama Hill, Mavrokoryfi, Sapes-Kassiteres, Pefka, Kalotycho) which evolved to Pb-Zn-Ag-Au intermediate-sulfidation state in later stages (Voudouris, 2006; Moritz et al., 2010). They mostly occur at the periphery of or superimposed on porphyry-style mineralization, and demonstrate a genetic relationship to the porphyry systems. This contrasts to the Bulgarian part of the eastern Rhodope, where intermediate-sulfidation Pb-Zn epithermal deposits dominate (Marchev et al., 2005; Moritz et al., 2010). End-member low-sulfidation epithermal Au-Ag mineralization, such as that present around the Kesebir-Kardamos metamorphic dome in Bulgaria (Marchev et al., 2005; Márton et al., 2010), has not been described from northern Greece.

The Perama Hill deposit is a high- and intermediate-sulfidation Au-Ag-Te-Se epithermal system (Voudouris et al., 2011a) located on the eastern margin of the Petrota graben (Fig. 3). The proven and probable reserves are 9.7 Mt containing 3.13 g/t Au and 4 g/t Ag, for a total of 0.975 Moz Au and 1.151 Moz Ag (Eldorado Gold Corp., 2017). The mineralization consists mainly of enargite-luzonite, tennantite, Au-Ag tellurides, and native gold, and is hosted in silicified and argillic-altered andesitic rocks, conglomerates, and sandstones. Whole-rock K-Ar ages of the andesites range between 33.1 and 30.8 Ma (Innocenti et al., 1984; Hague, 1993). The mineralization forms ore veins in the andesite and oxidized Au-rich stratabound mineralization in the overlying sedimentary rocks.

The Mavrokoryfi Cu-Ag-Au-Te high-sulfidation epithermal mineralization is hosted in the same andesite and hyaloclastite sequence as the neighboring Perama Hill deposit. The main hydrothermal alteration styles are silicification and advanced argillic, with a mineralogy of quartz, opal, alunite, allophane, minor smectite, kaolinite, pyrite, and marcasite (Voudouris, 2011). The silicic bodies are brecciated and contain pyrite and marcasite. Advanced argillic alteration extends around the mineralized zones and contains alunite supergroup minerals with extremely high Pb contents of up to 1.5 wt.%. The mineralization mainly forms massive sulfide bodies and veinlets, mainly composed of pyrite, famatinite, goldfieldite and acanthite, freibergite which are associated with the silicification (Voudouris, 2011). Chemical analyses of surface grab samples revealed up to 1.5 ppm Au and up to 162 ppm Ag.

The Sapes-Kassiteres district includes over twenty HS-IS-LS epithermal Au deposits hosted by Oligocene volcanic rocks (Fig. 3). The most important ones are Viper, St. Demetrios, Scarp, Sapana, Kameno, Galaxy, and St. Barbara. The total measured and indicated reserve of the combined deposits is 0.83 Moz containing 9.8 g/t Au, with a proven and probable reserve of 637,000 oz containing 15.1 g/t Au (using gold cut-off grades of 4 g/t Au for Viper and 1 g/t Au for St. Demetrios and Scarp). Viper contains a high-grade gold-sulfide zone, enriched in pyrite, chalcopyrite, galena, enargite, tetrahedrite-tennantite, Au-Ag tellurides and native gold at a depth of 200–250 m (e.g., 40 m in drill core containing 53.3 g/t Au), whereas St. Demetrios contains lower gold content which is associated with oxidized mineralization at surface (in average 2 g/t) and pyrite-chalcopyrite-enargite mineralization with grades of up to 22 g/t at depth (Border et al., 1999). The Viper deposit is related to a steeply dipping, NW-trending vein zone. Gold occurs in the form of native gold and gold tellurides, and is commonly associated with enargite, goldfieldite and alunite (Fig. 6a). The Viper and St. Demetrios high-to-intermediate sulfidation epithermal system is superimposed upon and also developed in the periphery of porphyry-style mineralization (Voudouris et al., 2006; Voudouris, 2014; this study). Preliminary $^{40}Ar/^{39}Ar$ data of magmatic-steam alunite and adularia from the Sapana and St Barbara deposits suggest almost identical ages (e.g. 31.2 ± 0.4 to 31.9 ± 0.6 Ma) for the ore formation in the high- and the intermediate-sulfidation environment (Ortelli et al., 2009, 2010).

The St. Philippos intermediate-to-high sulfidation epithermal Pb-Zn-Ag-Bi-Sn-In deposit (Fig. 3) is located in the Kirki ore field and is genetically related to a microgranite porphyry (Voudouris et al., 2013b). It contains an unusual ore mineralogy consisting of several Pb-As-Cu-Ag-Bi-Sn sulfosalts. Dickite, alunite, pyrophyllite, barite, and calcite are the main alteration minerals. Wurtzite and sphalerite contain considerable amounts of In (up to 3.5 wt.%), and Ga (up to 1.6 wt.%), whereas Ge is present in a smaller amounts (up to 0.3 wt.%; Driesner and Pintea, 1994). Past production has been 0.2 Mt of ore at 7.5% Pb + Zn.

The Pefka high-to-intermediate sulfidation epithermal Cu-Au-Ag-Te deposit located in the Evros mineralization district (Fig. 3) is hosted in andesitic to rhyolitic volcanic rocks. A whole rock K-Ar age of 30.7 ± 1.2 Ma was reported for a trachyandesite (Christofides et al., 2004). The main alteration styles are silicification, sericitization, and advanced argillic alteration, which are crosscut by late carbonate-bearing veins related to E- and

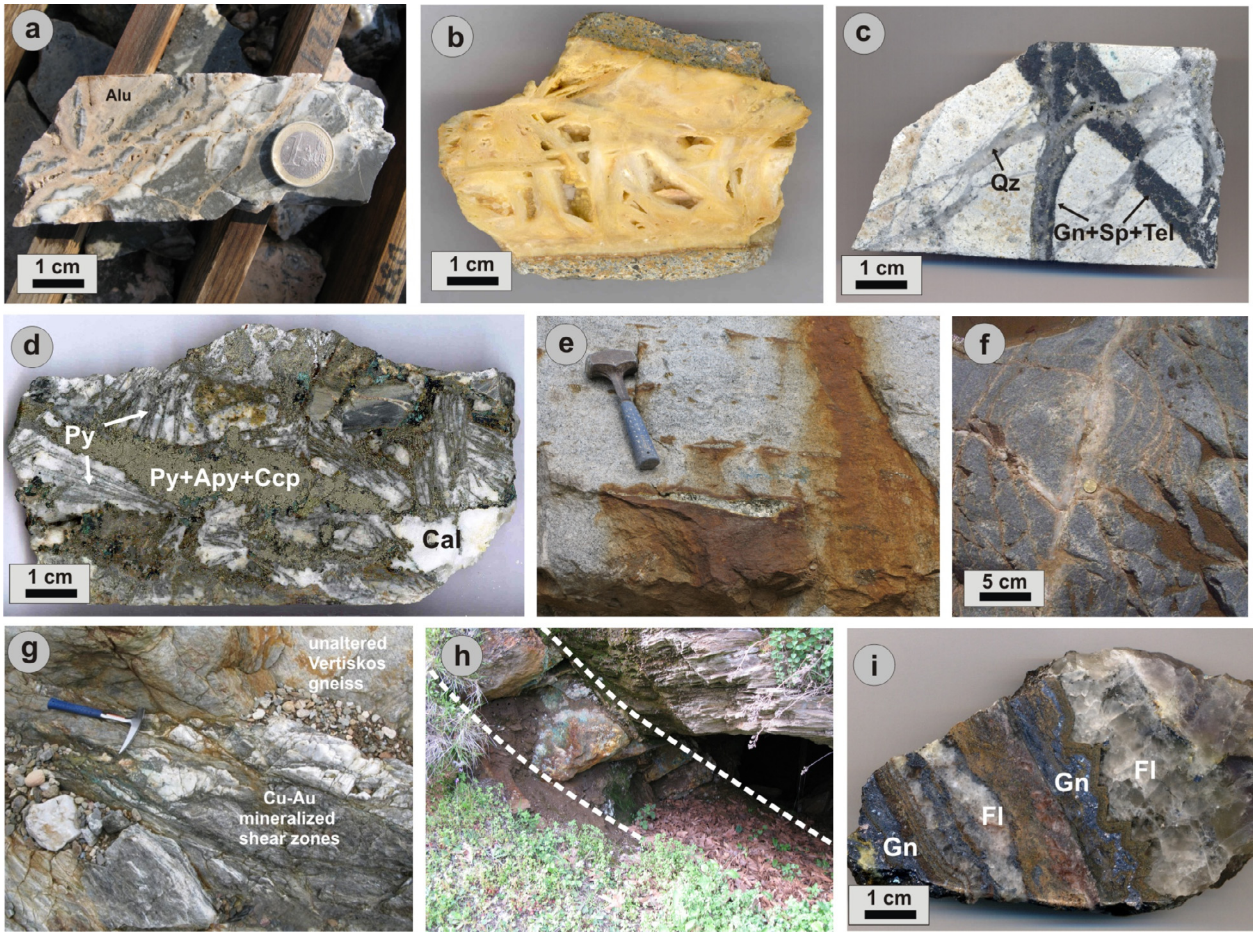

Fig. 6. Field photographs and hand specimens demonstrating various epithermal (a to c), carbonate-replacement (d), intrusion-related Au and Mo-W sheeted veins (e, f) and other intrusion-related(?) polymetallic veins (g to i) from Greece. (a) Hand specimen of Viper core material: early massive silica crosscut by milky chalcedonic quartz and then by alunite with pyrite; (b) platy calcite hosted in sericite-carbonate altered lava at Stipsi area; (c) drill core specimen of early massive sulfide veinlets composed of galena (Gn), sphalerite (Sp), and Au-Ag-tellurides (Tel), crosscut by late epithermal quartz veins; volcanic host rock is altered to quartz-adularia (base of Profitis Ilias deposit, Milos Island); (d) pyrite (Py), arsenopyrite (Apy), chalcopyrite (Ccp), and calcite (Cal) in marble; acicular crystals of pyrite are probably pyrrhotite pseudomorphs (Kamariza deposit, Lavrion); (e) Bi-Te ± Au-bearing pyrite boudins within the Kavala granodiorite; (f) granodiorite-hosted quartz veins with sericite-carbonate alteration containing molybdenite and pyrite (Xanthi intrusion-related Mo-W-Cu-Bi deposit); (g) mineralized shear zone within unaltered Vertiskos mica gneiss in Stanos area: hydrothermal alteration in the shear zone includes biotite and muscovite and is coeval with mineralization including pyrite, arsenopyrite, chalcopyrite, and native gold; (h) precious metal-bearing quartz veins crosscutting metamorphic fabrics of the schists (Kallianou deposits, Evia Island); (i) epithermal-style ore showing alternating bands of galena (Gn), siderite, and fluorite (Fl) (vein 80 from Plaka, Lavrion.

NNW-trending faults. Two distinct mineralization styles are observed in Pefka (Voudouris, 2006; Repstock et al., 2015): (1) early high-sulfidation veins with enargite, Bi-sulfosalts, and gold; and (2) late intermediate-sulfidation veins with tennantite/tetrahedrite and Au-Ag tellurides. Bulk analyses of mineralized samples from both epithermal mineralization styles contain up to 10 ppm Au, up to 23.5 ppm Mo, up to 105 ppm Bi, up to 468 ppm Te, up to 675 ppm In, 17 ppm Ga, 6 ppm Ge, >100 ppm Ag, >1 wt.% Cu and >1 wt.% As (Melfos and Voudouris, 2012; this study). Past mining operations produced 3 Kt ore at 7% Cu.

The Loutros area, close to the Greek-Turkish border (Fig. 3), hosts an intermediate-sulfidation epithermal deposit associated with a zeolite-altered rhyolitic lava dome, which yielded which yielded a whole rock K-Ar age of 19.53 ± 0.75 Ma (Christofides et al., 2004). The mineralization consists mainly of early NW-trending massive pyrite and marcasite veins and breccias, and late-stage barite-galena veins with sphalerite and minor chalcopyrite. The barite-galena veins contain up to 31 ppm Ag.

The Kalotycho high-sulfidation epithermal system covers a large area along the Greek-Bulgarian border (Fig. 3), and is hosted by Oligocene calc-alkaline and shoshonitic volcanic rocks. The volcanic rocks include andesites, dacites, trachytes, rhyodacitic ignimbrites and rhyolites, which were emplaced in a NE-SW trending sedimentary basin containing Eocene-Oligocene basal conglomerates and sandstones (Eleftheriadis, 1995). Whole-rock K-Ar ages of the volcanic rocks range from 33.0 ± 1.2 to 24.6 ± 0.6 Ma (Innocenti et al., 1984). The high-sulfidation epithermal alteration and mineralization are developed along NW-trending faults and are characterized by massive pyrite mineralization and advanced argillic, silicic-argillic, and propylitic alteration (Voudouris and Melfos, 2012).

3.2.2. Epithermal deposits in the northeastern Aegean region

In the northeastern Aegean islands of Limnos and Lesvos, epithermal mineralization is superimposed on or occurs peripherally to porphyry systems (Voudouris and Alfieris, 2005). The Fakos Au-Ag-Te high- to intermediate-sulfidation epithermal deposit on Limnos Island is associated with ∼20 Ma quartz monzonite and shoshonitic subvolcanic rocks which intruded Eocene to Miocene sedimentary rocks (Figs. 2 and 3; Voudouris and Alfieris, 2005; Fornadel et al., 2012). The epithermal mineralization is characterized by polymetallic veins containing pyrite, chalcopyrite, sphalerite, galena, enargite, bournonite, tetrahedrite-tennantite, hessite, petzite, altaite, an unknown cervelleite-like Ag-telluride, native Au, and Au-Ag alloy (Voudouris and Alfieris, 2005). Bulk chemical analyses of surface samples returned up to 11 ppm Au.

The Megala Therma Pb-Zn-Cu-Ag-Au intermediate-sulfidation epithermal deposit on Lesvos Island, is related to NNE–SSW- and NW–SE-trending quartz veins hosted in 21–18 Ma old andesite-latite lavas (Fig. 3; Kontis et al., 1994). Silicic, propylitic, argillic, and adularia-sericite are the main alteration types. The veins are enriched in Au (up to 21 ppm), Ag, Pb, Zn, Cu and Mo (Kontis et al., 1994). The Megala Therma epithermal system extends further to the south, where similar intermediate-sulfidation quartz-carbonate veins with platy calcite (Fig. 6b) overprint the porphyry Cu-Mo mineralization at Stipsi (Voudouris and Alfieris, 2005).

3.2.3. Epithermal deposits in the Cyclades

The island of Milos is located in the central part of the early Pliocene to Recent South Aegean Active Volcanic Arc, and belongs to the Cycladic Blueschist Unit of the Cyclades (Fytikas et al., 1986). Calc-alkaline volcanic activity in western Milos spans a period from ~3.5 to 0.9 Ma and originated from several emergent eruptive centers that produced submarine felsic pyroclastic deposits, pumice flows, dacitic-andesitic flow domes, lava flows, and felsic subvolcanic rocks (Fytikas et al., 1986; Stewart and McPhie, 2006; Alfieris et al., 2013). Milos Island is one of the most densely mineralized areas in Greece, characterized by intermediate-sulfidation epithermal Au-Ag-Te and base metal deposits (Fig. 6c) under transitional shallow submarine to subaerial conditions (Vavelidis and Melfos, 1998; Kilias et al., 2001; Naden et al., 2005; Alfieris et al., 2013; Papavassiliou et al., 2017). Epithermal-type mineralization rich in Au-Ag-Te occurs at Profitis Ilias (reserves: 5 Mt at 4.4 g/t Au) and Chondro Vouno (reserves: 3.3 Mt at 4.2 g/t Au), whereas Pb-Zn-Cu-Ag-Mn-Ba-rich mineralization occurs at in the Triades-Galana (resources: 1.2 Mt at 1 g/t Au and 124 g/t Ag) and Kondaros-Katsimouti-Vani districts (Fig. 4). The deposits are closely associated with active geothermal systems that are characterized by mixing of seawater, meteoric and, minor magmatic water (Naden et al., 2005; Alfieris et al., 2013; Papavassiliou et al., 2017).

3.3. Carbonate-hosted replacement and skarn deposits

3.3.1. Carbonate-hosted replacement and skarn deposits in the Rhodope Massif

The Olympias Au-Ag-Pb-Zn carbonate-replacement polymetallic deposit (Fig. 3; Siron et al., 2016) is hosted mainly within the lower calcitic marble horizon of the Kerdylion Unit and along the contact with the upper biotite gneiss. It forms mainly massive stratabound (manto), disseminated and cavity- or fracture-filling ore bodies consisting of various proportions of pyrite, aresonopyrite, chalcopyrite, marcasite, sphalerite, galena, bournonite, boulangerite, (Kalogeropoulos et al., 1989). Deformed sulfide ore is also present and is characterized by brecciation, mylonitization, folding and shearing. Mineralogical and geochemical features of the Olympias mineralization in both deformed and undeformed ores styles suggest that they were derived from the same system and were deposited after the onset of regional metamorphism (Kalogeropoulos et al., 1989; Gilg, 1993). Two major parts of the ore body are distinguished: the western section is approximately 250 m wide and extends 1500 m to the southwest dipping 30–35° to the east, whereas the eastern ore body is ~75 m wide and dips 25–30° to the southeast (Forward et al., 2011). The proven and probable reserves are 16.1 Mt containing 4.3% Pb, 5.7 % Zn, 128 g/t Ag and 7.9 g/t Au, for a total of 66.3 Moz Ag and 4.1 Moz Au (Eldorado Gold Corp., 2017). The Olympias deposit is currently in development with a planned annual production of approximately 190,000 oz Au per year by 2018, and with an expected mine life of over 25 years. The deposit is open at depth and the mineralization extends approximately 790 m below sea level. The majority of gold is "invisible", incorporated in arsenian pyrite and arsenopyrite (average ~50 ppm for both minerals; Chryssoulis and Cabri, 1990). Re-Os dating of arsenopyrite yielded an age of 26.1 ± 5.3 Ma (Hahn et al., 2012).

Two major carbonate-replacement deposits occur in the Kerdylion Unit along the Stratoni fault, at Madem Lakkos and Mavres Petres (Fig. 3). The Madem Lakkos has been exhausted, but past mining produced 13.5 Mt of Ag-Pb-Zn ore. Reserves at Mavres Petres are estimated to be 1.87 Mt at 160 g/t Ag, 6% Pb and 8.8% Zn (Eldorado Gold Corp., 2017). Two ore stages occur at the two deposits: early replacement-style massive sulfide forming undeformed and deformed (folded, sheared, brecciated) ore bodies consisting dominantly of galena and sphalerite with lesser pyrite and arsenopyrite, is overprinted by pyrite-rich disseminations that form the matrix to breccias and surrounds previous base metal-rich sulfide mineralization (Siron et al., 2016). Quartz, calcite and minor rhodochrosite form the gangue minerals. The average gold grade is ~5 g/t Au and is related to the arsenian pyrite and arsenopyrite as "invisible" gold (Forward et al., 2010).

The Piavitsa prospect is a siliceous-manganese carbonate-replacement deposit with associated Au-rich veins with a typical epithermal affiliation, located at the Stratoni area (Fig. 3; Siron et al., 2016). Piavitsa was the focus of exploration drilling by Eldorado Gold in 2012, which resulted in the discovery of a new resource estimated to be 10.54 Mt at 5.7 g/t Au and 57 g/t Ag (Eldorado Gold Corp., 2017). The Piavitsa ore deposit occurs along and adjacent to the Stratoni fault and was explored and exploited in the 1960s for manganese at the surface. The mineralization styles at Piavitsa vary and include brecciated semi-massive to massive sulfide lenses, banded epithermal quartz-rhodochrosite-gold veins, and hydrothermal breccias containing clasts of altered marble and massive sulfide (Siron et al., 2016).

The Thermes prospect is a polymetallic Zn-Pb-Fe-Cu-As-Ag-Au-Te carbonate-replacement deposit located in Xanthi area, NE Greece, at the southernmost part of the Arda dome (Fig. 3; Arvanitidis and Dimou, 1990; Kalogeropoulos et al., 1996). Veins and breccias containing Pb-Zn-(Fe-Cu) mineralization also occur, associated with NNW- and NNE-trending faults. The deposit contains a resource of ~1 Mt with grades of <4 g/t Au, 10–340 g/t Ag, 1.2–14.5% Pb, 2.1–16.7% Zn and 0.06–0.10% Cu (Gialoglou and Drymniotis, 1983). Thermes represents the southern extension of the Madan ore field in Bulgaria (Kaiser-Rohrmeier et al., 2013).

At Kimmeria a massive Cu-W-Mo-Au-bearing skarn-type mineralization consisting of chalcopyrite, magnetite, pyrrhotite, scheelite, and minor molybdenite and gold, is genetically related to the Xanthi I-type pluton (Fig. 3; Walenta and Pantzartzis, 1969; Vavelidis et al., 1990; Voudouris et al., 2010). The Xanthi pluton ranges in composition from gabbro through monzonite to granodiorite, and has an Oligocene age (28.8 ± 0.7 and 26.3 ± 0.1 Ma; Rb-Sr in whole rock and biotite; Kyriakopoulos, 1987). The emplacement of the pluton is controlled by two major regional structures: the Kavala-Xanthi-Komotini normal fault and the Nestos thrust fault (Fig. 3). The pluton intrudes gneisses, mica schists, amphibolites and marbles of the Northern Rhodope Domain. Mining operations in the 1930s, including underground galleries as well as surface excavations, extracted the magnetite-pyrrhotite-rich skarn mineralization and the Cu-Mo ore. The remaining resource is estimated to be ~2 Mt with 20 g/t Ag and 1.98% Cu (Gialoglou and Drymniotis, 1983).

Thasos Island contains silver-rich Pb-Zn carbonate-replacement deposits hosted in rocks of the Southern Rhodope Core Complex (Fig. 3; Vavelidis and Amstutz, 1983). The deposits were mined for silver and gold during antiquity, and for Fe, Pb and Zn between 1905 and 1964. These past mining operations produced a total of 2 Mt of ore containing 12% Zn + Pb, and 3 Mt of ore containing

44% Fe (Gialoglou and Drymniotis, 1983). Vavelidis and Amstutz (1983) distinguished four Pb-Zn-Ag-bearing horizons in carbonate rocks (marbles and dolomites) and schists, located on the eastern and the southern parts of the island. The mineralization occurs as veins and mantos of massive to semi-massive sulfides in the carbonate rocks, and veins crosscutting the schists. The main ore minerals are galena, sphalerite, pyrite, marcasite, arsenopyrite, chalcopyrite, cerussite, smithsonite, and Fe-Mn oxides; gangue minerals include calcite, ankerite, siderite, barite, and quartz.

3.3.2. Carbonate-hosted replacement and skarn deposits in the Attic-Cycladic belt

In the Attic-Cycladic Belt, the Lavrion ore district (Figs. 2 and 4) is a world-class carbonate-replacement deposit. It covers an area of ~150 km^2, and is famous for the exploitation of Pb-Ag-rich ore during ancient times, mainly during the Classical period, from 6th to 4th century B.C. (Conophagos, 1980). According to ancient writers (e.g., Aeschylus, Herodotos, Xenophon, Strabo) the Lavrion mines contributed significantly to the power of ancient Athens. After the decline of Athens, the mines were closed and then operated again in the 19th century. The exploitation of sulfide ores continued until the 1970s. Conophagos (1980) estimated that ~2.3 million metric tons of Pb and 7800 metric tons of Ag were extracted during the antiquity era. Remaining resources are estimated to be 4 Mt of ore containing 7% Pb + Zn. The carbonate-replacement Pb-Zn-Ag mineralization is the most economically important in the Lavrion district and occurs in the form of strata-bound lenses, bedded replacements (mantos), and chimneys up to tens of meters in length, in the Kamariza and Sounion areas (Marinos and Petrascheck, 1956; Voudouris et al., 2008a,b; Bonsall et al., 2011). According to Voudouris et al. (2008a,b), Bonsall et al. (2011), and Berger et al. (2013) the ore deposits in Lavrion are genetically related to the Miocene Lavrion granitoids, and ore formation occurred under extensional kinematic conditions. The carbonate-replacement and vein mineralogy is dominated by pyrite, arsenopyrite, sphalerite, chalcopyrite and galena (Fig. 6d), with various silver sulfosalts and native gold (Voudouris et al., 2008b), and quartz, fluorite, calcite and sericite gangue. Skarn deposits also occur around the Lavrion granodioritic body, and consist of early magnetite followed by pyrrhotite, pyrite, arsenopyrite, sphalerite, chalcopyrite, galena, bismuthinite, tetradymite, and native bismuth (Voudouris et al., 2008a,b; Bonsall et al., 2011). Extensive zones of supergene mineralization occur above the primary mineralization zones (Marinos and Petrascheck, 1956; Skarpelis and Argyraki, 2009). Various critical and rare elements occur in the mineralization, including Ag, Au, Bi, Sn, Ga, Ge, In, Sb, W, Ni, Te, and Se (Voudouris et al., 2008a,b; Zaimis et al., 2016). The sulfur isotope compositions of sulfides ($\delta^{34}S = -4.9$ to $+5.3$‰) in carbonate-replacement and vein style mineralization, along with the presence of elevated Ag, Bi, As, Sn, In, and Sb contents, point to a magmatic source for those elements, but is unclear whether the source was the Plaka granodiorite, the mafic to felsic dikes, or a granitoid at depth (Bonsall et al., 2011).

On Serifos Island (Fig. 4), a skarn deposit was mined for iron in antiquity and from 1869 to 1940, producing 6.6 Mt of ore. The mineralization is associated with a shallow intrusion of I-type granodiorite with an age of 11.6 ± 0.1 to 9.5 ± 0.1 Ma, based on zircon U–Pb dating (Iglseder et al., 2009). The granodiorite was intruded along the West Cycladic detachment fault into a series of gneisses, marbles and schists, producing a contact metamorphic aureole and extensive Ca-Fe-Mg skarns and iron ores, demonstrating ductile and brittle structures as a consequence of the activity of the detachment fault (Ducoux et al., 2017). The ore consists of pyrite, chalcopyrite, arsenopyrite, galena, sphalerite, tennantite, and is extensively oxidized. Calcite, barite, garnet, pyroxene, epidote, fluorite, talc, chlorite, adularia are the main gangue minerals.

The Sifnos Island carbonate-replacement Pb-Zn-Ag-Au deposits occur within marbles of the Cycladic Blueschist Unit (Fig. 4). Three main types of mineralization are distinguished in Sifnos (Vavelidis et al., 1985; Vavelidis, 1997; Neubauer, 2005): (1) Subconcordant ore bodies along shear zones composed mainly of pyrite and chalcopyrite; (2) Au bearing (6 ppm on average) quartz veins in the footwall of the detachment faults with pyrite, chalcopyrite, pyrrhotite, gold, and various undefined Ag-minerals; (3) Fe-Mn-Pb-Zn-Ag mineralization related to a major normal fault forming subhorizontal layers and lenses or irregular oxidized ore bodies in the marble. Sulfur isotope analyses in pyrites from the quartz veins ($\delta^{34}S = +1.59$ to $+1.73$‰ show a magmatic origin of the sulfur. On Sifnos Island, the various lithological units (marbles, schists, etc.) are separated by several shear zones and detachment faults, dominated by the Sifnos detachment (Avigad, 1993; Ring et al., 2011). Sifnos has been undergoing normal faulting from 30 to 23 Ma, and top-to-the-SSW extension along the Sifnos detachment was nucleated in the brittle-ductile transition zone at 13 Ma or slightly earlier, and continued to ~10 Ma (constrained by zircon fission track ages; Brichau et al., 2010). Structural relationships suggest that ore formation occurred under extensional kinematic conditions when the Sifnos metamorphic core complex reached a near-surface level during the late Miocene (<11 Ma; Neubauer, 2005, 2007).

Polymetallic Pb-Zn-Ag-Au mineralization in the southern part of Syros Island occurs as disseminations and massive sulfide bodies replacing marbles, along schist foliation planes and in veins crosscutting the marbles and schists in the Cycladic Blueschist Unit. The mineralization consists of base metal sulfides (pyrite, arsenopyrite, Fe-rich sphalerite, galena, pyrrhotite, stibnite, molybdenite), sulfosalts (Ag-rich tetrahedrite, famatinite, bournonite, bismuthinite, cosalite, stannite), tellurides (hessite), and Fe-oxides (magnetite, hematite). Bulk ore analyses show elevated contents of Mo, Sn, Te, Se, and Hg, in addition to Pb, Zn, Ag, and Au. Voudouris et al. (2014) suggested an intrusion-related origin for the Syros mineralization, assuming the presence of a Miocene granitoid at depth that fed the system with volatiles and metals. Deformation and mineralization at Syros were contemporaneous, occurring under brittle-ductile conditions probably related to detachment faulting. The Syros mineralization resembles other intrusion-related systems in the Attic-Cycladic Belt such as the Lavrion deposit.

3.4. Reduced intrusion-related gold systems in the Rhodope Massif

Various ore deposits in the Rhodope Massif are suggested here to belong to the reduced intrusion-related gold deposit classification (sensu Hart et al., 2002; Baker et al., 2005), although they have previously been classified as different deposit types, e.g. carbonate-replacement type, shear zone hosted mineralization or metamorphic rock hosted veins. The most important reduced intrusion-related systems occur in the Southern Rhodope Core Complex (Fig. 3; Palea Kavala and Pangeon).

In the Palea Kavala area (Fig. 3), metamorphic rocks of the lower tectonic unit of the Southern Rhodope Core Complex were intruded by the ~22–19 Ma Kavala (or Symvolon) pluton (Christofides et al., 1998) along the trend of the Kavala-Komotini fault zone. The Kavala pluton is an I-type intrusion and is dominantly composed of amphibole-biotite granodiorite with subordinate amounts of diorite, tonalite, monzogranite, and monzodiorite. The Palea Kavala region contains ~150 base- and precious-metal occurrences within the Kavala pluton and the surrounding metamorphic rocks. They were exploited in ancient times for gold or lead and silver, and in modern times (early 20th century) for iron and manganese, with considerable exploitation by both underground and surface mining techniques. These occurrences have variable metal contents and are mostly weathered and oxidized (particularly those that contain Mn). The estimated total resources are 1.5 Mt containing up to

34.5 g/t Au, up to 180 g/t Ag, up to 13% Pb + Zn, up to 40% Fe, and up to 42% Mn (Chatzipanagis and Dimitroula, 1996). Oxidized Fe-Mn-Au and Fe-Mn (Pb ± Zn ± Ag) bodies are localized in marbles, whereas Fe-As-Au, Fe-Cu-Au, and Bi-Te-Au deposits occur in gneisses and granitoids, as well as along the gneiss-marble contact of the lower tectonic unit in milky quartz veins. The Miocene Kavala pluton is crosscut by an approximately 4 km-long sheeted-quartz vein system (Kavala vein) that contains Bi-Te-Pb-Sb ± Au mineralization (Melfos et al., 2008; Fornadel et al., 2011) and the the 30 m-long Chalkero quartz vein (Chalkero vein). The Kavala quartz vein system is characterized by several parallel to subparallel quartz veins ~1 m thick and tens of meters apart. The SW–NE orientation of the vein system reflects both large- and small-scale regional structures, such as the Kavala–Komotini fault. The Bi-Te-Au mineralization is dominantly hosted in the Kavala vein, though, rare pods of massive pyrite, up to 30 cm long, are found in the granodiorite (Fig. 6e).

On Pangeon mountain (Fig. 3), a reduced intrusion-related gold system contains Au-Ag ± Bi ± Te ± W mineralization, which is genetically associated with the Pangeon granitoids (Vaxevanopoulos, 2017). These granitoids (Nikisiani, Mesoropi, Podochori, Messolakkia bodies) are the surface exposures of the same pluton, which occupies the core of a large anticline and extends ~25 km in a SW-NE direction, intruded into the Southern Rhodope Core Complex along the Strymon detachment fault (Eleftheriadis and Koroneos, 2003). The Pangeon granitoids consist of tonalite, granodiorite, and granite, and have high-K calc-alkaline metaluminous to the slightly peraluminous post-collisional character. They have hornblende $^{40}Ar/^{39}Ar$ ages of 21.7 ± 0.5 to 18.8 ± 0.6 Ma. Mineralization is hosted in marble, schist, gneiss, and amphibolite (Eliopoulos and Kilias, 2011) as well as in the granitoids, especially in the Nikisiani pluton, and is mainly structurally controlled. Three different mineralization styles are distinguished, intrusion-hosted sheeted veins, metamorphic rock hosted veins, and carbonate replacements, which show a slight zonation centered on the granitoids. The majority of this mineralization is oxidized and only small proportions contain primary ore minerals. Bulk sample analyses from Pangeon yielded up to 315 ppm W, up to 60 ppm Te, >2000 ppm Bi, >2000 ppm Sb, >100 ppm Ag, >100 ppm Au (Vaxevanopoulos, 2017).

3.5. Intrusion-hosted Mo-Cu-W deposits

The Oligocene Kimmeria intrusion-hosted Mo-Cu-W-Bi-Au deposit is located close to the Nestos thrust in the Rhodopes and is associated with the Oligocene Xanthi pluton (Figs. 2 and 3), described above in terms of its skarn mineralization. The Kimmeria ore district includes sheeted quartz veins crosscutting sericite-carbonate-altered granodiorite and contains pyrite, molybdenite, scheelite, wolframite, and chalcopyrite (Fig. 6f; Walenta and Pantzartzis, 1969; Voudouris et al., 2010; Theodoridou et al., 2016). Vein hosted mineralization contains >1 wt.% Cu, >0.2 wt.% Mo, up to 2.7 g/t Au, up to 79.5 g/t W, up to 456.6 g/t Bi, and traces of Te (up to 4 g/t) (Theodoridou et al., 2016). Primary fluid inclusion studies indicate CO_2 in the sheeted veins. Underground galleries as well as surface excavations aimed at the extraction of the Cu-Mo ore date back to the 1930s, but no production data are available. Similar Mo-Cu-W-Bi-Au veins occur also at the plutons of Samothraki and Tinos islands.

3.6. Other intrusion-related polymetallic vein deposits

Polymetallic quartz veins cutting metamorphic rocks in the Rhodope massif (e.g. Kallintiri, Thasos Island, Stanos, Nea Madytos, Drakontio, Koronouda, Stefania, and Laodikino; Fig. 3) and Cyclades (e.g. Kallianou, Tinos Island, Sifnos Island, Antiparos Island, and "Vein 80" in Lavrion; Fig. 4), are thought to have formed in response to Tertiary extensional tectonics in the Aegean.

3.6.1. Intrusion-related polymetallic vein deposits in the Rhodope Massif

The Kallintiri deposit on the southwestern edge of the Biala Reka-Kechros metamorphic dome (Fig. 2) is characterized as a detachment-related, epithermal deposit, hosted in silicified marble and argillic-sericitic-altered schists of the Mesozoic Makri Unit, as well as in Paleogene supra-detachment sedimentary rocks (Kanellopoulos et al., 2014). This deposit shares some similarities to low-sulfidation detachment-related deposits in Bulgaria, but Kallintiri is Sb-rich with additional Pb-Zn-Ag-Au-Te-Hg-Tl. The mineralization was deposited at the brittle-to-ductile transition within and above a detachment fault, and occurs in the form of disseminations, quartz-barite-carbonate veins, and breccias (Kanellopoulos et al., 2014).

Thasos Island (Fig. 3), besides the previously mentioned Pb-Zn-Ag carbonate-replacement deposits, also hosts several Au-rich Cu-Bi-Ag ± Te deposits hosted within schist, gneiss, and amphibolite of the Southern Rhodope Core Complex in the northern and western parts of the island (Vavelidis and Amstutz, 1983; Vavelidis et al., 1995; Vavelidis and Melfos, 2004). Where veins crosscut marble, small massive sulfide bodies also form. The mineralization contains chalcopyrite, pyrite, magnetite, pyrrhotite, gersdorffite, bismuthinite, tetrahedrite, tennantite, tetradymite, hessite, Fe- and Mn-oxides, and gold. Gold-grain size reaches up to 500 μm. The gangue minerals consist of quartz, calcite, ankerite, and barite. The relatively high homogenization temperatures of fluid inclusions and the presence of Te in the Cu-Au-Bi-Ag mineralization (Vavelidis et al., 1995; Vavelidis and Melfos, 2004) may indicate a magmatic source at depth.

Shear zone-hosted Cu-As-Pb-Bi-Au-Te deposits (e.g., Stanos, Nea Madytos, Drakontio, Koronouda, Stefania, and Laodikino) are found in metamorphic rocks of the Vertiskos Unit at Chalkidiki and Kilkis (Fig. 2). All these deposits share common mineralogical composition, fluid characteristics, and host rocks, but exploration projects are very limited or are lacking (Bristol et al., 2015).

The Stanos Cu-Au-Bi-Pb-Ag-Te deposit in the NE Chalkidiki area (Fig. 3) is hosted in marble, amphibolite, gneiss, metagabbro, and schist of the Vertiskos Unit, and is spatially related to regional NW–SE-trending shear zones (Voudouris et al., 2013a; Bristol et al., 2015). The mineralization forms disseminated to massive ore bodies along foliation planes and in boudinaged quartz veins (Fig. 6g). A Re-Os isochron age of 19.2 ± 2.1 Ma was obtained for pyrite in Stanos (Bristol et al., 2015).

Shear-related Au-Ag-Cu-Te-Bi mineralization in the NE Chalkidiki (Nea Madytos) and Kilkis (Drakontio, Koronouda, Stefania, Laodikino) areas (Fig. 3; Table 4) hosted by the Vertiskos Unit is considered to have a genetic affiliation to magmatic rocks of a possible Oligocene-Miocene age, although these intrusions are not exposed in the area (Bristol et al., 2015). These mineralizations are enriched in Au (up to 28.3 ppm) and also contain Ag (up to 765 ppm) and Cu (up to 4.3 wt.%), consisting mainly of chalcopyrite and pyrite, with traces of galena, sphalerite, Cu-Au-Ag-Bi sulfides, and gold (Thymiatis, 1995; Vavelidis and Tarkian, 1995; Vavelidis et al., 1996, 1999; Melfos et al., 2001). The ore bodies are associated with quartz boudins, veins and segregations, which were emplaced along shear and strike-slip zones, operated under ductile-to-brittle conditions.

3.6.2. Intrusion-related polymetallic vein deposits in the Attic-Cycladic belt

The Kallianou mining district in south Evia Island is famous for the exploitation of gold-silver-rich ore during ancient and recent times. Indicated mineral resources are 500,000 tons at an average grade of 2–2.4% Pb, 0.7% Zn, 0.5–0.8% Cu, 35–60 ppm Ag and 5 ppm Au (Voudouris et al., 2011b and references therein). However, the sulfide-bearing quartz veins contain up to 9 ppm Au and 202 ppm Ag and the oxidized ore up to 30 ppm Au. Mineralization is hosted in mica schists and marbles of the Cycladic Blueschists and occurs either as dissemination within brecciated marbles or as quartz veins that crosscut the foliation of the schists (Fig. 6h). The quartz veins (up to 3 m thick and 100 m long) generally strike NW-SE, are discordant to metamorphic structures and were formed close to the brittle-ductile transition (Voudouris et al., 2011b). Ore minerals in the quartz veins occur in masses to disseminations, filling fractures, or cementing brecciated quartz fragments. There is a district-scale zonation at Kallianou with Au and Te enriched in the lower topographic levels and Ag at higher elevations (Voudouris, Unpublished data). This may suggest the presence of a buried granitoid at depth. The host rocks of the Kallianou deposit represent the footwall of the North Cycladic Detachment System (Ring et al., 2007; Jolivet et al., 2010). High-P conditions of the Cycladic Blueschists at south Evia Island persisted until ~33 Ma, when the rocks started to be exhumed and finally re-equilibrated under greenschist-facies conditions at ~21 Ma (Ring et al., 2007). The veins were probably formed during the Miocene.

The vein hosted Au-Ag-Te rich mineralization at Tinos Island consists of quartz veins crosscutting Triassic marbles and schists of the Cycladic Blueschist Unit (Tombros et al., 2007). The mineralization contains electrum and an extremely rich suite of tellurides, including Au-Ag tellurides and silver sulfotellurides. Mineralization occurs in the footwall of the North Cycladic Detachment (Fig. 4). The intrusion of a granodiorite of ~18 to 15 Ma age was followed by the intrusion of a boron and fluorine-rich leucogranite peripheral to the granodiorite at ~14 Ma (Altherr et al., 1982). The mineralization at Panormos Bay is considered to be genetically related to the 14 Ma old, peraluminous leucogranite (Tombros et al., 2007).

On Sifnos Island, a vein hosted mineralization occurs in the southern part of the island, hosted in greenschists and gneisses of the Cycladic Blueschist Unit (Vavelidis, 1997; Vavelidis et al., 1985; Neubauer, 2005). Mineralization occurs as subconcordant and subvertical pyrite-chalcopyrite-pyrrhotite ore bodies with Fe-rich carbonates and quartz. These ores occur in the footwall of low-angle normal faults, which separate greenschists and gneisses from overlying marbles. The quartz veins formed during subhorizontal extension and their gold contents range from 1.5 to 12.2 ppm (Neubauer, 2005). E-W extension during movement of a NNE-directed semi-ductile normal fault in the hanging wall of the greenschist-gneiss unit was responsible for the formation of Au-bearing quartz veins.

Steeply dipping quartz veins containing galena with 800–2000 ppm Ag crosscut biotite-muscovite schists and marbles of the Cycladic Blueschist Unit at Agios Georgios of Antiparos Island (Kevrekidis et al., 2015). The mineralized veins were deposited from fluids in the epithermal stage with a significant magmatic contribution mixed with meteoric water. Kevrekidis et al. (2015) suggested that the mineralization is genetically related to the neighboring Miocene Paros leucogranite.

A major Pb-As-Sb-Cu-Ag rich banded vein with epithermal affinities (Fig. 6i), known as "Vein 80" or "Filoni 80", crosscuts pyrrhotite bearing hornfelses and carbonate-replacement mineralization at Plaka area, Lavrion deposit (Voudouris et al., 2008a). The Filoni 80 vein trending ESE-WNW, is up to 2 m thick and up to 1 km long. This vein includes early deposition of pyrrhotite followed by arsenopyrite, löllingite, pyrite, marcasite, a Cu-Bi bearing assemblage including lillianite homologues, pyrargyrite, chalcopyrite, Bi-bearing tetrahedrite/tennantite, bournonite, lead sulfantimonides and finally by galena and native arsenic. Quartz, siderite, fluorite and calcite are the main gangue minerals. An estimated total production of this vein is 90,000 t with an average Pb + Zn content of 14–15 wt.% and 500 ppm Ag (Conophagos 1980).

4. Discussion

4.1. Time-space relationships between detachment systems, magmatism and ore deposition

In the northern Rhodope core complexes of Bulgaria and Greece the Arda, Biala Reka-Kechros and Kesebir-Kardamos domes were exhumed from ~42 to 35 Ma along the ductile- to brittle Madan-Xanthi, Kechros and Tokachka-Kardamos low-angle detachment faults respectively (Bonev et al., 2006a,b, 2010, 2013; Wüthrich, 2009; Moritz et al., 2010; Márton et al., 2010; Kaiser-Rohrmeier et al., 2013). Exhumation of the metamorphic rocks in the southern Rhodope core complex occurred along the ductile Kerdylion detachment, active from ~42 Ma until ~24 Ma, and the ductile-to-brittle Strymon detachment from 24 Ma until 12 Ma (Brun and Sokoutis, 2007; Wüthrich, 2009; Kounov et al., 2015). As a consequence of the metamorphic core complex exhumation along large detachment faults, magmas were emplaced along the transition from ductile to brittle deformation related to shear zones attributed to post-orogenic exhumation (Jones et al., 1992; Kilias et al., 2013a; Siron et al., 2016).

Around the Arda, Biala Reka-Kechros and Kesebir-Kardamos domes, the Oligocene porphyry Cu-Mo-Au deposits are associated with plutonic and subvolcanic intrusions either in the footwall of detachment fault systems that accommodated their exhumation (e.g., Maronia deposit, M. Sanchez, pers. commun., 2013), or located in supra-detachment grabens (Konos Hill, Pagoni Rachi, Myli, Melitena, etc). In association with the porphyry deposits, the high-sulfidation style epithermal gold deposits (e.g., Sapes, Perama Hill etc), occur within the supra-detachment basins, where mineralization is controlled by steeply-dipping extensional faults and associated fractures. An interesting aspect for the Oligocene plutonic intrusions of Maronia, Kassiteres, Kirki and Leptokarya is their alignment along a NE-SW direction (Fig. 2), which parallels to the NE-trending axis of Oligo-Miocene intrusive centers in the Kassandra mining district and also to the NE-elongated Early Miocene Kavala pluton (Siron et al., 2016). This direction parallels the NE-SW back-arc extension and according to Siron et al. (2016), this indicates a northeast-oriented principal axis of extension evidenced by crustal-scale ruptures developed prior to Early Miocene and believed to have localized magmatism. At Kassandra mining district in Chalkidiki, the exhumation of the southern Rhodope core complex may have influenced ascent of magmas to shallow crustal levels, preferentially exploiting favorable oblique structural intersections between NE-trending transtensional faults and ENW - trending structures (Siron et al., 2016).

A subsequent metallogenic episode is associated with the magmatism of Early Miocene at ~22–19 Ma and is restricted: (a) in southern Rhodope core complex, either along the Strymon detachment fault (e.g., Pangeon and Palea Kavala reduced intrusion-related gold systems, and Thasos Pb-Zn carbonate-replacement deposits and intrusion-related (?) polymetallic veins), (b) along a NW-trending corridor through Chalkidiki and Kilkis regions including the Skouries, Vathi and Gerakario porphyry Cu-Au deposits, as well as the Stanos, Koronouda and Laodikino shear-zone intrusion-related(?) polymetallic deposits, (c) along a NE-trending direction at Loutros north of the island of Samothraki, and (d) at Limnos and Lesvos Islands occurring in the western extension of Biga Peninsula.

The ductile shear zone at Stanos area occurs west of the Kerdylion detachment and within the Athos-Volvi Suture Zone and coincides with Cu-Au ore deposition at ~19 Ma (Bristol et al., 2015).

This may indicate operation of a previously unrecognized NW-trending ductile detachment zone, which accommodated emplacement of granitoids and ore deposition in Chalkidiki and Kilkis during the Early Miocene. During the same period (~19 Ma) the Loutros rhyolites and the Samothraki granite were emplaced and exhumed during NE directed extension, like the coeval Kavala granodiorite beneath the Strymon Detachment (Dinter and Royden, 1993; Lips et al., 2000). Mineral deposits are classified as intrusion-hosted Cu-W with peripheral intrusion- and metamorphic rock-hosted Pb-Zn-Ag sulfide veins (Samothraki) or as epithermal styles at Loutros.

The porphyry-epithermal systems at Fakos and Sardes in Limnos Island, and Megala Therma and Stipsi in Lesvos Island occur along major E-W and NNE-trending steep-dipping extensional faults and associated fractures, like those considered to control porphyry and epithermal ore formation at Biga Peninsula (Sanchez et al., 2016).

During the Miocene back-arc extension of the Cyclades, stretching was accommodated mainly by the North Cycladic Detachment System, which is exposed at Mykonos, Tinos and further to Evia offshore Kallianou ore district (Jolivet et al., 2010) and the West Cycladic Detachment System which is exposed on Lavrion, Kea, Kythnos, and Serifos (Grasemann et al., 2012; Scheffer et al., 2016; Ducoux et al., 2017). The evolution of the Cyclades can be resolved into SSW- and NE directed ductile to a brittle extension, localized plutonism, and rapid cooling of the footwall of both detachment faults during Middle and Late Miocene. At Lavrion, the West Cycladic Detachment Fault operated under ductile-to-brittle conditions (Grasemann et al., 2012; Scheffer et al., 2016) and, based on U-Th/He dating of titanite, zircon and apatite (Seman et al., 2013a,b), accommodated exhumation of the metamorphic rocks in at least two major periods: Middle Miocene (16–12 Ma) and Late Miocene (6–9 Ma), the latter also coinciding with mineralization. Similarly to Lavrion, other mineral occurrences in the Cyclades are in part spatially associated with Miocene plutonic rocks, which intrudes the footwall units along detachment faults under ductile to brittle extensional kinematic conditions (e.g., Mykonos, Menant et al., 2013), in part by extensional structures in the footwall of detachment faults without any adjacent granitoids (e.g., Tinos, Sifnos, Syros, Kallianou) (Neubauer, 2005; Tombros et al., 2007; Voudouris et al., 2014; Kevrekidis et al., 2015). On Mykonos Island (Cyclades), epithermal style barite-base metal mineralization occurred when the pluton crossed the ductile-to-brittle transition during its exhumation below the North Cycladic Detachment System at ~11–10 Ma (Menant et al., 2013; Tombros et al., 2015).

In this broad geodynamic regime, the Oligocene-Miocene to Pliocene-Pleistocene magmatic-hydrothermal ore deposits in Greece were mostly formed in four periods: Oligocene (33–25 Ma), Early Miocene (22–19 Ma), Middle to Late Miocene (14–7 Ma) and Pliocene-Pleistocene (3 to 1.5 Ma). A compilation of magmatic and mineralization ages and metal content of known systems, is demonstrated in the time–space plot of Fig. 7.

4.2. Comparison to Cenozoic deposits in southern Balkans and Western Anatolia

The Biga Peninsula in northwestern Turkey shares many similarities in tectono-magmatic and metallogenetic history to the Oligocene-Miocene Rhodope and Serbo-Macedonian Massifs (Yigit, 2012). Several porphyry, HS-IS and LS epithermal and skarn/carbonate-replacement deposits in Biga are associated with Late Eocene-Oligocene magmatism (38–25 Ma; Yigit, 2012), mostly contemporaneous to the major Oligocene magmatic-metallogenetic event (~33–25 Ma) that took place in the western part of the belt in Greece and FYROM.

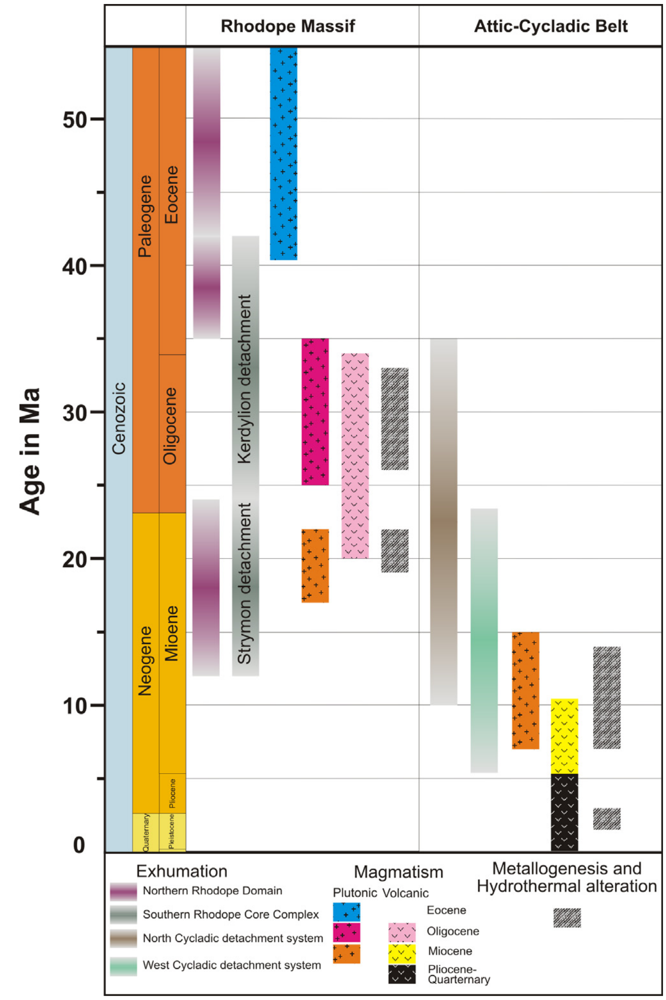

Fig. 7. Time-space diagram demonstrating major tectonic, magmatic, and metallogenetic events in the Rhodope and Attic-Cycladic Massifs of Greece. Data from Pe-Piper and Piper (2006), Jolivet and Brun (2010), Ersoy and Palmer (2013), Jolivet et al. (2013, 2015), Menant et al. (2016), and this study.

In addition, the Cu-Au belt of the Greek part of the Rhodopes extends further to the southeast, at the Biga Peninsula in Turkey. Yigit (2012) distinguished at least three phases of porphyry Cu–Au–Mo mineralization and two phases of high sulfidation epithermal gold mineralization in Biga Peninsula, where porphyry deposits as well as causative intrusions have a younger age from north to south. The oldest phase (52–47 Ma) of porphyry Cu–Au–Mo mineralization is related to the Dikmen and Karabiga stocks and belongs to the adakitic-magmatism in NW Anatolia described by Ersoy and Palmer (2013). The second phase is associated with the Early Oligocene Alankoy granodiorite (~28 Ma), and coincides with the second phase of high sulfidation epithermal mineralization (~28 Ma). The third late Oligocene porphyry phase (~25 Ma) is related to the Tepeoba and Kestane granodiorite porphyries. A late Eocene (~38–39 Ma) age for the early phase in high sulfidation epithermal systems at Kartaldag and Kuscayiri prospects and an Early Oligocene age (~25–31 Ma) for the second high sulfidation phase at Agi Dagi, Anankoy, Kirazli, Küçükdağ, are considered by Yigit (2012), Sanchez et al. (2016) and Leroux (2016).

Finally, major carbonate-hosted deposits, such as the Papazlik Pb–Zn (Au–Ag) deposit and base-metal skarns in the Yenice district, are considered as a part of Oligocene magmatic-hydrothermal systems at Biga and comparable to the polymetallic Pb-Zn-Ag-Au deposits in the Rhodope Massif (e.g., Olympias, Madan), and low-sulfidation epithermal deposits and prospects (e.g., Ovacik and Kisacik) are related to Miocene volcanic rocks (Yigit, 2012). According to Yigit (2012) and Sanchez et al. (2016), the Latest Oligocene porphyry Cu-Au-Mo deposits are associated with plutonic intrusions in the footwall of detachment fault systems that accommodated exhumation of the Kazdağ Massif metamorphic core complex. Both the Kestane (Halilaga) Cu-Au porphyry and Tepeoba Cu-Mo-Au porphyry deposits (~25–26 Ma) are located in supra-detachment grabens on the north and south of the Kazdağ core complex. In association with the porphyry deposits, the high-sulfidation style epithermal gold deposits (e.g., TV Tower, etc), occur within the supra-detachment basins, where mineralization is controlled by steep-dipping extensional faults and associated fractures (Leroux, 2016; Sanchez et al., 2016). The Kestane porphyry Cu-Au and Tepeoba porphyry Cu-Mo-Au deposits are hosted in granodiorite porphyries and are characterized by potassic and phyllic alteration bearing pyrite, magnetite, chalcopyrite and minor molybdenite. The phyllic alteration at Topeoba includes tourmaline, a feature also observed from Limnos porphyry Cu-Mo-Au deposits (Voudouris and Alfieris, 2005; Fornadel et al., 2012). Reduced intrusion-related gold deposits, like those present in the Greek part of Rhodope (e.g., Miocene age), might be present in Biga, at the Mo-rich porphyry Au Dikmen prospect, which is related to quartz–feldspar porphyry, granodiorite and aplitic dikes. Finally, the Kizildam and Findikli prospects in the eastern Biga Peninsula have many similarities to Carlin-type gold deposits (e.g., presence of antimonite, As-rich pyrite, jasperoid formation. etc) and can be classified as distal-disseminated gold deposits (Yigit, 2012).

The Late Oligocene-Early Miocene shoshonitic Chalkidiki-Kilkis porphyry Cu-Au trend of Greece, extends further to the NW through FYROM, where the Bucim porphyry Cu-Au deposit is related to shoshonitic intrusives dated between 24.04 ± 0.77 and 24.51 ± 0.89 Ma, based on U-Pb in zircons (Lehmann et al., 2013). Bucim belongs to the so-called Lece-Chalkidiki metallogenetic zone, that also includes other major deposits like the Ilovica (FYROM) and Kiseljak porphyry Cu-Au (Serbia), the Lece Pb-Zn-Ag-Au skarn-carbonate-replacement deposits (Serbia), the Plavica high sulfidation epithermal Cu-Au mineralization (FYROM), with all of them situated on the east of the Vardar suture zone, within rocks of the eastern Vardar ophiolites and the Serbo-Macedonian Massif (Serafimovski, 2000; Lehmann et al., 2013). Within the Oligocene Lece magmatic complex of southern Serbia, the Tulare dioritic porphyry cluster (33.0–31.8 Ma), host the Kiseljak Cu-Au deposit (Dragić et al., 2014). In common to ages of magmatic (and ore) processes described from the Serbo-Macedonian/Rhodope region, Schefer et al. (2011) distinguished both Oligocene (31.7–30.6 Ma) and Miocene (20.58–17.74 Ma) ages (by U-Pb dating in zircons) for the Cenozoic granitoids in the Dinarides of southern Serbia.

4.3. Metal enrichment in Cenozoic deposits in Greece

Cenozoic magmatic-hydrothermal deposits in Greece demonstrate various enrichment in precious, critical, and energy critical metals (e.g., Melfos and Voudouris, 2012; Tsirambides and Filippidis, 2012), as defined by John and Taylor (2016) and Kelley and Spry (2016). Tellurium is a common constituent throughout Oligocene to Pliocene-Pleistocene Greek deposits (Voudouris et al., 2007) and PGE and Re enrichment has been reported for Skouries (Economou-Eliopoulos and Eliopoulos, 2000) and the porphyry Cu-Mo-Au deposits in the Rhodope Massif (Voudouris et al., 2013c), respectively.

The Re, Te (and Au) enrichment in the high-K calc-alkaline porphyry Cu-Mo-Au mineralization at Pagoni Rachi, Konos Hill, Maronia, Melitena, and the associated epithermal Au-Ag-Te deposits at Sapes, Perama Hill, and Pefka, expanding over an area of ~5400 km^2, is a case study attributed to anomalous concentration of these elements in source areas of magma generation (Voudouris et al., 2013c). The Au, Re and Te enrichment in the eastern Rhodope Oligocene-Miocene magmatic-hydrothermal systems is also present at the shoshonitic Miocene porphyry deposits of Limnos and Lesvos Islands (Voudouris et al., 2013c). This metal enrichment belt seems to continue further to the east in the Biga Peninsula, where Au-Ag tellurides were described from the high-sulfidation Küçük dağ deposit (Smith et al., 2014) and also to the west where, besides the Skouries deposit, also the Oligocene-Miocene Vathi and Bucim porphyry Cu-Au deposits are enriched in Au, Ag, and Pd-tellurides (Eliopoulos and Economou-Eliopoulos, 1991; Tarkian et al., 1991; Economou-Eliopoulos and Eliopoulos, 2000; Serafimovski et al., 2013).

This enrichment is common in porphyry and epithermal style ore deposits in post-subduction settings elsewhere, where partial melting of the residues of previous cycles of calc-alkaline arc magmatism, may generate high-K calc-alkaline to shoshonitic post-collisional magmas (Richards, 2009, 2011, 2015). Delamination of sub-continental mantle lithosphere and slab retreat, associated with the ingress of asthenospheric melts into the lower crust, can cause small volume partial melting of arc-metasomatized lithosphere and/or hydrous, amphibolitic, lower crustal cumulates (Richards, 2011). Small amounts of chalcophile and siderophile element-rich sulfides left in these cumulates may be redissolved during partial melting thus giving rise to Au rich as well as normal Cu ± Mo porphyry and epithermal Au systems. Potential source regions of lithospheric contamination include subduction-modified lower crust, sub-continental lithospheric mantle, or juvenile lower crust formed by underplated arc basalts (Richards, 2015 and references therein).

Ersoy and Palmer (2013) suggested for the Rhodope-Aegean-west Anatolian Oligocene–Miocene high-K calc-alkaline magmatic rocks crustal hybridization processes involving lower crustal melting, and mixing of these magmas with mantle-derived mafic melts, and subsequent AFC (assimilation and fractional crystallization) processes. Throughout the Oligocene and Miocene, the magmatic activity was derived from subcontinental mantle lithosphere that had been intensely contaminated by the Late Eocene and onwards by oceanic and continental subduction (Ersoy and Palmer, 2013). A slab retreat after ~35 Ma (Jolivet et al., 2013) associated with a southward fast migration of the magmatic centers, may have caused upwelling of asthenospheric mantle, melting of metabasaltic amphibolites that underplated subducted continental crust and high-K calc-alkaline to shoshonitic magmatism (Pe-Piper et al., 2009).

Melting of mafic or ultramafic rocks, as well as involvement of mantle metasomatism in the source rocks, could contribute to Re enrichment as proposed elsewhere (Stein et al., 2001). Previous subduction magmatism may be responsible for the enrichment in Au, Te, Re together with other fluid-mobile elements such as Pb, As, Sb, Cu and the platinum group elements (PGE) in the mantle lithosphere, probably due to fluids released from the oceanic and continental subducted slab and associated sediments (Sun et al., 2003; Tessalina et al., 2008; Cook et al., 2009; Grabezhev and Voudouris, 2014). Tellurium enrichment is also present in epithermal deposits at Milos Island in the South Aegean Volcanic Arc, which are typical of subduction-related magmatic activity and their mantle source was metasomatized by subduction of oceanic assemblages (Ersoy and Palmer, 2013).

Less fertile magma sources beneath the Bulgarian part of the Rhodope may be the reason for the rarity of Au-bearing tellurides from the Oligocene volcanic-hosted intermediate sulfidation deposits in the eastern Rhodope, Bulgaria, compared to their abundance in northeastern Greek high sulfidation epithermal

Au-Ag-Cu-Te deposits. At these deposits Au-Ag-tellurides were introduced by fluids of intermediate sulfidation states and contribute to their total gold potential (Voudouris, 2006). Marchev et al. (2005) have already pointed out significant geographical variations in the style and composition of the Early Oligocene Rhodopean deposits, from Pb-Zn-Ag veins, skarns and carbonate-replacement base-metal deposits in the central Rhodope (e.g., Madan ore field), through intermediate sulfidation epithermal Pb-Zn-Ag-Au deposits (Madjarovo, Zvezdel, Spahievo) in volcano-sedimentary basins at the Bulgarian part of the eastern Rhodope, to high-intermediate sulfidation epithermal Au-Ag-Cu-Te polymetallic deposits in the Greek part of the Rhodope (Sapes, Perama Hill). Based on Sr and Pb isotope systematics on igneous rocks, sulfides and gangue minerals from the southeastern Bulgarian ore deposits, Marchev et al. (2005) demonstrated a decreasing input to the hydrothermal systems of Palaeozoic or older crustal material, from the much thicker continental crust in the central Rhodope and an increase of mantle contributions towards the eastern Rhodope, which is underlain by a thinner crust. The increasing amount of crustal components, from the SE Rhodope towards the central Rhodope, also coincides with an increasing proportion of acid rocks in the central Rhodope, where crustal contamination could have diluted original mantle magmas containing Cu and Au with an increasing contribution of Pb from a continental basement source.

However, further to the north, the Cretaceous arc-related porphyry-epithermal deposits in the Srednogorie-Pontides Belt are quite similar to those in northern Greece in respect to Au, Te, Re and PGE enrichment (Zimmerman et al., 2008; Eliopoulos et al., 2014). These deposits, as for example, Majdanpek, Elatsite, and Assarel, are related to subduction of the Vardar Ocean (Gallhofer et al., 2015), and a melt-metal source in fertile mantle and/or juvenile lower crust was responsible for the relatively high Re concentrations (up to 0.35 wt.%) in molybdenite from the Majdanpek (Serbia) and Elatsite (Bulgaria) Cu-Mo porphyry deposits (Zimmerman et al., 2008).

4.4. Perspectives for future exploration

The Greek part of the Western Tethyan metallogenic belt has been recognized as a favorable metallogenic province representing the link between Balkans and Anatolides-Taurides, where intensive precious metal exploitation currently takes place. Although mineral exploration and mining activity for precious and base metals in Greece date back to ancient times, only a few major magmatic-hydrothermal prospects have been studied with modern exploration methods. With the exception of drilled projects/deposits at Chalkidiki (e.g., Skouries, Olympias) and western Thrace (Sapes, Perama Hill) in northern Greece, by Eldorado Gold Corp., in recent years, the rest of mineralization in the Rhodope, the eastern Aegean islands and the Cyclades, are insufficient explored and only limited information exists in addition to the evidence from historic exploitation.

Several questions remain open and are related to issues about gold, the age of magmatism and associated mineralization and metal enrichment in the Cenozoic metallogenic provinces of Greece. Future investigations should focus on exploring gold potential at the porphyry deposits, like in Pagoni Rachi, Maronia, Konos Hill, Vathi, Fakos. Exploration targets for porphyry Au-ore should not only be the potassic- but also the sodic-calcic-potassic alteration, which usually is barren and occurs in the periphery of other porphyry systems (Halley et al., 2015). The enrichment in rare and critical metals, like Re, Te, Se, and PGE, in several northern Greek porphyry systems, may increase their economic potential since they could be extracted by-products in metallurgy processing.

Although the Oligocene-Miocene Western Tethyan metallogenic belt in Balkan-Western Turkey has prospects mainly for porphyry, epithermal, skarn, and carbonate-replacement deposits, there is increasing evidence that there may also be a province for Reduced Intrusion-Related Gold, Carlin-style Sb-Au, as well as low sulfidation epithermal Au deposits. These three styles of ore deposits have been discovered in various regions along the Western Tethyan belt and it is only a matter of future exploration for additional discoveries.

Typical end-member low-sulfidation gold-silver deposits are not yet discovered in Greece, but present both in western Turkey (e.g., Kucukdere and Kisacik deposits) where they are related to Miocene volcanic rocks (Yigit, 2012) and also in SE Bulgaria, (e.g., Ada Tepe, Rosino, Stremtsi, etc.) where they are older than the adjacent magmatic-related deposits and are mainly hosted in Maastrichtian-Paleocene sedimentary rocks, above detachment fault contacts with the underlying Palaeozoic metamorphic rocks (Marchev et al., 2005; Márton et al., 2010).

Carlin-style gold deposits are also missing in Greece, but present in western Turkey, at the Kizildam and Findikli prospects in the eastern Biga Peninsula and also at several deposits at Menderes Massif (Yigit, 2012). Carlin-style gold mineralization also occurs in Allchar deposit FYROM (Percival and Radtke, 1994). The Kallintiri Sb-As-Ag deposit is a polymetallic ore, sharing some affinities to Carlin-style mineralization, however, its exact classification is a matter of further investigations (Kanellopoulos et al., 2014).

Reduced intrusion-related gold deposits, like those present in the Greek part of Rhodope (e.g., Miocene age), might be present in Biga, at the Mo rich porphyry Au Dikmen prospect which is related to quartz-feldspar porphyry, granodiorite and aplitic dikes.

The Rhodope and Cyclades region also include ore mineralization enriched in Au, Ag, Cu, Bi, and Te, which is associated with detachment faults, shear zones and metamorphic rock-hosted veins in Stanos, Nea Madytos, Drakontio, Koronouda, Stefania, Laodikino, Lavrion, Kallianou, Sifnos, Tinos, Syros, and Antiparos. They are considered to have a genetic affiliation to magmatic rocks of a possible Miocene age, although these intrusions are not exposed and are deduced to be buried at shallow depths. It is suggested that ore fluids derived from the magmas, circulated at low depths along extension-related shear zones and interacted with the country rocks of the exhumed metamorphic core complexes. These large tectonic structures should also be exploration targets.

Acknowledgments

The authors are thankful for the comments and suggestions given from the two reviewers, Thomas Bissig and Ladislav Palinkas. Tim Baker and Jeremy Richards are sincerely thanked for their reviews and their constructive and valuable comments on an earlier version of this manuscript. Editor Franco Pirajno is greatly acknowledged for editorial handling.

References

Alfieris, D., Voudouris, P., Spry, P.G., 2013. Shallow submarine epithermal Pb-Zn-Cu-Au-Ag-Te mineralization on western Milos Island, Aegean Volcanic Arc, Greece: Mineralogical, Geological and Geochemical constraints. Ore Geol. Rev. 53, 159–180.

Altherr, R., Kreuzer, H., Wendt, I., Lenz, H., Wagner, G.A., Keller, J., Harre, W., Höndorf, A., 1982. A late Oligocene/early Miocene high temperature belt in the Attic-Cycladic crystalline complex (SE Pelagonian, Greece). Geol. Jahrb. 23, 97–164.

Altherr, R., Siebel, W., 2002. I-type plutonism in a continental back-arc setting: Miocene granitoids and monzonites from the central Aegean Sea, Greece. Contrib. Miner. Petrol. 143, 397–415.

Anders, B., Reischmann, T., Kostopoulos, D., 2006. The oldest rocks of Greece: first evidence for a Precambrian terrane within Pelagonian Zone. Geol. Mag. 143, 41–58.

Arikas, K., Voudouris, P., 1998. Hydrothermal alterations and mineralizations of magmatic rocks in the southern Rhodope Massif. Acta Vulcanol. 10, 353–365.

Arvanitidis, N., 2010. New metallogenetic concepts and substainability perspectives of non-energy metallic minerals in Central Macedonia, Greece. Bull. Geol. Soc. Greece 43, 2437–2445.
Arvanitidis, N., Dimou, E., 1990. Electrum and silver telluride occurrences in the polymetallic sulfide mineralization of the Thermes ore-field, N. Greece. Geol. Rhodopica 2, 309–325.
Avigad, D., 1993. Tectonic juxtaposition of blueschists and greenschists in Sifnos Island (Aegean Sea)–implications for the structure of the Cycladic blueschist belt. J. Struct. Geol. 15, 1459–1469.
Baker, T., Pollard, P., Mustard, R., Mark, G., Graham, J., 2005. A comparison of granite-related tin, tungsten and gold-bismuth deposits: implications for exploration. Soc. Econ. Geol. Newsl. 61, 5–17.
Berger, A., Schneider, D.A., Grasemann, B., Stockli, D., 2013. Footwall mineralization during Late Miocene extension along the West Cycladic Detachment System, Lavrion, Greece. Terra Nova 25, 181–191.
Biggazzi, G., Del Moro, A., Innocenti, F., Kyriakopoulos, K., Manetti, P., Papadopoulos, P., Norelliti, P., Magganas, A., 1989. The magmatic intrusive complex of Petrota, west Thrace: age and geodynamic significance. Geol. Rhodopica 1, 290–297.
Bonev, N., Beccaletto, L., 2007. From syn- to post-orogenic Tertiary extension in the north Aegean region: constraints on the kinematics in the eastern Rhodope-Thrace, Bulgaria-Greece and the Biga Peninsula, NW Turkey. Geol. Soc. London Spec. Publ. 291, 113–142.
Bonev, N., Burg, J.P., Ivanov, Z., 2006a. Mesozoic-Tertiary structural evolution of an extensional gneiss dome – the Kesebir-Kardamos dome, E. Rhodopes, Bulgaria. Int. J. Earth Sci. 95, 318–340.
Bonev, N., Marchev, P., Moritz, R., Collings, D., 2015. Jurassic subduction zone tectonics of the Rhodope Massif in the Thrace region (NE Greece) as revealed by new U-Pb and $^{40}Ar/^{39}Ar$ geochronology of the Evros ophiolite and high-grade basement rocks. Gondwana Res. 27, 760–775.
Bonev, N., Marchev, P., Singer, B., 2006b. $^{40}Ar/^{39}Ar$ geochronology constraints on the Middle Tertiary basement extensional exhumation, and its relation to ore-forming and magmatic processes in the Eastern Rhodope (Bulgaria). Geodin. Acta 19, 265–280.
Bonev, N., Moritz, R., Márton, I., Chiaradia, M., Marchev, P., 2010. Geochemistry, tectonics, and crustal evolution of basement rocks in the Eastern Rhodope Massif, Bulgaria. Int. Geol. Rev. 52, 269–297.
Bonev, N., Spikings, R., Moriz, R., Marchev, P., 2013. $^{40}Ar/^{39}Ar$ age constraints on the timing of Tertiary crustal extension and its temporal relation to ore-forming and magmatic processes in the Eastern Rhodope Massif, Bulgaria. Lithos 180–181, 264–278.
Bonneau, M., 1984. Correlation of the Hellenic nappes in the south-east Aegean and their tectonic reconstruction. Geol. Soc. London Spec. Publ. 17, 517–527.
Bonsall, T.A., Spry, P.G., Voudouris, P., Tombros, S., Seymour, K., Melfos, V., 2011. The geochemistry of carbonate-replacement Pb-Zn-Ag mineralization in the Lavrion District, Attica, Greece: fluid inclusion, stable isotope, and rare earth element studies. Econ. Geol. 106, 619–651.
Border, A., Constantinides, D., Michael, C., 1999. Discovery and evaluation of the Sappes gold deposit, northeastern Greece, in: Currie, D., Nielsen, K. (Eds.), Proceedings of the Australian Mineral Foundation Conference: New generation gold mines '99, case histories of discovery, Perth, pp. 29–38.
Boronkay, K., Doutsos, T., 1994. Transpression and transtension within different structural levels in the central Aegean region. J. Struct. Geol. 16, 1555–1573.
Brichau, S., Thomson, S., Ring, U., 2010. Thermochronometric constraints on the tectonic evolution of the Serifos detachment, Aegean Sea, Greece. Int. J. Earth Sci. 99, 379–393.
Bristol, S.K., Spry, P.G., Voudouris, P.Ch., Melfos, V., Fornadel, A.P., Sakellaris, G.A., 2015. Geochemical and geochronological constraints on the formation of shear-zone hosted Cu-Au-Bi-Te mineralization in the Stanos area, Chalkidiki, northern Greece. Ore Geol. Rev. 66, 266–282.
Bröcker, M., Pidgeon, R.T., 2007. Protolith ages of meta-igneous and metatuffaceous rocks from the Cycladic Blueschist Unit, Greece: results of a reconnaissance U-Pb zircon study. J. Geol. 115, 83–98.
Brun, J.-P., Faccenna, C., 2008. Exhumation of high-pressure rocks driven by slab roll-back. Earth Planet. Sci. Lett. 272, 1–7.
Brun, J.-P., Faccenna, C., Gueydan, F., Sokoutis, D., Philippon, M., Kydonakis, K., Gorini, C., 2016. The two-stage Aegean extension, from localized to distributed, a result of slab rollback acceleration. Can. J. Earth Sci. 53, 1142–1157.
Brun, J.-P., Sokoutis, D., 2007. Kinematics of the Southern Rhodope core complex (Northern Greece). Int. J. Earth Sci. 96, 1079–1099.
Burchfiel, B.C., Nakov, R., Dumurdzanov, N., Papanikolaou, D., Tzankov, T., Serafimovski, T., King, R.W., Kotzev, V., Todosov, A., Nurce, B., 2008. Evolution and dynamics of the Cenozoic tectonics of the South Balkan extensional system. Geosphere 4, 919–938.
Burg, J.-P., 2012. Rhodope: from Mesozoic convergence to Cenozoic extension. Review of petro-structural data in the geochronological frame. J. Virtual Explorer 42, 44, paper 1.
Burg, J.P., Ricou, L.E., Ivano, Z., Godfriaux, I., Dimov, D., Klain, L., 1996. Syn-metamorphic nappe complex in the Rhodope Massif. Structure and kinematics. Terra Nova 8, 6–15.
Chatzipanagis, I., Dimitroula, M., 1996, Investigation of gold in the area of Palea Kavala. Institute of Geology and Mineral Exploration Internal Report. 120 p (in Greek).
Christofides, G., Pecskay, Z., Eleftheriadis, G., Soldatos, T., Koroneos, A., 2004. The Tertiary Evros volcanic rocks (Thrace, northeastern Greece): petrology and K-Ar geochronology. Geol. Carpath. 55, 397–410.
Christofides, G., Soldatos, T., Elefthertiadis, G., Koroneos, A., 1998. Chemical and isotopic evidence for source contamination and crustal assimilation in the Hellenic Rhodope plutonic rocks. Acta Volcanol. 10, 305–318.
Chryssoulis, S.L., Cabri, L.J., 1990. Significance of gold mineralogical balances in mineral processing. Trans. Inst. Min. Metall. 99, C1–C10.
Conophagos, C., 1980. The Lavrion and the ancient Greek techniques for silver production. Athens. Ekdotiki Athinion, Athens. 458 p. (in Greeek).
Cook, N.J., Ciobanu, C.L., Spry, P.G., Voudouris, P., 2009. Understanding gold-(silver)-telluride-(selenide) mineral deposits. Episodes 32, 249–263.
Cvetković, V., Prelević, D., Downes, H., Jovanović, M., Vaselli, O., Pécskay, Z., 2004. Origin and geodynamic significance of Tertiary postcollisional basaltic magmatism in Serbia (central Balkan Peninsula). Lithos 73, 161–186.
de Boorder, H., Spakman, W., White, S.H., Wortel, M.J.R., 1998. Late Cenozoic mineralization, orogenic collapse and slab detachment in the European Alpine Belt. Earth Planet. Sci. Lett. 164, 569–575.
Del Moro, A., Innocenti, F., Kyriakopoulos, C., Manetti, P., Papadopoulos, P., 1988. Tertiary granitoids from Thrace (Northern Greece): Sr isotopic and petrochemical data. Neues Jahrb. Mineral. Abh. 159, 113–135.
Denèle, Y., Lecomte, E., Jolivet, L., Lacombe, O., Labrousse, L., Huet, B., Le Pourhiet, L., 2011. Granite intrusion in a metamorphic core complex: the example of the Mykonos laccolith (Cyclades, Greece). Tectonophysics 501, 52–70.
Dinter, D., Royden, L., 1993. Late Cenozoic extension in northeastern Greece: Strymon Valley detachment system and Rhodope metamorphic core complex. Geology 21, 45–48.
Dinter, D.A., Macfarlane, A., Hames, W., Isachsen, C., Bowring, S., Royden, L., 1995. U-Pb and $^{40}Ar/^{39}Ar$ geochronology of the Symvolon granodiorite: implications for the thermal and structural evolution of the Rhodope metamorphic core complex, northeastern Greece. Tectonics 14, 886–908.
Dragić, D., Mišković, A., Hart, C., Tosdal, R., Dunav, P.F., Glisic, S., 2014. Spatial and temporal relations between epithermal and porphyry style mineralization in the Lece magmatic complex, Serbia. Extended Abstracts of the Conference: Building Exploration Capability for the 21st century. Keystone, Colorado.
Driesner, T., Pintea, I., 1994. Constraints on the conditions of wurtzite formation at the Agios Philippos Pb-Zn deposit, NE-Greece. Ber. Dtsch. Mineralogischen Ges., Beihefte zum European Journal of Mineralogy 6, 54.
Ducoux, M., Branquet, Y., Jolivet, L., Arbaret, L., Grasemann, B., Rabillard, A., Gumiaux Drufin, S., 2017. Synkinematic skarns and fluid drainage along detachments: The West Cycladic Detachment System on Serifos Island (Cyclades, Greece) and its related mineralization. Tectonophysics 695, 1–26.
Economou-Eliopoulos, M., Eliopoulos, D.G., 2000. Palladium, platinum and gold concentration in porphyry copper systems of Greece and their genetic significance. Ore Geol. Rev. 16, 59–70.
Eldorado Gold Corp., 2017. Assets; Resources and Reserves. http://www.eldoradogold.com (accessed 20th May 2017).
Eleftheriadis, G., 1995. Petrogenesis of the Oligocene volcanics from the Central Rhodope massif (N. Greece). Eur. J. Mineral. 7, 1169–1182.
Eleftheriadis, G., Koroneos, A., 2003. Geochemistry and petrogenesis of post-collision pangeon granitoids in central Macedonia, Northern Greece. Chem. Erde 63, 364–389.
Eliopoulos, D., Kilias, S.P., 2011. Marble-hosted submicroscopic gold mineralization at Asimotrypes area, Mount Pangeon, southern Rhodope Core Complex, Greece. Econ. Geol. 106, 751–780.
Eliopoulos, D.G., Economou-Eliopoulos, M., 1991. Platinum-group element and gold contents in the Skouries porphyry copper deposit, Chalkidiki peninsula, Northern Greece. Econ. Geol. 86, 740–749.
Eliopoulos, D.G., Economou-Eliopoulos, M., Zelyaskova-Panayiotova, M., 2014. Critical factors controlling Pd and Pt potential in porphyry Cu–Au deposits: evidence from the Balkan Peninsula. Geosciences 4, 31–49.
Ersoy, E.Y., Palmer, M.R., 2013. Eocene-Quaternary magmatic activity in the Aegean: implications for mantle metasomatism and magma genesis in an evolving orogeny. Lithos 180–181, 5–24.
Fornadel, A.P., Spry, P.G., Melfos, V., Vavelidis, M., Voudouris, P., 2011. Is the Palea Kavala Bi-Te-Pb-Sb±Au district, northeastern Greece, a reduced intrusion-related system? Ore Geol. Rev. 39, 119–133.
Fornadel, A.P., Voudouris, P.C., Spry, P.G., Melfos, V., 2012. Mineralogical, stable isotope, and fluid inclusion studies of spatially related porphyry Cu and epithermal Au-Te mineralization, Fakos Peninsula, Limnos Island, Greece. Mineral. Petrol. 105, 85–111.
Forward, P., Francis, A., Lidell, N., 2010. Technical Report on the Stratoni Project Pb-Zn-Ag Deposit, Northern Greece. European Goldfields Limited, p. 49.
Forward, P., Francis, A., Lidell, N., 2011. Technical Report on the Olympias Project Au-Pb-Zn-Ag Deposit, Northern Greece. European Goldfields Limited, p. 207.
Frei, R., 1992. Isotope (Pb, Rb-Sr, S, O, C, U-Pb) geochemical investigations on Tertiary intrusives and related mineralizations in the Serbo-Macedonian Pb-Zn, Sb+Cu-Mo metallogenic province in Northern Greece. Unpublished Doctoral dissertation, Zürich, Switcherland, ETH Zürich. 231 p.
Frei, R., 1995. Evolution of mineralizing fluid in the porphyry copper system of the Skouries deposit, northeast Chalkidiki (Greece): evidence from combined Pb-Sr and stable isotope data. Econ. Geol. 90, 746–762.
Fytikas, M., Innocenti, F., Kolios, N., Manneti, P., Mazzuoli, R., Poli, G., Rita, F., Villari, L., 1986. Volcanology and petrology of volcanic products from the island of Milos and neighbouring islets. J. Volcanol. Geoth. Res. 28, 297–317.
Fytikas, M., Innocenti, F., Manetti, P., Mazzuoli, R., Peccerillo, A., Villari, L., 1984. Tertiary to Quaternary evolution of volcanism in the Aegean region. Geol. Soc., London, Spec. Publ. 17, 687–699.

Gallhofer, D., von Quadt, A., Peytcheva, I., Schmid, S.M., Heinrich, C.A., 2015. Tectonic, magmatic and metallogenetic evolution of the Late Cretaceous arc in the Carpathian-Balkan orogen. Tectonics, 1813–1836.
Gautier, P., Brun, J.-P., 1994. Ductile crust exhumation and extensional detachments in the central Aegean (Cyclades and Evvia islands). Geodin. Acta, 57–85.
Gialoglou, G., Drymniotis, D., 1983. Northeastern Greece: mining activities, mineral exploration and future developments. Trans. Inst. Min. Metall., Sect. A 92, A180–183.
Gilg A.G., 1993. Geochronology (K-Ar), fluid inclusion and stable isotope (C, O, H) studies of skarn, porphyry copper, and carbonate-hosted Pb-Zn (Ag-Au) replacement deposits in the Kassandra mining district (Eastern Chalkidiki, Greece). Unpublished Doctoral dissertation, Züich, Switcherland, ETH Zürich. 152 p.
Gilg, H.A., Frei, R., 1994. Chronology of magmatism and mineralization in the Kassandra mining area, Greece: The potentials and limitations of dating hydrothermal illites. Geochim. Cosmochim. Acta 58, 2107–2122.
Glory Resources, 2012. High grade gold in Greece. Unpublished report, 31 p.
Grabezhev, A., Voudouris, P., 2014. Rhenium distribution in oscillatory zoned molybdenite from Vosnesensk porphyry Cu ± (Mo-Au) deposit (southern Urals, Russia). Can. Mineral. 52, 671–686.
Grasemann, B., Schneider, D.A., Stöckli, D.F., Iglseder, C., 2012. Miocene bivergent crustal extension in the Aegean: evidence from the western Cyclades (Greece). Lithosphere 4, 23–39.
Hague, P.F., 1993. The structural and volcanic evolution of tertiary basins along the southern margin of the Rhodope Massif, northeastern Greece. Unpublished Doctoral dissertation, Southampton, Great Britain, The University of Southampton. 227 p.
Hahn, A., Naden, J., Treloar, P.J., Kilias, S.P., Ranking, A.H., Forward, P., 2012. A new time frame for the mineralisation in the Kassandra mine district, N. Greece: deposit formation during metamorphic core complex exhumation. European Mineralogical Conference 1, EMC2012-742.
Halley, S., Dilles, J.H., Tosdal, R.M., 2015. Footprints: Hydrothermal alteration and geochemical dispersion around porphyry copper deposits. SEG Newsletter 100, 1 & 12–17.
Hart, C.J.R., McCoy, D., Goldfarb, R.J., Smith, M., Roberts, P., Hulstein, R., Bakke, A.A., Bundtzen, T.K., 2002. Geology, exploration and discovery in the Tintina gold province, Alaska and Yukon. Soc. Econ. Geol. Spec. Publ. 9, 241–274.
Heinrich, C.A., Neubauer, F., 2002. Cu-Au-Pb-Zn-Ag metallogeny of the Alpine-Balkan-Carpathian-Dinaride geodynamic province. Miner. Deposita 37, 533–540.
Himmerkus, F., Reischmann, T., Kostopoulos, D., 2006. Late Proterozoic and Silurian basement units within the Serbo-Macedonian Massif, northern Greece: the significance of terrane accretion in the Hellenides. Geol. Soc. London, Spec. Publ. 260, 35–50.
Himmerkus, F., Reischmann, T., Kostopoulos, D.K., 2009a. Serbo-Macedonian revisited: a Silurian basement terrane from the northern Gondwana in the Internal Hellenides, Greece. Tectonophysics 473, 20–35.
Himmerkus, F., Reischmann, T., Kostopoulos, D.K., 2009b. Triassic rift-related metagranites in the Internal Hellenides, Greece. Geol. Mag. 146, 252–265.
Iglseder C., Grasemann B., Rice A.H., Petrakakis K., Schneider D., 2011. Miocene south directed low-angle normal fault evolution on Kea Island (West Cycladic Detachment System, Greece). Tectonics 30, TC4013.
Iglseder, C., Grasemann, B., Schneider, D.A., Petrakakis, K., Miller, C., Klötzli, U.S., Thöni, M., Zámolyi, A., Rambousek, C., 2009. I and S-type plutonism on Serifos (W-Cyclades, Greece). Tectonophysics 473, 69–83.
Innocenti, F., Kolios, N., Manetti, O., Mazzuoli, R., Peccerilo, G., Rita, F., Villari, L., 1984. Evolution and geodynamic significance of the Tertiary orogenic volcanism in northeastern Greece. Bull. Volcanol. 47, 25–37.
Janković, S., 1997. The Carpatho-Balkanides and adjacent area: a sector of the Tethyan Eurasian metallogenic belt. Miner. Deposita 32, 426–433.
John, D.A., Taylor, R.D., 2016. By-products of porphyry copper and molybdenum deposits. Rev. Econ. Geol. 18, 137–164.
Jolivet, L., Brun, J.-P., 2010. Cenozoic geodynamic evolution of the Aegean region. Int. J. Earth Sci. 99, 109–138.
Jolivet, L., Faccenna, C., Huet, B., Labrousse, L., Le Pourhiet, L., Lacombe, O., Lecomte, E., Burov, E., Denèle, Y., Brun, J.-P., Philippon, M., Paul, A., Salaün, G., Karabulut, H., Piromallo, C., Monié, P., Gueydan, F., Okay, A.I., Oberhänsli, R., Pourteau, A., Augier, R., Gadenne, L., Driussi, O., 2013. Aegean tectonics: strain localization, slab tearing and trench retreat. Tectonophysics 597, 1–33.
Jolivet, L., Lecomte, E., Huet, B., Denèle, Y., Lacombe, O., Labrousse, L., Le Pourhiet, L., Mehl, C., 2010. The North Cycladic detachment system. Earth Planet. Sci. Lett. 289, 87–104.
Jolivet, L., Menant, A., Sternai, P., Rabillard, A., Arbaret, L., Augier, R., Laurent, V., Beaudoin, A., Grasemann, B., Huet, B., Labrousse, L., Le Pourhiet, L., 2015. The geological signature of a slab tear below the Aegean. Tectonophysics 659, 166–182.
Jones, C.E., Tarney, J., Baker, J.H., Gerouki, F., 1992. Tertiary granitoids of Rhodope, northern Greece: magmatism related to extensional collapse of the Hellenic Orogen? Tectonophysics 210, 295–314.
Kaiser-Rohrmeier, M., von Quadt, A., Driesner, T., Heinrich, C.A., Handler, R., Ovtcharova, M., Ivanov, Z., Petrov, P., Sarov, S., Peytcheva, I., 2013. Post-orogenic extension and hydrothermal ore formation: high precision geochronology of the Central Rhodopian metamorphic core complex (Bulgaria-Greece). Econ. Geol. 108, 691–718.
Kalogeropoulos, S.I., Kilias, S.P., Arvanitidis, N.D., 1996. Physicochemical conditions of deposition and origin of carbonate-hosted base metal sulfide mineralization, Thermes ore-field, Rhodope Massif, northeastern Greece. Miner. Deposita 31, 407–418.
Kalogeropoulos, S.I., Kilias, S.P., Bitzios, D.C., Nicolaou, M., Both, R.A., 1989. Genesis of the Olympias carbonate-hosted Pb-Zn (Au, Ag) sulfide ore deposit, eastern Chalkidiki Peninsula, northern Greece. Econ. Geol. 84, 1210–1234.
Kanellopoulos, C., Voudouris, P., Moritz, R., 2014. Detachment-related Sb-As-Au-Ag-Te mineralization in Kallintiri area, northeastern Greece: Mineralogical and geochemical constraints. Proceedings 20th CBGA Congress, Tirana, Albania, Buletini i Shkencave Gjeologjike Special Issue 1, 162–165.
Katzir, Y., Garfunkel, Z., Avigad, D., Matthews, A., 2007. The geodynamic evolution of the Alpine orogen in the Cyclades (Aegean Sea, Greece): insights from diverse origins and modes of emplacement of ultramafic rocks. Geol. Soc. London, Spec. Publ. 291, 17–40.
Kelley, K.D., Spry, P.G., 2016. Critical elements in alkaline igneous rock-related epithermal gold deposits. Rev. Econ. Geol. 18, 195–216.
Kevrekidis, E., Seymour, K.St., Tombros, S., Zhai, D., Liu, J., Zouzias, D., 2015. The Agios Georgios argentiferous galena deposit on Antiparos island, Cyclades, Hellas and its relationship to the Paros leucogranite. Neues Jahrb. Mineral. 192, 239–261.
Kilias, A., Falalakis, G., Mountrakis, D., 1999. Cretaceous-Tertiary structures and kinematics of the Serbo-Macedonian metamorphic rocks and their relation to exhumation of the Hellenic hinterland (Macedonia, Greece). Int. J. Earth Sci. 88, 513–531.
Kilias, A., Falalakis, G., Sfeikos, A., Papadimitriou, E., Vamvaka, A., Gkarlaouni, C., 2013. The Thrace basin in the Rhodope province of NE Greece – a Tertiary supradetachment basin and its geodynamic implications. Tectonophysics 595–596, 90–105.
Kilias, S.P., Naden, J., Cheliotis, I., Shepherd, T.J., Constandinidou, H., Crossing, J., Simos, I., 2001. Epithermal gold mineralization in the active Aegean volcanic arc: the Profitis Ilias deposit, Milos island, Greece. Miner. Deposita 36, 32–44.
Kilias, S.P., Nomikou, P., Papanikolaou, D., Polymenakou, P.N., Godelitsas, A., Argyraki, A., Carey, S., Gamaletsos, P., Mertzimekis, T.J., Stathopoulou, E., Goettlicher, J., Steihninger, R., Betzelou, K., Livanos, I., Christakis, C., Croff Bell, K., Scoullos, M., 2013b. New insights into hydrothermal vent processes in the unique shallow-submarine arc-volcano, Kolumbo (Santorini), Greece. Nature Scientific Reports 3, Article number: 2421 doi: 10.1038/srep02421.
Kirchenbaur, M., Pleuger, J., Jahn-Awe, S., Nagel, T.J., Froitzheim, N., Fonseca, R.O.C., Münker, C., 2012. Timing of high-pressure metamorphic events in the Bulgarian Rhodopes from Lu–Hf garnet geochronology. Contrib. Miner. Petrol. 163, 897–921.
Kockel, F., Mollat, H., Gundlach, H., 1975. Hydrothermally altered and (copper) mineralized porphyritic intrusions in the Serbo-Macedonian Massif (Greece). Miner. Deposita 10, 195–204.
Kontis, E., Kelepertsis, A.E., Skounakis, S., 1994. Geochemistry and alteration facies associated with epithermal precious metal mineralization in an active geothermal system, northern Lesvos, Greece. Miner. Deposita 29, 430–433.
Kounov, A., Wüthrich, E., Seward, D., Burg, J.P., Stockli, D., 2015. Low-temperature constraints on the Cenozoic thermal evolution of the Southern Rhodope Core Complex (Northern Greece). Int. J. Earth Sci. 104, 1337–1352.
Kroll, T., Müller, D., Seifert, T., Herzig, P.M., Schneider, A., 2002. Petrology and geochemistry of the shoshonite-hosted Skouries porphyry Cu-Au deposit, Chalkidiki, Greece. Miner. Deposita 37, 137–144.
Kydonakis, K., Brun, J.-P., Poujol, M., Monié, P., Chatzitheodoridis, E., 2016. Inferences on the Mesozoic evolution of the North Aegean from the isotopic record of the Chalkidiki block. Tectonophysics 682, 65–84.
Kydonakis, K., Brun, J.-P., Sokoutis, D., 2015a. North Aegean core complexes, the gravity spreading of a thrust wedge. J. Geophys. Res. Solid Earth 120, 595–616.
Kydonakis, K., Brun, J.-P., Sokoutis, D., Gueydan, F., 2015b. Kinematics of Cretaceous subduction and exhumation in the western Rhodope (Chalkidiki block). Tectonophysics 665, 218–235.
Kyriakopoulos, K., 1987. A geochronological, geochemical and mineralogical study of some Tertiary plutonic rocks of the Rhodope Massif and their isotopic characteristics, Greece. Unpublished Doctoral dissertation, Athens, Greece, University of Athens. 343 p (in Greek).
Laurent, V., Huet, B., Labrousse, L., Jolivet, L., Monie, P., Augier, R., 2017. Extraneous argon in high-pressure metamorphic rocks: distribution, origin and transport in the Cycladic Blueschist Unit (Greece). Lithos 272, 315–335.
Lehmann, S., Barcikowski, J., von Quadt, A., Gallhofer, D., Peytcheva, I., Heinrich, C.A., Serafimovski, T., 2013. Geochronology, geochemistry and isotope tracing of the Oligocene magmatism of the Buchim-Damjan-Borov Dol ore district: implications for timing, duration and source of the magmatism. Lithos 180–181, 216–233.
Leroux, G.M., 2016. Stratigraphic and petrographic characterization of HS epithermal Au-Ag mineralization at the TV Tower district, Biga Peninsula, NW Turkey. Unpublished Master thesis, Vancouver, University of British Columbia. 198 p.
Liati, A., 1986. Regional metamorphism and overprinting contact metamorphism of the Rhodope zone, near Xanthi (N. Greece): petrology, geochemistry, geochronology. Unpublished Doctoral dissertation, Braunschweig, Germany, University of Braunschweig. 186 p.
Lips, A.L.W., Stanley, H.W., Wijbrans, J.R., 2000. Middle-Late Alpine thermo-tectonic evolution of the southern Rhodope Massif, Greece. Geodin. Acta 13, 281–292.
Lister, G.S., Banga, G., Feenstra, A., 1984. Metamorphic core complexes of cordilleran type in the Cyclades, Aegean Sea, Greece. Geology 12, 221–225.
Marchev, P., Georgiev, S., Raicheva, R., Peytcheva, I., von Quadt, A., Ovtcharova, M., Bonev, N., 2013. Adakitic magmatism in post-collisional setting: an example

from the early–middle Eocene Magmatic Belt in Southern Bulgaria and Northern Greece. Lithos 180–181, 159–180.
Marchev, P., Kaiser-Rohrmeier, B., Heinrich, C., Ovtcharova, M., von Quadt, A., Raicheva, R., 2005. Hydrothermal ore deposits related to post-orogenic extensional magmatism and core complex formation: the Rhodope Massif of Bulgaria and Greece. Ore Geol. Rev. 27, 53–89.
Marinos G., Petrascheck W.E., 1956. Lavrion: geological and geophysical research. Institute of Geological and Subsurface Research Greece 4. 246 p (in Greek).
Márton, I., Moritz, R., Spikings, R., 2010. Application of low-temperature thermochronology to hydrothermal ore deposits: formation, preservation and exhumation of epithermal gold systems from the Eastern Rhodope, Bulgaria. Tectonophysics 483, 240–254.
McFall, K.A., Roberts, S., Teagle, D., Naden, J., Lusty, P., Boyce, A., 2016. The origin and distribution of critical metals (Pd, Pt, Te & Se) within the Skouries Cu-Au porphyry deposit, Greece. Extended Abstracts of the Conference: Mineral Deposits Study Group meeting, 39th, Dublin, Ireland, 1 p.
Meinhold, G., Kostopoulos, D.K., 2013. The Circum-Rhodope Belt, northern Greece: age, provenance, and tectonic setting. Tectonophysics 595–596, 55–68.
Melfos, V., Arikas, M., Vavelidis, K., 2001. A new occurrence of argentopentlandite and gold from the Au-Ag-rich copper mineralisation in the Paliomylos area, Serbo-Macedonian massif, Central Macedonia, Greece. Bull. Geol. Soc. Greece 34, 1065–1072.
Melfos, V., Vavelidis, M., Christofides, G., Seidel, E., 2002. Origin and evolution of the Tertiary Maronia porphyry copper-molybdenum deposit, Thrace, Greece. Miner. Deposita 37, 648–668.
Melfos, V., Voudouris, P., 2012. Geological, mineralogical and geochemical aspects for critical and rare metals in Greece. Minerals 2, 300–317.
Melfos, V., Voudouris, P., 2016. Fluid evolution in Tertiary magmatic-hydrothermal ore systems at the Rhodope metallogenic province, NE Greece. A review. Geol. Croat. 69, 157–167.
Melfos, V., Voudouris, P., Vavelidis, M., Spry, P.G., 2008. Microthermometric results and formation conditions of a new intrusion-related Bi-Te-Pb-Sb ± Au deposit in the Kavala pluton, Greece. In: Proceedings of the XIII All-Russian conference on thermobaro-geochemistry in conjunction with IV APIFIS symposium, Moscow 2, 165–168.
Melidonis, N., Constantinides, D., 1983. The stratabound sulphide Mineralisation of Syros (Cyclades, Greece). Zeitschrift der Deutschen Geologischen Gesellschaft 134, 555–575.
Menant, A., Jolivet, L., Augier, R., Skarpelis, N., 2013. The North Cycladic Detachment System and associated mineralization, Mykonos, Greece: insights on the evolution of the Aegean domain. Tectonics 32, 433–452.
Menant, A., Jolivet, L., Vrielynck, B., 2016. Kinematic reconstruction and magmatic evolution illuminating crystal and mantle dynamics of the eastern Mediterranean region since the late Cretaceous. Tectonophysics 675, 103–140.
Moritz, R., Márton, I., Ortelli, M., Marchev, P., Voudouris, P., Bonev, N., Spikings, R., Cosca, M., 2010. A review of age constraints of epithermal precious and base metal deposits of the Tertiary Eastern Rhodopes: coincidence with Late Eocene-Early Oligocene tectonic plate reorganization along the Tethys. In: Christofides, G., et al. (Eds.), Proceedings of the XIX Congress of the Carpathian-Balkan Geological Association, Thessaloniki. Scientific Annals of the School of Geology A.U.Th. 100, 351–358.
Mposkos, E.D., Kostopoulos, D.K., 2001. Diamond, former coesite and supersilicic garnet in metasedimentary rocks from the Greek Rhodope: a new ultrahighpressure metamorphic province established. Earth Planet. Sci. Lett. 192, 497–506.
Naden, J., Kilias, S.P., Darbyshire, D.B.F., 2005. Active geothermal systems with entrained seawater as analogues for transitional continental magmato-hydrothermal and volcanic-hosted massive sulfide mineralization-the example of Milos Island, Greece. Geology 33, 541–544.
Neubauer, F., 2002. Contrasting Late Cretaceous with Neogene ore provinces in the Alpine-Balkan-Carpathian-Dinaride collision belt. In: Blundell, D.J., Neubauer, F., von Quadt, A., (Eds.). Timing and Location of Major Ore Deposits in an Evolving Orogen: Geological Society of London, pp. 81–102.
Neubauer, F., 2005. Structural control of mineralization in metamorphic core complexes. In: Mao, J., Bierlein, F.P. (Eds.), Mineral Deposit Research: Meeting the Global Challenge. Springer, Berlin, pp. 561–564.
Neubauer, F., 2007. Geodynamic control of shear reversal, exhumation of metamorphic core complexes and ore mineralization in the Aegean arc. Geophysical Research Abstracts 9, 07042 (SRef-ID: 1607–7962/gra/EGU2007-A-07042).
Ortelli, M., Moritz, R., Voudouris, P., Cosca, M., Spangenberg, J., 2010. Tertiary porphyry and epithermal association of the Sapes-Kassiteres district, Eastern Rhodopes, Greece. In: Proceedings of the 8th Swiss Geoscience Meeting, Fribourg, 19th-20th November 2010, pp. 83–84.
Ortelli, M., Moritz, R., Voudouris, P., Spangenberg, J., 2009. Tertiary porphyry and epithermal association of the Sapes-Kassiteres district, Eastern Rhodopes, Greece. In: Williams, P., et al., (Eds.), Smart science for exploration and mining. Proceedings, of the 10th SGA meeting, Townsville, Australia, pp. 536–538.
Papavassiliou, K., Voudouris, P., Kanellopoulos, C., Glasby, G., Alfieris, D., Mitsis, I., 2017. New geochemical and mineralogical constraints on the genesis of the Vani hydrothermal manganese deposit at NW Milos island, Greece: comparison with the Aspro Gialoudi deposit and implications for the formation of the Milos manganese mineralization. Ore Geol. Rev. 80, 594–611.
Parra, T., Vidal, O., Jolivet, L., 2002. Relation between the intensity of deformation and retrogression in blueschist metapelites of Tinos Island (Greece) evidenced by chlorite-mica local equilibria. Lithos 63, 429–450.
Pe-Piper, G., Christofides, G., Eleftheriadis, G., 1998. Lead and neodymium isotopic composition of Tertiary igneous rocks of northeastern Greece and their regional significance. Acta Vulcanol. 10, 255–263.
Pe-Piper, G., Piper, D.J.W., 1993. Revised stratigraphy of the Miocene volcanic rocks of Lesbos, Greece. Neues Jarbuchfwr Geologie und Palaontologie Monatschefte 2, 97–110.
Pe-Piper, G., Piper, D.J.W, 2002. The igneous rocks of Greece. The anatomy of an orogen, Beiträge der regionalen Geologie der Erde 30. Berlin-Stuttgart. 573 p.
Pe-Piper, G., Piper, D.J.W., 2006. Unique features of the Cenozoic igneous rocks of Greece. Geol. Soc. Am. Spec. Pap. 409, 259–281.
Pe-Piper, G., Piper, D.J.W., Koukouvelas, I., Dolansky, L.M., Kokkalas, S., 2009. Postorogenic shoshonitic rocks and their origin by melting underplated basalts: the Miocene of Limnos Island, Greece. Geol. Soc. Am. Bull. 121, 39–54.
Percival, T.J., Radtke, A.S., 1994. Sedimentary-rock-hosted disseminated gold mineralization in the Alsar district, Macedonia. Can. Mineral. 32, 649–655.
Perugini, D., Poli, G., Christofides, G., Eleftheriadis, G., Koroneos, A., Soldatos, T., 2004. Mantle-derived and crustal melts dichotomy in northern Greece: spatiotemporal and geodynamic implications. Geol. J. 39, 63–80.
Prelević, D., Foley, S.F., Romer, R.L., Cvetković, V., Downes, H., 2005. Tertiary ultrapotassic volcanism in Serbia: constraints on petrogenesis and mantle source characteristics. J. Petrol. 46, 1443–1487.
Reinecke, T., Altherr, R., Hartung, B., Hatzipanagiotou, K., Kreuzer, H., Harre, W., Klein, H., Keller, J., Geenen, E., Boeger, H., 1982. Remnants of a Late Cretaceous high temperature belt on the island of Anafi (Cyclades, Greece). Neues Jahrb. Mineral. 145, 157–182.
Reischmann, T., Kostopoulos, D., 2007. Terrane accretion in the internal Hellenides. Geophys. Res. Abstracts 9, 05337.
Repstock, A., Voudouris, P., Kolitsch, U., 2015. New occurrences of watanabeite, colusite, "arsenosulvanite" and Cu-excess tetrahedrite-tennantite at the Pefka high-sulfidation epithermal deposit, northeastern Greece. Neues Jahrb. Mineral. 192, 135–149.
Richards, J.P., 2009. Post-subduction porphyry Cu-Au and epithermal Au deposits: products of remelting of subduction-modified lithosphere. Geology 37, 247–250.
Richards, J.P., 2011. Magmatic to hydrothermal metal fluxes in convergent and collided margins. Ore Geol. Rev. 40, 1–26.
Richards, J.P., 2015. Tectonic, magmatic, and metallogenic evolution of the Tethyan orogen: from subduction to collision. Ore Geol. Rev. 70, 323–345.
Ring, U., Glodny, J., Will, T.M., Thomson, S., 2011. Normal faulting on Sifnos and the South Cycladic Detachment System, Aegean Sea, Greece. J. Geol. Soc. London 168, 751–768.
Ring, U., Glodny, J., Will, T., Thomson, S., 2007. An Oligocene extrusion wedge of blueschist-facies nappes on Evia, Aegean Sea, Greece: implications for the early exhumation of high-pressure rocks. J. Geol. Soc. London 164, 637–652.
Ring, U., Glodny, J., Will, T., Thomson, S., 2010. The Hellenic subduction system: highpressure metamorphism, exhumation, normal faulting, and large-scale extension. Annu. Rev. Earth Planet. Sci. 38, 45–76.
Robertson, A.H., 2002. Overview of the genesis and emplacement of Mesozoic ophiolites in the Eastern Mediterranean Tethyan region. Lithos 65, 1–67.
Robertson, A.H., Trivić, B., Derić, N., Bucurc, I.I., 2013. Tectonic development of the Vardar ocean and its margins: evidence from the Republic of Macedonia and Greek Macedonia. Tectonophysics 595–596, 25–54.
Salemink, J., 1985. Skarn and ore formation at Seriphos, Greece as a consequence of granodiorite intrusion. Geologica Untrajectina 40, 231 p.
Sanchez, M.G., McClay, K., King, A., 2016. Crustal extension and its relationship to porphyry Cu-Au and epithermal Au mineralization in the Biga Peninsula, NW Turkey. Soc. Econ. Geol. Spec. Publ. 19, 113–156.
Schefer, S., Cvetkovic, Fügenschuh, B., Kounov, A., Ovtcharova, M., Schaltegger, U., Schmid, S.M., 2011. Cenozoic granitoids in the Dinarides of southern Serbia: age of intrusion, isotope geochemistry, exhumation history and significance for the geodynamic evolution of the Balkan Peninsula. Int. J. Earth Sci. 100, 1181–1206.
Scheffer, C., Vanderhaeghe, O., Lanari, P., Tarantola, A., Ponthus, L., Photiades, A., France, L., 2016. Syn- to post-orogenic exhumation of metamorphic nappes: structure and thermobarometry of the western Attic-Cycladic metamorphic complex (Lavrion, Greece). J. Geodyn. 96, 174–193.
Schmid, S.M., Bernoulli, D., Fügenschuh, B., Matenco, L., Schefer, S., Schuster, R., Tischler, M., Ustaszewski, K., 2008. The Alpine-Carpathian-Dinaridic orogenic system: correlation and evolution of tectonic units. Swiss J. Geosci. 101, 139–183.
Seman, S., Soukis, K., Stockli, D.F., Skourtsos, E., Kranis, H., Lozios, S., Shin, T., 2013a. Provenance of metasediments and Miocene exhumation history of the Lavrion Peninsula, South Attica, Greece: a combined structural, (U-Th)/He, and detrital zircon U-Pb study. EGU General Assembly Conference Abstracts 15, 12605.
Seman, S., Stockli, D.F., Soukis, K., Shin, T.A., Hernandez-Goldstein, E., 2013b. Unraveling the tectonostratigraphy of a HP-LT metamorphic belt using combined detrital zircon U-Pb and trace element analysis: an example from the Cycladic Blueschist Unit, Cyclades, Greece. In 2013 GSA Annual Meeting in Denver.
Serafimovski, T., 2000. The Lece-Chalkidiki metallogenic zone: geotectonic setting and metallogenic features. Geologija 42, 159–164.
Serafimovski, T., Tasev, G., Stefanova, V., 2013. Rare mineral phases related with major sulfide minerals in the Bučim porphyry copper deposit, R. Macedonia. Geol. Macedonica 27, 43–54.

Siron, C.R., Thompson, J.F.H., Baker, T., Friedman, R., Tsitsanis, P., Russell, S.V., Randall, S.B., Mortensen, J.K., 2016. Magmatic and metallogenic framework of Au-Cu porphyry and polymetallic carbonate-hosted replacement deposits of the Kassandra mining district, Northern Greece. Soc. Econ. Geol. Spec. Publ. 19, 29–55.
Skarpelis, N., Argyraki, A., 2009. Geology and origin of supergene ore at the Lavrion Pb-Ag-Zn deposit, Attica, Greece. Resour. Geol. 59, 1–14.
Skarpelis, N., Tsikouras, B., Pe-Piper, G., 2008. The Miocene igneous rocks in the Basal unit of Lavrion (SE Attica, Greece): petrology and geodynamic implications. Geol. Mag. 145, 1–15.
Smith, M.T., Lepore, W.A., Incekaraoğlu, T., Shabestari, P., Boran, H., Raabe, K., 2014. Küçükdağ: a new high-sulfidation epithermal Au-Ag-Cu deposit at the TV Tower property in western Turkey. Econ. Geol. 109, 1501–1511.
Stein, H.J., Markey, R.J., Morgan, J.W., Hannah, J.L., Scherstén, A., 2001. The remarkable Re–Os chronometer in molybdenite: how and why it works. Terra Nova 13, 479–486.
Stergiou, C., Melfos, V., Voudouris, P., Michailidis, K., Spry, P., Chatzipetros A. 2016. Hydrothermal alteration and structural control of the Vathi porphyry Cu-Au-Mo-U ore system, Kilkis district, N. Greece. Scientific Annals of the School of Geology, Aristotle University of Thessaloniki (Honorary Publication in Memory of Professor A. Kasoli-Fournaraki) 105, 69–74.
Stewart, A.L., McPhie, J., 2006. Facies architecture and Late Pliocene-Pleistocene evolution of a felsic volcanic island, Milos, Greece. Bull. Volcanol. 68, 703–726.
Stouraiti, C., Mitropoulos, P., Tarney, J., Barreiro, B., McGrath, A.M., Baltatzis, E., 2010. Geochemistry and petrogenesis of late Miocene granitoids, Cyclades, southern Aegean: nature of source components. Lithos 114, 337–352.
Sun, W., Arculus, R.J., Bennett, V.C., Eggins, S.M., Binns, R.A., 2003. Evidence for rhenium enrichment in the mantle wedge from submarine arc like volcanic glasses (Papua New Guinea). Geology 31, 845–848.
Tarkian, M., Eliopoulos, D.G., Economou-Eliopoulos, M., 1991. Mineralogy of precious metals in the Skouries porphyry copper deposit, N. Greece. Neues Jahrb. Mineral. 12, 529–537.
Tessalina, S.G., Yudovskaya, M.A., Chaplygin, I.V., Birck, J.-L., Capmas, F., 2008. Sources of unique rhenium enrichment in fumaroles and sulfides at Kudryavy volcano. Geochim. Cosmochim. Acta 72, 889–909.
Theodoridou, S., Melfos, V., Voudouris, P., Miscovic, A., 2016. Mineralogical and geochemical characterization of the Kimmeria Intrusion-Related deposit, Xanthi, NE Greece. Geophysical Research Abstracts 18, EGU2016-8933.
Thymiatis, G.E., 1995. Metallogenesis of Laodikino-Lipsidrio area, Kilkis/Mecedonia, Northern Greece. Unpublished Doctoral dissertation, Thessaloniki, Greece, Aristotle University of Thessaloniki. 240 p (in Greek).
Tombros, S., St. Seymour, K., Spry, P.G., Williams-Jones, A., 2007. The genesis of epithermal Au-Ag-Te mineralization, Panormos Bay, Tinos Island, Cyclades, Greece. Econ. Geol. 102, 1269–1294.
Tombros, S.F., Seymour, K.S., Williams-Jones, A.E., Zhai, D., Liu, J., 2015. Origin of a barite-sulfide ore deposit in the Mykonos intrusion, Cyclades: trace element, isotopic, fluid inclusion and Raman spectroscopy evidence. Ore Geol. Rev. 67, 139–157.
Tompouloglou, C., 1981. Les mineralisations tertiaires, type cuivre porphyrique, du massif Serbo-Macedonien (Macedoine Grece) dans leur contexte magmatique (avec un traitement geostatistique pour les donnees du prospect d' Alexia). Unpublished Doctoral dissertation, Paris, France, Ecole National Superieure des Mines de Paris. 230 p.
Tsirambides, A., Filippidis, A., 2012. Metallic mineral resources of Greece. Central Eur. J. Geosci. 4, 641–650.
Turpaud, P., Reischmann, T., 2010. Characterisation of igneous terranes by zircon dating: implications for UHP occurrences and suture identification in the Central Rhodope, northern Greece. Int. J. Earth Sci. 99, 567–591.
van Hinsbergen, D.J.J., Hafkenscheid, E., Spakman, W., Meulenkamp, J.E., Wortel, R., 2005. Nappe stacking resulting from subduction of oceanic and continental lithosphere below Greece. Geology 33, 325–328.
Vavelidis, M., Melfos, V., 2004. Bi-Ag-bearing tetrahedrite-tennantite in the Kapsalina copper mineralisation, Thasos island, Northern Greece. Neues Jahrb. Mineral. – Abh. (J. Mineral. Geochem.) 180, 149–169.
Vavelidis M., Melfos V., Kilias A., 1999. The gold-bearing quartz veins in the metamorphic rocks at the Drakontio area, central Macedonia, northern Greece. In: Stanley, C.J. et al., Mineral Deposits: Processes to Processing. Proceedings, pp. 209–212.
Vavelidis, M., Tarkian, M., 1995. Mineralogy of the gold-silver-bearing copper mineralized zones in the Paliopyrgos (Nea Madytos-Stanos) area, Northern Greece. Neues Jahrb. Mineral. Monatsh. 3, 133–143.
Vavelidis, M., 1997. Au-bearing quartz veins and placer gold on Sifnos island, Aegean Sea, Greece. In: Papunen, H. (Ed.), Mineral Deposits: Research and Exploration Where do They Meet? Balkema, pp. 335–338.
Vavelidis, M., Amstutz, G.C., 1983. New genetic investigations on the Pb-Zn deposits of Thasos (Greece). In: Mineral Deposits of the Alps and of the Alpine Epoch in Europe: Berlin-Heidelberg, Springer, pp. 359–365.
Vavelidis, M., Bassiakos, I., Begemann, F., Patriarcheas, K., Pernicka, E., Wagner, G.A., 1985. Geologie und Erzvorkommen von Sifnos. Anschnitt Beihefte 3, 59–80.
Vavelidis, M., Kilias, A., Melfos, V., Schmidt-Mumm, A., 1996. New investigations in the Au-Ag-bearing Cu mineralization and its structural control in the Koronouda area, central Macedonia, Northern Greece. In: Knežević, V., Krstić, B., (Eds.), Terranes of Serbia, Proceedings, pp. 317–322.
Vavelidis, M., Melfos, V., 1998. Fluid inclusion evidence for the origin of the barite silver-gold-bearing Pb–Zn mineralization of the Triades area, Milos Island, Greece. Bull. Geol. Soc. Greece 32, 137–144.
Vavelidis, M., Michailidis, K., Christofides, G., Boboti-Tsitlakides, I., 1990. Geochemical study of placer gold and the gold-bearing skarn-type mineralization of Kimmeria area, Xanthi disctrict, NE Greece. Geol. Rhodopica 2, 297–307.
Vavelidis, M., Schmidt-Mumm, A., Melfos, V., 1995. Microthermometric investigations in the Bi-Te-Ag bearing Cu-mineralization of Panagia area, Thasos Island, Greece. Bol. Soc. Esp. Mineral. 18–1, 261–262.
Vaxevanopoulos, M., 2017. Recording and study of ancient mining activity on Mount Pangaeon, E. Macedonia, Greece. Unpublished Doctoral dissertation, Thessaloniki, Greece, Aristotle University of Thessaloniki. 337 p (in Greek).
Veranis, N., Tsamantouridis, P., 1991. Using panning method to the exploration of auriferous mineralizations of Krousia metallogenic province. Institute of Geology and Mineral Exploration Internal Report (in Greek).
Voudouris, P., 2006. Comparative mineralogical study of Tertiary Te-rich epithermal and porphyry systems in northeastern Greece. Mineral. Petrol. 87, 241–275.
Voudouris, P., 2011. Conditions of formation of the Mavrokoryfi high-sulfidation epithermal Cu-Ag-Au-Te deposit (Petrota Graben, NE Greece). Mineral. Petrol. 101, 97–113.
Voudouris, P., 2014. Hydrothermal corundum, topaz, diaspore and alunite supergroup minerals in the advanced argillic alteration lithocap of the Kassiteres-Sapes porphyry-epithermal system, western Thrace, Greece. Neues Jahrb. Mineral. 191, 117–136.
Voudouris, P., Alfieris, D., 2005. New porphyry-Cu ± Mo occurrences in northeastern Aegean/Greece: ore mineralogy and transition to epithermal environment. In: Mao, J., Bierlein, F.P. (Eds.), Mineral Deposit Research: Meeting the Global Challenge. Springer, Berlin, pp. 473–476.
Voudouris, P., Manoukian, E., Veligrakis, Th., Sakellaris, G.A., Koutsovitis, P., Falalakis, G., 2014. Carbonate-replacement and vein-type Pb-Zn-Ag-Au mineralization at Syros Island, Cyclades: Mineralogical and geochemical constraints. In: Proceedings 20th CBGA Congress, Tirana, Albania, Buletini i Shkencave Gjeologjike Special Issue 1, 183–186.
Voudouris, P., Melfos V., Moritz R., Spry P.G., Ortelli M., Kartal T., 2010. Molybdenite occurrences in Greece: mineralogy, geochemistry and depositional environment. In: Christofides, G., et al. (Eds.), Proceedings of the XIX Congress of the Carpathian-Balkan Geological Association, Thessaloniki. Scientific Annals of the School of Geology A.U.Th. 100, pp. 369–378.
Voudouris, P., Melfos, V., Spry, P.G., Bonsall, T., Tarkian, M., Economou-Eliopoulos, M., 2008a. Mineralogical and fluid inclusion constraints on the evolution of the Plaka intrusion-related ore system, Lavrion, Greece. Mineral. Petrol. 93, 79–110.
Voudouris, P., Melfos, V., 2012. Aluminum-phosphate-sulfate (APS) minerals in the sericitic advanced argillic alteration zone of the Melitena porphyry-epithermal Mo-Cu ± Au ± Re prospect, western Thrace, Greece. Neues Jahrb. Mineral. – Abh. (J. Mineral. Geochem.) 190, 11–27.
Voudouris, P., Melfos, V., Spry, P.G., Baker, T., 2016b. Cenozoic Porphyry-Epithermal and Other Intrusion-Related Deposits in Northeastern Greece: Geological, Mineralogical and Geochemical Constraints. Society of Economic Geologists, Guidebook Series 54, 43–82.
Voudouris, P., Melfos, V., Spry, P.G., Bindi, L., Kartal, T., Arikas, K., Moritz, R., Ortelli, M., 2009. Rhenium-rich molybdenite and rheniite (ReS_2) in the Pagoni Rachi-Kirki Mo-Cu-Te-Ag-Au deposit, Northern Greece: implications for the rhenium geochemistry of porphyry style Cu-Mo and Mo mineralization. Can. Mineral. 47, 1013–1036.
Voudouris, P., Melfos, V., Spry, P.G., Bindi, L., Moritz, R., Ortelli, M., Kartal, T., 2013c. Extremely Re-rich molybdenite from porphyry Cu-Mo-Au prospects in northeastern Greece: mode of occurrence, causes of enrichment, and implications for gold exploration. Minerals 3, 165–191.
Voudouris, P., Melfos, V., Spry, P.G., Bonsall, T., Tarkian, M., Solomos, Ch., 2008b. Carbonate-replacement Pb-Zn-Ag ± Au mineralization in the Kamariza area, Lavrion, Greece: mineralogy and thermochemical conditions of formation. Mineral. Petrol. 94, 85–106.
Voudouris, P., Melfos, V., Spry, P.G., Kartal, T., Schleicher, H., Moritz, R., Ortelli, M., 2013b. The Pagoni Rachi/Kirki Cu-Mo-Re-Au-Ag-Te deposit, northern Greece: mineralogical and fluid inclusion constraints on the evolution of a telescoped porphyry-epithermal system. Can. Mineral. 51, 411–442.
Voudouris, P., Melfos, V., Spry, P.G., Moritz, R., Papavasiliou, C., Falalakis, G., 2011a. Mineralogy and geochemical environment of formation of the Perama Hill high-sulfidation epithermal Au-Ag-Te-Se deposit, Petrota graben, NE Greece. Mineral. Petrol. 103, 79–100.
Voudouris, P., Siron, C.R., Márton, I., Melfos, V., Baker, T., Spry, P.G., 2016a. Eocene to Miocene Hydrothermal Deposits of Northern Greece and Bulgaria: Relationships between Tectonic-Magmatic Activity, Alteration, and GoldMineralization - A Preface. Society of Economic Geologists, Guidebook Series 54, 1–15.
Voudouris, P., Spry, P.G., Mavrogonatos, C., Sakellaris, G.A., Bristol, S.K., Melfos, V., Fornadel, A., 2013. Bismuthinite derivatives, lillianite homologues, and bismuth sulfotellurides as indicators of gold mineralization at the Stanos shear-zone related deposit, Chalkidiki, northern Greece. Can. Mineral. 51, 119–142.
Voudouris, P., Spry, P.G., Melfos, V., Alfieris, D., 2007. Tellurides and bismuth sulfosalts in gold occurrences of Greece: mineralogy and genetic considerations. In: Proceedings of the Field Workshop of IGCP-486, Espoo, Finland, August 26th-31st 2007, Geological Survey of Finland 53, 85–94.
Voudouris, P., Spry, P.G., Sakellaris, G.A., Mavrogonatos, C., 2011b. A cervelleite-like mineral and other Ag-Cu-Te-S minerals [Ag_2CuTeS and $(Ag, Cu)_2TeS$] in gold-bearing veins in metamorphic rocks of the Cycladic Blueschist Unit, Kallianou, Evia Island, Greece. Mineral. Petrol. 101, 169–183.

Voudouris, P., Tarkian, M., Arikas, K., 2006. Mineralogy of telluride-bearing epithermal ores in Kassiteres-Sappes area, western Thrace, Greece. Mineral. Petrol. 87, 31–52.

Walenta, K., Pantzartzis, P., 1969. The molybdenite deposit of Kimmeria, Xanthi, northern Greece. Erzmetall 22, 272–278.

Wüthrich, E., 2009. Low temperature thermochronology of the Northern Aegean Rhodope Massif. Unpublished Doctoral thesis, Zürich, Switzerland, ETH Zürich. 216 p.

Yigit, O., 2009. Mineral deposits of Turkey in relation to Tethyan metallogeny: implications for future mineral exploration. Econ. Geol. 104, 19–51.

Yigit, O., 2012. A prospective sector in the Tethyan Metallogenic Belt: geology and geochronology of minerals deposits in the Biga Peninsula. Ore Geol. Rev. 46, 118–148.

Zaimis S., Gutzmer J., Voudouris P., Melfos V., 2016. Indium, germanium and gallium enrichments in the carbonate-replacement Pb-Zn-Ag ore deposit at Kamariza, Lavrion (SE Attica, Greece). Abstract Volume of the 1st Postgraduate conference on the "Geology Of Ore Deposits", Freiberg, Germany, March 15–18, 2016.

Zimmerman, A., Stein, H.J., Hannah, J.L., Kozelj, D., Bogdanov, K., Berza, T., 2008. Tectonic configuration of the Apuseni-Banat-Timrok-Srednogorie belt, Balkans-South Carpathians, constrained by high precision Re-Os. Miner. Deposita 43, 1–21.